Regulation of chromosome morphology by histone modifications in pig oocytes

Bui, Hong Thuy

(Degree)
博士（学術）

(Date of Degree)
2005-03-25

(Date of Publication)
2020-07-13

(Resource Type)
doctoral thesis

(Report Number)
甲3281

(URL)
https://hdl.handle.net/20.500.14094/D1003281

Doctoral Dissertation

Regulation of Chromosome Morphology by Histone Modifications in Pig Oocytes

(ブタ卵母細胞におけるヒストン蛋白質の修飾
による染色体の形態の制御に関する研究)

Hong Thuy Bui

Graduate School of Science and Technology

Kobe University

January 2005

CONTENTS

Abbreviations

APMSF: 4-amidinobenzylsulfonyl fluoride hydrochloride
ATP: adenosine-triphosphate
Ac-H3-K9: acetylated histone H3 at lysine 9
Ac-H3-K14: acetylated histone H3 at lysine 14
Ac-H3-K18: acetylated histone H3 at lysine 18
BSA: bovine serum albumin
CHX: cycloheximide
CL-A: calyculin A
DAPI: 4,6-diamidino-2-phenylindole
DMEM: Dulbecco's modified Eagle's medium
DTT: dithiothreitol
EGTA: ethylene glycol-bis(β-Aminoethyl ether) N, N, N', N' – tetraacetic acid
ERK: extracellular signal-regulated kinase
FCS: fetal calf serum
GVBD: germinal vesicle breakdown
H1: histone H1
H3: histone H3
HAT: histone acetyltransferase
HDAC: histone deacetylase
HP1: heterochromatin protein 1
MAP kinase: mitogen-activated protein kinase
MBP: myelin basic protein
MEK: MAP kinase kinase
MPF: maturation promoting factor
Me-H3-K9: methylated histone H3 at lysine 9
OA: okadaic acid
OCC: oocyte-cumulus complex
P-H3-S10: phosphorylated histone H3 at serine 10
P-H3-S28: phosphorylated histone H3 at serine 28
PBD: Dulbecco's phosphate-buffered saline
PI: propidium iodide
PP1/PP2A: protein phosphatase 1 and 2A
PTPase: protein tyrosine phosphatase
PVA: polyvinyl alcohol
PVP: polyvinylpyrrolidone
SDS: sodium dodecyl sulfate
TCM-199: tissue cultured medium 199
TSA: trichostatin A
U0126: a MAP kinase inhibitor
Va: sodium orthovanadate

Chapter 1. General Introduction

Meiosis in mammalian oocytes starts during embryonic life and arrests around birth at the diplotene stage of the first prophase which corresponds to the G2 phase of the mitotic cell cycle. Oocytes stop the meiotic progression until the animal reaches the puberty. During the arrest, some oocytes start to grow. The oocytes increase the volume remarkably approximately 100-fold during the growth phase. For example, mouse oocytes of 15-20 μm in diameter grow to their final size of 70-75 μm (without zona pellucida), and pig and bovine oocytes grow from 30 μm to 120-125 μm. Oocyte growth and differentiation are coordinated with the development of the surrounding somatic components. During the oocyte growth, the surrounding granulosa cells proliferate and the follicles increase in their size (Fig. 1.1). After morphological change followed by a series of mitotic division of granulosa cells, the primordial follicles are converted to the primary follicles and then secondary follicles. With the formation of an antral cavity, the secondary follicles are converted to antral follicles.

Oocytes acquire the meiotic competence after a long series of preparatory processes involving transcription and subsequent translation of messages during the growth phase (Szöllösi, 1993). Studies in pig (Motlik et al., 1984), bovine (Fair et al., 1996), and goat oocytes (de Smedt et al., 1994) suggest that the transcriptional activity decreases as oocytes approach to their final size. At the same time, oocyte chromatin and nucleolus show dramatic changes in their structure. Although they are a continuous process, the nucleus changes toward the typical morphology showing a rim of condensed chromatin around a nucleolus. Acquisition of the meiotic competence during oocyte growth phase has been correlated with the change in the nuclear morphology (Motlik et al., 1984; Hirao et al., 1995). In pig, formation of chromatin peri-nucleolar rim appears to be correlated with the competence of oocytes to mature to the second metaphase (Hirao et al., 1995).

After reaching the full size, oocytes resume meiosis in response to gonadotropic stimuli. Reinitiation of meiosis represents transition from the G2 to M phase in the cell cycle and is manifested by chromosome condensation, disintegration of the nuclear membrane (germinal vesicle break down), and spindle formation. The continuation of the meiotic process includes discharge of one set of homologous chromosomes into the first polar body and arrest at

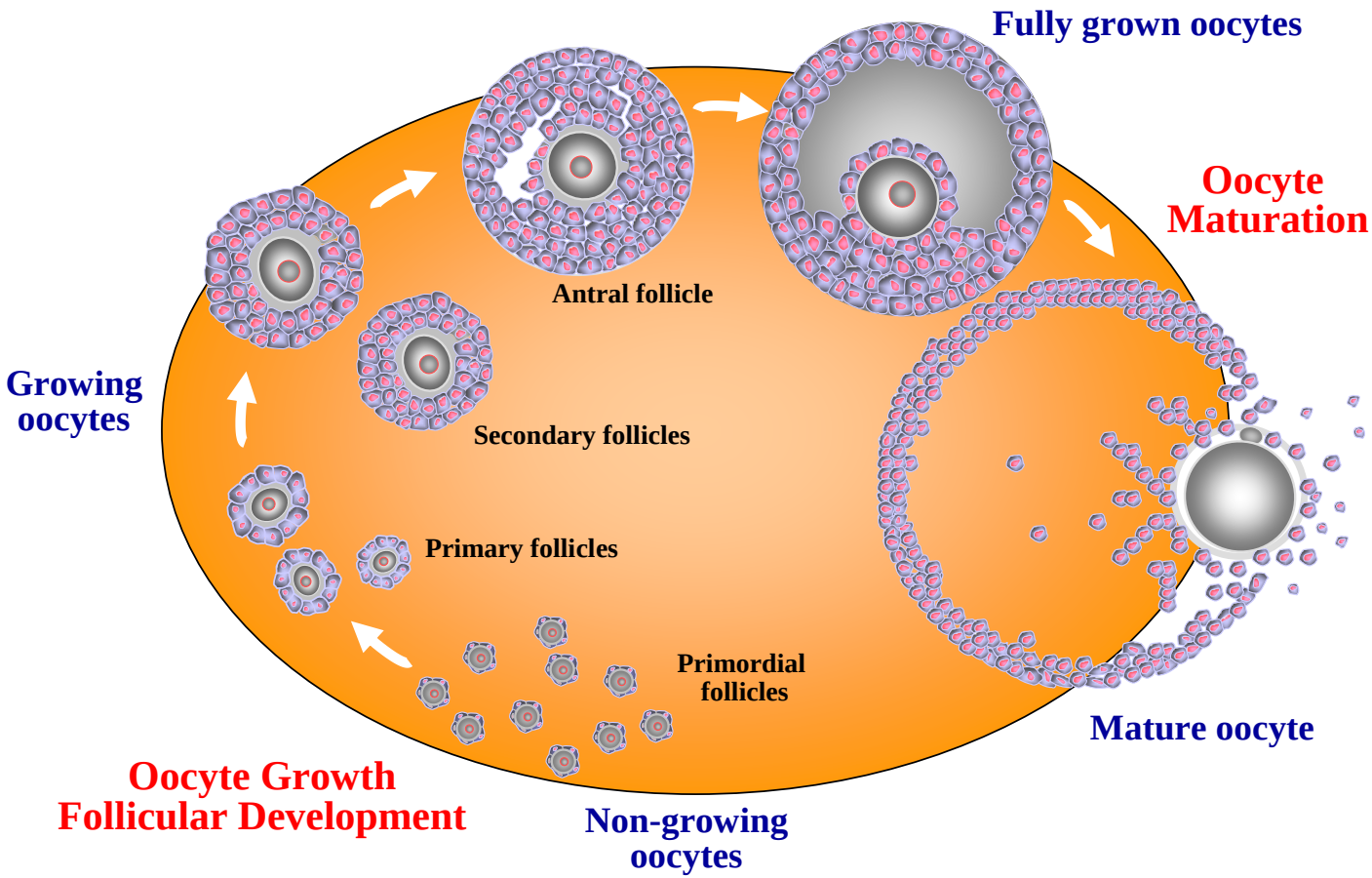

Fig. 1.1. Oocyte growth and maturation in the pig ovary

metaphase of the second meiotic division (MII). A series of these changes is called oocyte maturation.

Evidence of cell cycle studies shows that both the mitotic and meiotic cycles are driven by a protein kinase, known as maturation promoting factor (MPF). The MPF activity was first discovered by Masui and Markert in the cytoplasm of metaphase-arrested frog oocytes in 1971. The MPF activity was later found in mammals, and is now known as Cdc2 kinase which is a heterodimeric protein kinase consisting of a 34 kDa catalytic subunit ($p34^{cdc2}$) and a regulatory subunit (cyclin B) (Nurse, 1990; Murray, 1992). Cdc2 kinase is a serine/threonine protein kinase and phosphorylates many cellular substrates, such as histone H1 and nuclear lamin (Nigg, 1993). Another enzyme that has shown to be activated during oocyte maturation is the mitogen-activated protein kinase (MAPK), also known as extracellular signal-regulated kinase (ERK1/ERK2) in mammals.

The chromosome condensation is the first step of oocyte maturation and has been thought to be induced by Cdc2 kinase. However, based on the studies of the pig oocyte maturation, chromosomes start to condense before full activation of Cdc2 kinase (Miyano et al., 2003). Moreover, it is suggested that MAP kinase substitutes for the role of Cdc2 kinase in inducing chromosome condensation (Kubelka et al., 2002). These findings suggest that chromosome condensation is induced by either some kinase(s) other than Cdc2 kinase or by some phosphatase(s).

Recently, the morphological change in the chromosome has been implicated by the histone modification. Genomic DNA is packaged with histone proteins into chromatin, compacting DNA approximately 10,000-fold. Four core histone molecules, H2A, H2B, H3, and H4, associate with DNA to form the basic nucleosome structure in which DNA wraps around the histone proteins in eukaryotic cells (Arents et al., 1991) (Fig. 1.2). Each core histone is composed of a structured domain and an unstructured N-terminal tail, and the latter contains 25-40 amino acid residues (Luger et al., 1997). This unstructured tail extends through the DNA gyres and into the space surrounding the nucleosomes. Histone N-terminal tails provide sites for a variety of posttranslational modifications, including acetylation, phosphorylation, and methylation (Strahl and Allis, 2000). It is becoming increasingly apparent that such modifications of histone tails determine the interactions of histone with other proteins, which may in turn regulate chromatin

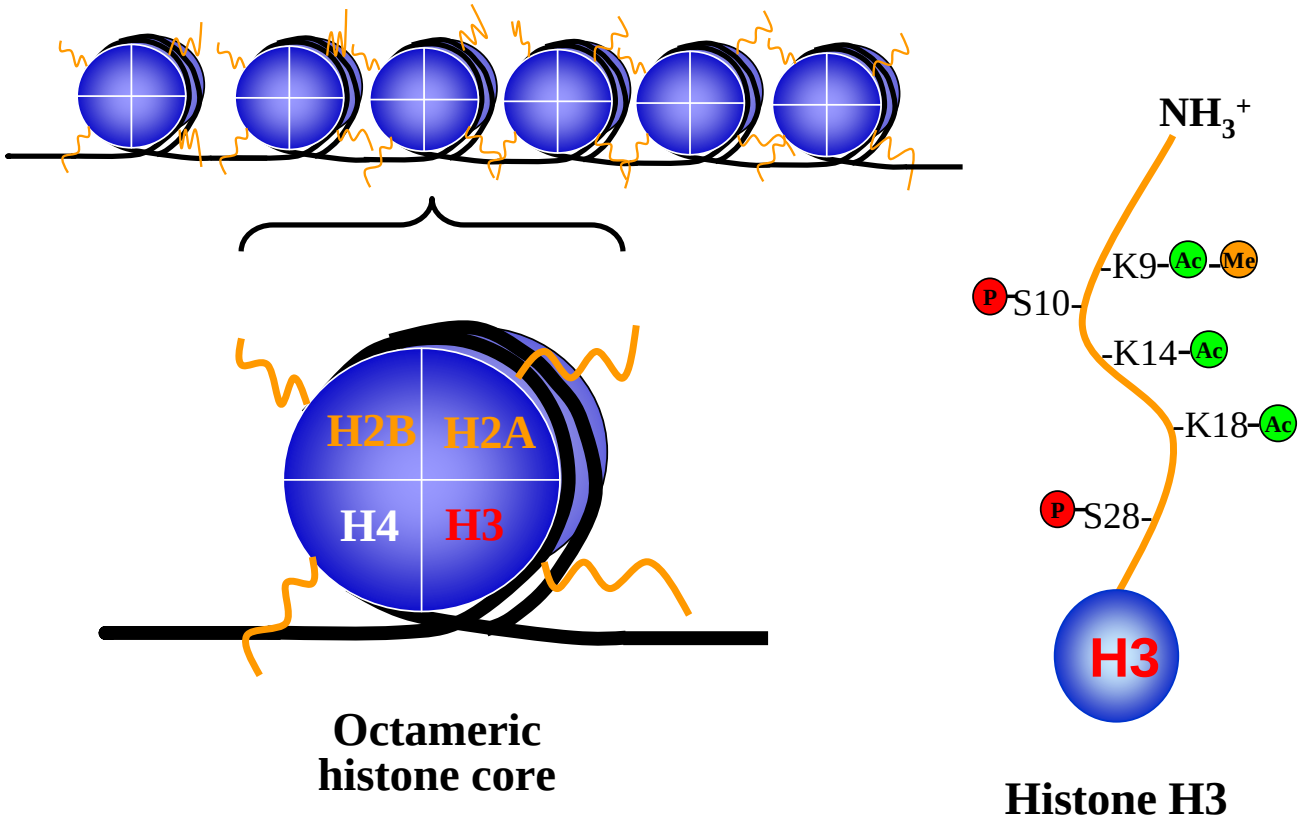

Fig. 1.2. Chromatin fiber, nucleosome, and core histones

structure (Wu and Grunstein, 2000). The change in chromatin configuration in growing oocytes correlates with the decline of transcriptional activity (Christians et al., 1999; De La Fuente and Eppig, 2001). Acetylated histones are associated with transcriptionally active chromatin and deacetylated histones with inactive chromatin in somatic cells (Allfrey et al., 1964). The highly conserved histone H3 lysines at 9, 14, 18, and 23 are frequently targeted for the modifications.

Phosphorylation of the serine 10 residue of the N-terminal tail of histone H3 is crucial for chromosome condensation during mitosis. Beside that, phosphorylation of serine 28 in histone H3 has the kinetics similar to those of serine 10. Both phosphorylation occur early in mitosis of somatic cells and the levels of phosphorylation seem to be regulated via an interplay between the activities of its protein kinase and phosphatase.

The localization of the serine 10 residue in close proximity to other modifiable amino acids in the histone H3 tail enables the possible interactions between phosphorylation of serine 10, methylation of lysine 9, and acetylation of lysine 9 and lysine 14 (Fig. 1.2). Recent studies identified methylation of histone H3 tail as an epigenetic mark that affects acetylation and phosphorylation of histone tail residues and also acts as a recognition signal for heterochromatin formation (Lachner et al., 2001; Bannister et al., 2001). Epigenetic modification means heritable but occurs independently of the gene sequence. It has become increasingly evident that the controlled expression of genes can not be accounted for by DNA sequences alone. Epigenetic regulation of gene transcription must be maintained and propagated across cell division cycles and throughout the development of the organism proper in order for cells to establish and maintain their identities as specialized cell types.

The success in the production of clone animals by somatic nuclear transfer has shown that the oocyte cytoplasm has the ability to reprogram gene expression (Wilmut et al., 1997; Wakayama et al., 1998). The breakthrough of animal cloning by using adult somatic cells has opened new ways of investigation in basic cell and reproductive sciences. Following nuclear transfer, the nuclear membrane breakdown, premature chromosome condensation, and nuclear swelling are well-known morphological changes (Campbell et al., 1996). It is thought that the chromosome condensation and remodeling of injected somatic cell nuclei are controlled by oocyte cell cycle. Oocyte cytoplasm may reprogram epigenetic modifications of somatic cell nuclei in a similar manner in fertilized oocytes. The change in phosphorylation, methylation, and

acetylation of histones H3 is thought to play important roles in the regulation of gene expression in reconstructed embryos and to be essential for their normal development. However, little has been understood about the change in the histone modifications of somatic cell nuclei transferred into oocytes.

Pig oocytes have been used as a model to study the maturation of mammalian oocytes because their maturation period is longer than those in any other mammalian species, and the chromatin condensation progresses gradually to make the metaphase chromosome. Moreover, pig oocytes are almost freely available from commercially slaughtered animals, and under our culture conditions, it is easy to obtain the specific stage of oocytes progressing to MII synchronously in response to gonadotropic stimulation.

The objective of the research in this dissertation is to investigate the regulation of chromosome morphology by histone modifications in pig oocytes. First, the experiments were designed to show that histone H3 phosphorylation was involved in the chromosome condensation during oocyte maturation in Chapter 2. The relation of histone H3 phosphorylation with the activity of kinases such as Cdc2 kinase and MAP kinase was also investigated. The results in Chapter 2 showed that chromosome condensation during oocyte maturation was correlated with phosphorylation of histone H3 by histone H3 kinase activity in pig oocytes. In Chapter 3, the focus was to find out the correlation between morphology of chromatin/chromosome and histone H3 phosphorylation, acetylation and methylation throughout oocyte growth, maturation and activation. In Chapter 4, chromosome condensation and decondensation of injected somatic cell nuclei in mature pig oocytes were investigated in relation to the histone H3 modifications of the somatic cell nuclei. In Chapter 5, the possible involvement of histone modifications in the change in the chromosome morphology in pig oocytes induced by some inhibitors were investigated.

Chapter 2. Chromosome Condensation and Histone H3 Phosphorylation During Oocyte Maturation

2.1. INTRODUCTION

The meiotic resumption of oocytes is controlled by protein kinase MPF (maturation-promoting factor or M-phase promoting factor), which is now also known as Cdc2 kinase. Cdc2 kinase is activated around the germinal vesicle breakdown (GVBD) of oocytes, and has been thought to be the key regulator of such major morphological changes during oocyte maturation as chromosome condensation, GVBD and spindle formation. Mitogen-activated protein (MAP) kinase (ERK1/ERK2 in mammals) is another kinase known to become active during oocyte maturation in a number of species, including *Xenopus* (Haccard et al., 1990), clams (Shibuya et al., 1992), and also in mammalian species such as mice (Sobajima et al., 1993), pigs (Inoue et al., 1995), goats (Dedieu et al., 1996), cattle (Fissore et al., 1996), and humans (Sun et al., 1999). The role of MAP kinase during oocyte maturation has not been firmly established, although it is known that its activation modulates microtubule dynamics.

Fully-grown pig oocytes have a condensed heterochromatin ring around the nucleolus in the germinal vesicle (GV). When the oocytes resume meiosis by hormonal stimuli, chromosomes start to condense and oocytes reach the first metaphase. They finish the first meiosis, go to the second meiosis without the interphase, and become arrested at metaphase of the second meiosis to complete the maturational process. Chromosome condensation is the first step of oocyte maturation. It is a unique process characterized by a dramatic change in chromosome morphology, and is required for the correct segregation of chromosomes. The precise change in the nucleus in pig oocytes during maturation has been described by Motlik and Fulka (1976). The heterochromatin in the fully-grown oocytes at GVI stage changes the morphology as the chromatin condenses to form the metaphase chromosome from GVI to GVIV stage. After GVIV stage, chromosomes condense into a single clump at the stage of diakinesis and nuclear membrane breaks down (germinal vesicle break down: GVBD). Then at metaphase I, paired homologs of chromosomes align on the metaphase plate of the spindle poised for segregation.

During anaphase I, chromosomes move to opposite ends of the spindle. At telophase I, the repulsion of the two sets of chromosomes is complete and the area of the spindle between them is elongated. Finally, one set of homologs with small volume of oocyte cytoplasm is emitted to perivitelline space as the first polar body. The other set of homologs remain in the oocyte cytoplasm, and are aligned in the spindle at metaphase II (Fig. 2.1). This classical observation shows that chromosomes start to condense before GVBD in pig oocytes, although the chromosome condensation has been thought to be induced by Cdc2 kinase. Furthermore, the recent findings show that the chromosome condensation does not always correlate with Cdc2 kinase activity, and that MAP kinase substitutes for the role of Cdc2 kinase (Kubelka et al., 2002). The cause of the chromosome condensation has not been understood completely.

The chromatin fiber is composed of repetitive units, the nucleosomes, which are comprised of an octamer of two each of the core histones, H2A, H2B, H3, and H4, around which 146 base pairs of DNA are wrapped (Luger et al., 1997). Each histone contains an N-terminal "tail" domain which is involved in the stabilization of the chromatin fiber (Tse and Hansen, 1997). The phosphorylation of histone H3 is thought to be involved in transcriptional activation (Sassone-Corsi et al., 1999) and chromosome condensation during mitotic cell division (Wei et al., 1999). A strong correlation between the initial chromosome condensation and histone H3 phosphorylation has been observed in mammalian somatic cells (Van Hooser et al., 1998), and its phosphorylation at serine 10 (S10) has been suggested to play a key role in mitotic chromosome condensation (Wei et al., 1998). The spatio-temporal distribution of histone H3 phosphorylation is different among the cell types so far examined. However, there is no evidence about histone H3 phosphorylation in meiotic chromosome condensation in mammalian oocytes.

Both Ipl1/Aurora-B kinase and its genetically interacting protein phosphatase Glc7/PP1 has been shown to be required for H3 phosphorylation during mitosis in *Saccharomyces cerevisiae* and *Caenorhabditis elegans* (Hsu et al., 2000; Murnion et al., 2001). It is suggested in somatic cells that the balance of histone H3 kinase and PP1 acting on S10 of histone H3 regulates chromosome condensation. Inhibitors of the protein serine/threonine phosphatase PP1 and PP2A, such as okadaic acid and calyculin A, induce rapid chromosome condensation in oocytes (Lu et al., 2002). However, it remains to be elucidated whether the effect of PP1/PP2A inhibitors on the chromosome condensation correlates with Cdc2 kinase, MAP kinase, or histone H3 kinase.

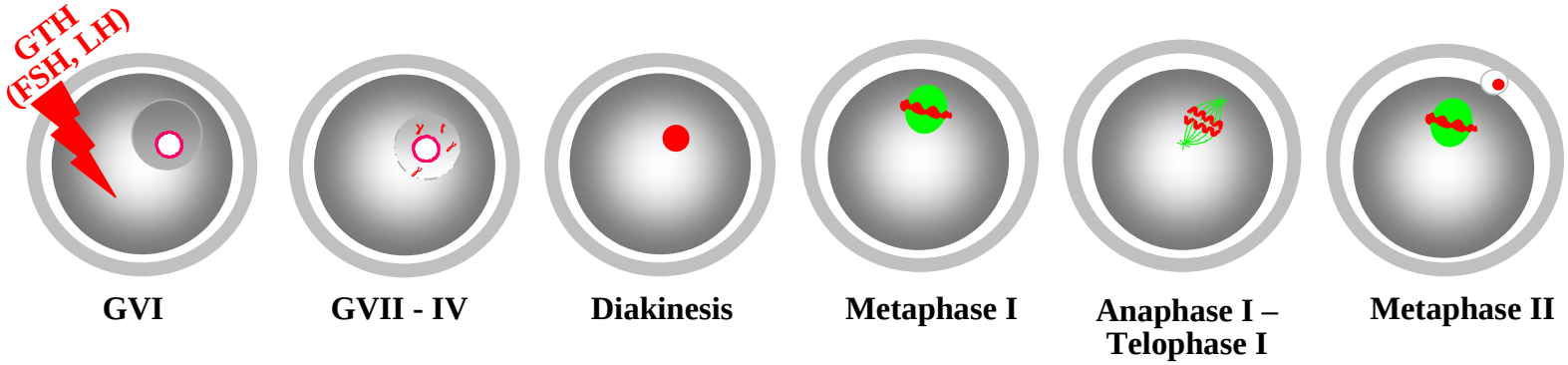

Fig. 2.1. The change in chromosome morphology during maturation of pig oocytes

The aim of this chapter is to investigate the involvement of histone H3 phosphorylation in the chromosome condensation during meiotic maturation of pig oocytes. First, the chromosome condensation and histone H3 phosphorylation at S10 during the maturation were examined immunocytologically. Next, the effects of protein phosphatase 1/2A (PP1/PP2A) inhibitors on the chromosome condensation and histone H3 phosphorylation were investigated. Moreover, the involvements of Cdc2 kinase, MAP kinase, and histone H3 kinase on the chromosome condensation and histone H3 phosphorylation were examined.

2.2. MATERIALS AND METHODS

2.2.1. Collection and Culture of Pig Oocytes

Pig ovaries were obtained from prepubertal gilts at a local slaughterhouse. The ovaries were washed once with 0.2% (w/v) cetyltrimethylammonium bromide and twice with Dulbecco's phosphate-buffered saline (PBS) containing 0.1% (w/v) polyvinyl alcohol (PBS-PVA; Sigma Chemical Co., St. Louis, MO). Antral follicles of 4-6 mm in diameter were dissected in PBS-PVA from ovaries following the technique described by Moor and Trounson (1977). After being opened in 25 mM HEPES buffered TCM-199 (Earl's salt; Nissui Pharmaceutical, Tokyo, Japan), oocyte-cumulus complexes with a piece of parietal granulosa tissue (oocyte-cumulus-granulosa cell complexes; OCGCs) were isolated from the follicles. Following two washes in HEPES buffered TCM-199, the OCGCs were cultured in 2 ml of maturation medium. The maturation medium was bicarbonate-buffered TCM-199 supplemented with 10% (v/v) heat-treated fetal calf serum (Biocell Inc., Carson, CA), 0.1 mg/ml sodium pyruvate, 0.08 mg/ml kanamycin sulphate (Sigma Chemical Co.), 2.2 mg/ml sodium bicarbonate, 0.1 IU/ml human menopausal gonadotropin (Pergonal; Teikoku Zoki, Tokyo, Japan), and two everted theca shells with gentle agitation in an atmosphere of 5% CO_2 in humidified air at 38.5^{o}C. The OCGCs were cultured for various time to obtain oocytes at the germinal vesicle (0 h), diakinesis (D, 18 h), metaphase I (MI, 27 h), anaphase I and telophase I (AI and TI, 30-33 h), and metaphase II (MII, 42 h) stages.

To examine the effects of the inhibition of PP1/PP2A on chromosome condensation, oocyte-cumulus complexes (OCCs) were used. The OCCs were cultured in maturation medium containing 50 nM calyculin A (CL-A; Sigma-Aldrich, Germany) or 2.5 μM okadaic acid (OA; sodium salt, Sigma-Aldrich) for 0, 0.5, 1, 2, 3, 4, and 6 h. To inhibit the activation of MAP kinase during the PP1/PP2A inhibition, the OCCs were cultured in maturation medium containing 50 nM CL-A and an MEK inhibitor, 0.1 mM U0126 (Promega, Madison, WI).

After culturing, some oocytes were mounted on slides, fixed in acetic alcohol (acetic acid: ethanol = 1: 3), and stained with 1% orcein. The chromatin and nucleolar morphology of oocytes were examined under a differential interference microscope (Optiphoto; Nikon, Tokyo, Japan). The meiotic stages of oocytes were determined based on the criteria by Motlik and Fulka (1976). Other oocytes were used for immunostaining or kinase assay.

2.2.2. Immunofluorescent Microscopy

Oocytes were collected after culture for maturation or inhibitor treatment. After oocytes were denuded and washed twice in PBS-PVA, they were fixed in PBS-PVA containing 4% (w/v) paraformaldehyde and 0.2% (v/v) Triton X-100 for 40 min. The fixed oocytes were washed twice in PBS-PVA for 15 min each and stored overnight in 1% (w/v) bovine serum albumin (BSA; International Reagents Corporation, Kobe, Japan) supplemented PBS-PVA (BSA-PBS-PVA) at 4ºC. The oocytes were blocked with 10% (v/v) goat serum (DakoCytomation A/S, Glost rup, Denmark) in BSA-PBS-PVA for 45 min, and then incubated for double labeling in a mixture of rabbit polyclonal anti-phospho-histone H3 at S10 (1:100 dilution; #9701, Cell Signaling Technology Inc., MA) and mouse monoclonal anti-lamin A/C (1:100 dilution; sc-7292, Santa Cruz Biotechnology Inc., CA) antibodies at 4ºC overnight. After being washed 3 times in BSA-PBS-PVA for 15 min each, the oocytes were incubated in the mixture of Alexa Fluor 488-labeled goat anti-rabbit IgG (1:400 dilution; Molecular Probes Inc., Eugene, OR) and Alexa Fluor 350-labeled goat anti-mouse IgG (1:400 dilution; Molecular Probes Inc.) as the conjugated second antibodies for 40 min at room temperature. After being washed 3 times in BSA-PBS-PVA for 15 min each, the chromosomes were stained with propidium iodide (400 μg/ml; Sigma Chemical Co.). Following complete washing, the oocytes were mounted on slides by Vectashield mounting medium (Vector Laboratories Inc., Burlingame, CA) and observed under a fluorescent

microscope (U-LH100HGAPO, Olympus Optical Co. Tokyo, Japan). Determination of the meiotic stages was based on the chromosome configuration described by Motlik and Fulka (1976). In the negative control, oocytes were reacted with nonimmune rabbit serum instead of rabbit polyclonal anti-phospho-histone H3 at S10 antibody, or with normal mouse IgG instead of mouse monoclonal anti-lamin A/C antibody.

2.2.3. Kinase Assay

To examine the activities of Cdc2 kinase, MAP kinase, and histone H3 kinase of pig oocytes, the phosphorylation of histone H1, myelin basic protein, and histone H3, respectively, were measured by *in vitro* kinase activity assay. Oocytes samples were collected after maturation culture or inhibitor treatment. After denudation and three washes in PBS-PVA, each group of oocytes was transferred into an Eppendorf tube with 1 μl of PBS-PVA for the double kinase assay following the technique described by Kanayama et al. (2002). To determine the meiotic stage of oocytes, they were stained with 12 μg/ml Hoechst 33342 (Polysciences Inc. Warrington, PA) for 20 min followed by observation under a fluorescent microscope. Each sample contained two oocytes for double assay of Cdc2 kinase and MAP kinase, and five oocytes for double assay of Cdc2 kinase and histone H3 kinase. Thereafter, 4 μl of ice cold extraction buffer was added, and the samples were frozen at -80^{o}C before the assay. The extraction buffer was composed of 80 mM β-glycerophosphate, 25 mM HEPES (pH 7.2), 20 mM EGTA, 15 mM $MgCl_2$, 1 mM dithiothreitol (DTT), 1 mM 4-amidinobenzylsulfonyl fluoride hydrochloride (APMSF, Sigma Chemical Co.), 0.1 mM Na_3VO_4, 1 μg/ml leupeptin (Sigma Chemical Co.), and 1 μg/ml aprotinin (Sigma Chemical Co.) (Nebreda et al., 1995). After being thawed, the oocytes were centrifuged at 10,000 *g* for 2 min at 2 ^{o}C, added with 5 μl of kinase buffer and 5 μl of substrate solution, and incubated for 20 min at 37^{o}C. The kinase buffer was composed of 75 mM HEPES (pH 7.2), 75 mM β-glycerophosphate, 75 mM $MgCl_2$, 6 mM DTT, 10 mM EGTA, 60 μM ATP, 15 μM cAMP-dependent protein kinase inhibitor peptide (Sigma Chemical Co.) and 0.3 μCi/μl [γ-^{32}P]ATP (250 μCi/25 μl, Amersham Pharmacia Biotech, UK). The substrate solution for the double assay of the Cdc2 kinase and MAP kinase was composed of 4.25 μl of histone H1 (5 mg/ml, from calf thymus; Roche Diagnostics GmbH, Mannheim, Germany), and 0.75 μl of myelin basic protein (5 mg/ml, MBP from bovine brain; Sigma Chemical Co.). The substrate

solution for the double assay of Cdc2 kinase and histone H3 kinase was composed of 2.5 µl of histone H1 and 2.5 µl of histone H3 (1 mg/ml, from calf thymus; Boehringer). The reaction was terminated by the addition of 5 µl of 4-times-concentrated SDS sample buffer (Laemmli, 1970) and boiling for 5 min. The samples were loaded onto a 15% SDS-polyacrylamide gel for separation of labelled myelin basic protein and histone H1, or histone H3 and histone H1. After running, the gels were dried and autoradiographed. The autoradiographs were scanned with an image analysis system with Image Master ID Elite software Version 3.00 (Amersham Pharmacia Biotech). The kinase activity in the oocytes at MI was arbitrarily set to 100%, and the others bands were expressed relative to that as a mean percentage ± SEM.

2.2.4. Statistical Analysis

At least 30 immunostained oocytes were examined by the immunofluorescent microscopy in each group. Each kinase assay experiment was performed at least 3 replicates. Statistical differences in the activities of the kinases were analysed by one-way ANOVA (F1-test) followed by the Tukey's multiple range test. Other values were analysed using the chi-square test. P values less than 0.05 were considered statistically significant.

2.3. RESULTS

2.3.1. Phosphorylation of Histone H3 Takes Place during Oocyte Maturation

Phosphorylated histone H3 at S10 was detected in maturing pig oocytes using the antibody against histone H3 with a single phosphorylated S10. Histone H3 phosphorylation was not detected in any oocytes at the GV stage before culture (0%, 0/41 oocytes, Fig. 2.2A"). Phosphorylation of histone H3 was first detected in the clump of condensed chromosomes (green color, Fig. 2.2B") in all of the examined oocytes (100%, 38/38 oocytes) at the diakinesis stage after 18 h of culture and thereafter it was maintained during oocyte maturation (Figs. 2.2C"-F").

The integrity of the nuclear envelope was monitored by immunostaining with the anti-lamin A/C antibody. At the GV stage, the lamin A/C antibody recognized the entire contour of the nuclear envelope (Fig. 2.2A). At the diakinesis stage, chromosomes were frequently in contact

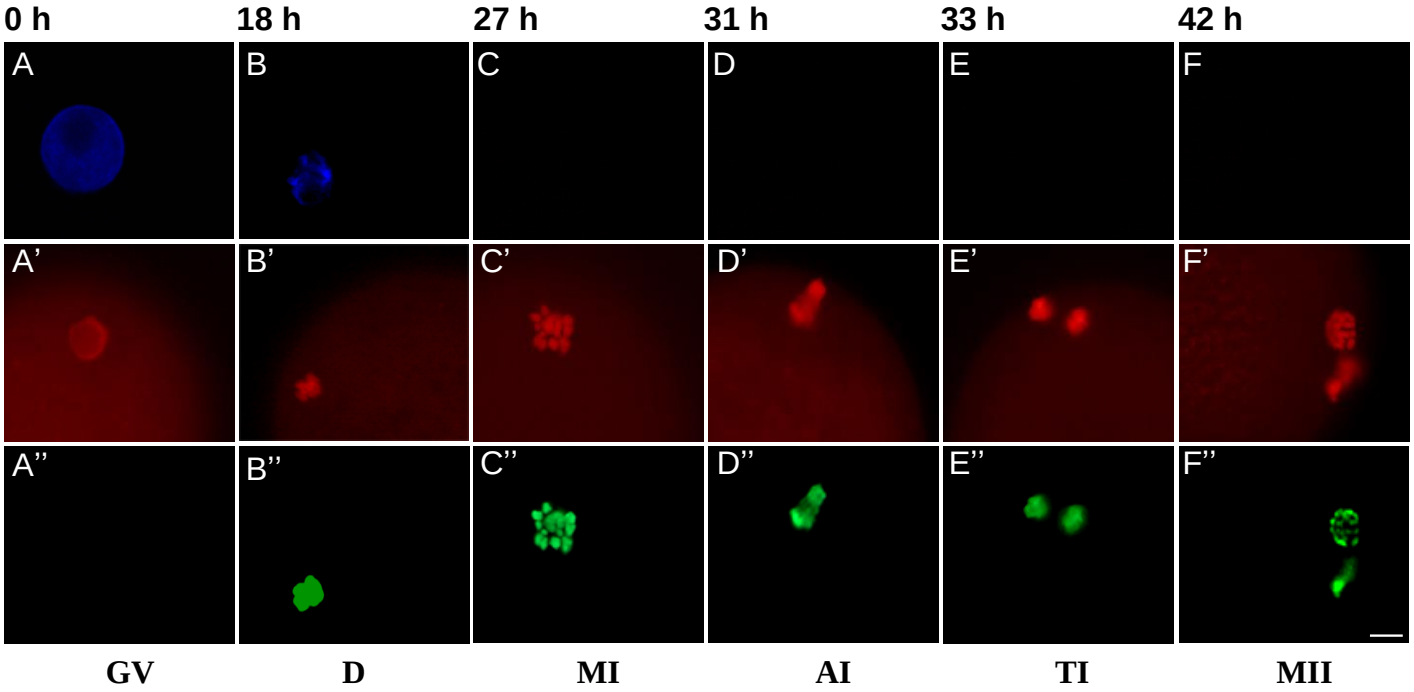

Fig. 2.2. Immunofluorescent localization of phosphorylated histone H3-S10 during maturation of pig oocytes. Anti-lamin A/C and Alexa 350-labeled antibodies stained the nuclear membrane (blue), PI stained the chromosome (red), and anti-phospho-histone H3-S10 and Alexa 488-labeled antibodies stained the phosphorylated histone H3 (green) in the same oocyte. The meiotic stages are **A**) Germinal vesicle stage (GV), **B**) Dakinesis (D), **C**) Metaphase I (MI), **D**) Anaphase I (AI), **E**) Telophase I (TI), and **F**) Metaphase II (MII). Scale bar = 10 µm.

with the envelope and lamin A/C staining was closely associated with the chromosomes (Figs. 2.2B and B'). The nuclear membrane breakdown initiated during the diakinesis stage and the nuclear membrane was completely disassembled when the oocytes entered MI (Figs. 2.2C-F). The control oocytes did not show any fluorescence at any stages.

The activities of Cdc2 kinase and MAP kinase during meiotic resumption were shown in Fig. 2.3. Following the stimulation with gonadotropin in culture medium, Cdc2 kinase activity gradually increased around GVBD at 24 h and reached a maximum level at MI at 27 h. The GV oocytes before culture had no MAP kinase activity, and this kinase became active after Cdc2 kinase activation. The changes in the activities of Cdc2 kinase and the histone H3 kinase during oocyte maturation were measured after determination of the meiotic stage of each oocyte by Hoechst 33342 (Fig. 2.4). Histone H3 kinase activity was lowest in the GV-stage oocytes, increased at the diakinesis stage, reached a peak at MI, and was maintained until MII (Fig. 2.4C). Cdc2 kinase was inactive at the GV and diakinesis stages. Thereafter, the activity increased and reached a peak at MI. The activity fell during AI and TI, and increased again at MII (Fig. 2.4B).

2.3.2. PP1/PP2A Inhibitors Induce Rapid Chromosome Condensation with Histone H3 Phosphorylation

The PP1/PP2A inhibitors induced morphological changes in chromosomes in a similar manner with normal maturation in pig oocytes. However, the time taking chromosome condensation was short. The typical chromosome morphologies of PP1/PP2A inhibitor treated oocytes were shown in Fig. 2.5.

The effects of PP1/PP2A inhibitors, CL-A and OA, on histone H3 phosphorylation, chromosome condensation, and nuclear membrane morphology were examined. Both CL-A (Fig. 2.6 and Table 2.1) and OA (Fig. 2.7 and Table 2.2) induced rapid chromosome condensation in a similar manner. Chromosomes started to condense after 2 h of treatment, but most of the chromosome configuration was still at the GVI-IV stages which were described by Motlik and Fulka for normal maturation of pig oocytes (Motlik and Fulka, 1976). Some oocytes had a chromosome configuration that looked like GVIII or GVIV, but the chromosomes were much more condensed (GV') (Fig. 2.6C' and Fig. 2.7C'). Chromosome condensation progressed throughout the treatment. After 6 h, in most of the oocytes, the condensation of the chromosomes

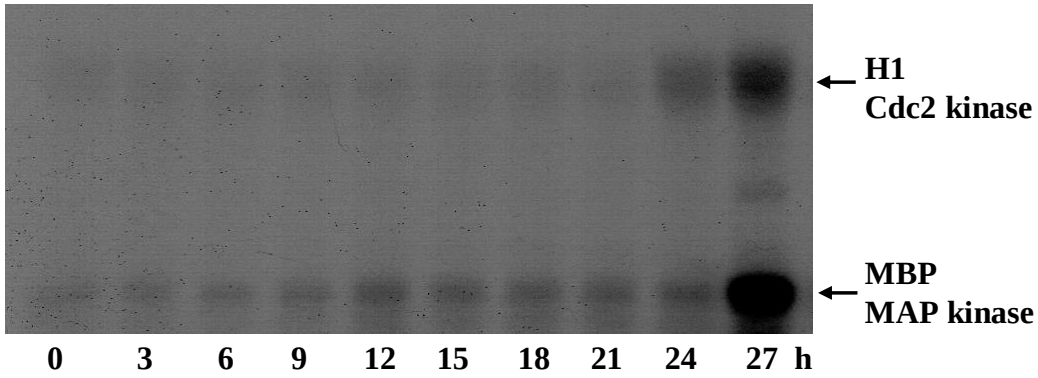

Fig. 2.3. The autoradiograph showing the changes in Cdc2 kinase and MAP kinase activities during meiotic resumption of pig oocytes. Histone H1 (H1) and myelin basic protein (MBP) were used for the substrates of Cdc2 kinase and MAP kinase, respectively. The lower figures present the hours of maturation culture.

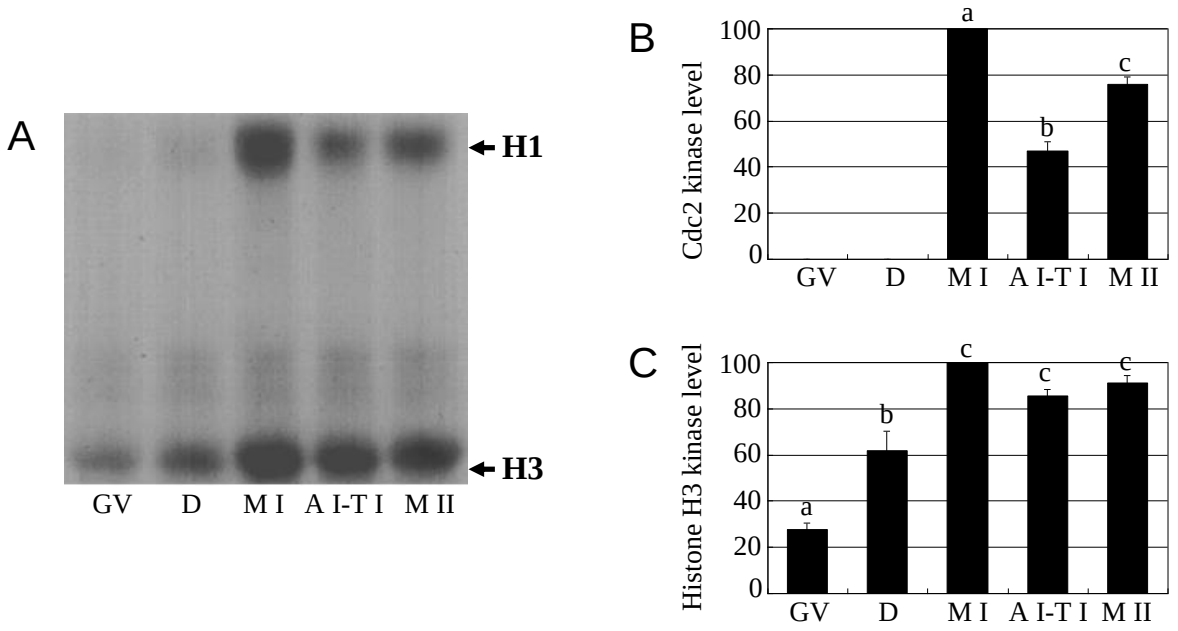

Fig. 2.4. A) The autoradiograph showing the changes in Cdc2 kinase and histone H3 kinase activities during maturation of pig oocytes. Histone H1 (H1) and histone H3 (H3) were used for the substrates of Cdc2 kinase and histone H3 kinase, respectively. **B**, **C**) The intensity of each phosphorylated histone H1 and histone H3 were measured by densitometry analysis of blots. The data are represented as the mean ± SEM. The lower figures of the graphs show the meiotic stages of oocytes as presented in the legend for Fig. 2.2. The experiments were conducted three times. Values with different superscripts were significantly different ($P<0.05$).

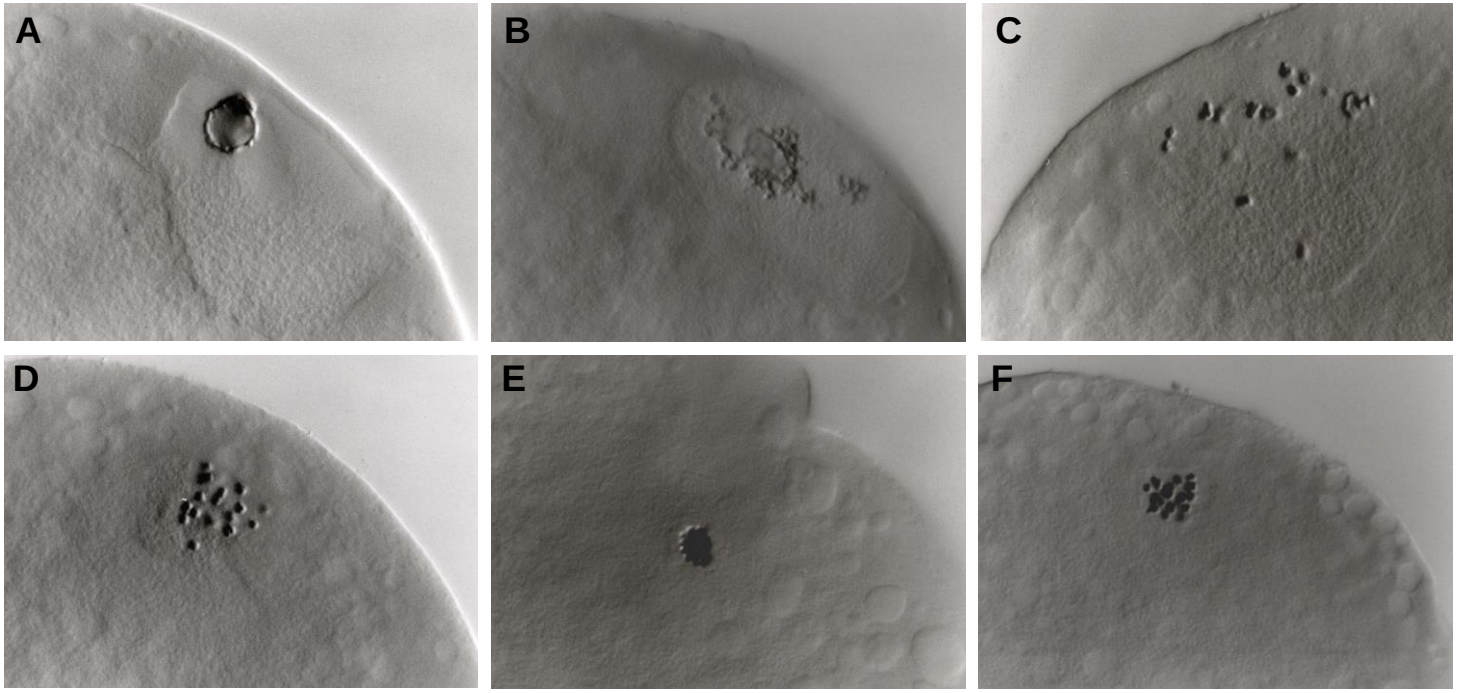

Fig. 2.5. The typical chromosome morphologies of PP1/PP2A inhibitor-treated oocytes. Each treated oocyte was fixed in acetic alcohol (1/3, v/v), stained with 1% orcein, and examined under a differential interference microscope. Chromosome configurations of oocytes were classified as described by Motlik and Fulka (1976). **A)** Germinal vesicle stage I (GVI), **B)** Condensing chromosomes like in GVIII stage, **C)** Condensing chromosomes like in GVIV stage, **D)** Condensed chromosomes like in early diakinesis stage (ED), **E**) Condensed chromosomes like in late diakinesis stage (LD), and **F**) Condensed chromosomes like in metaphase I (MI).

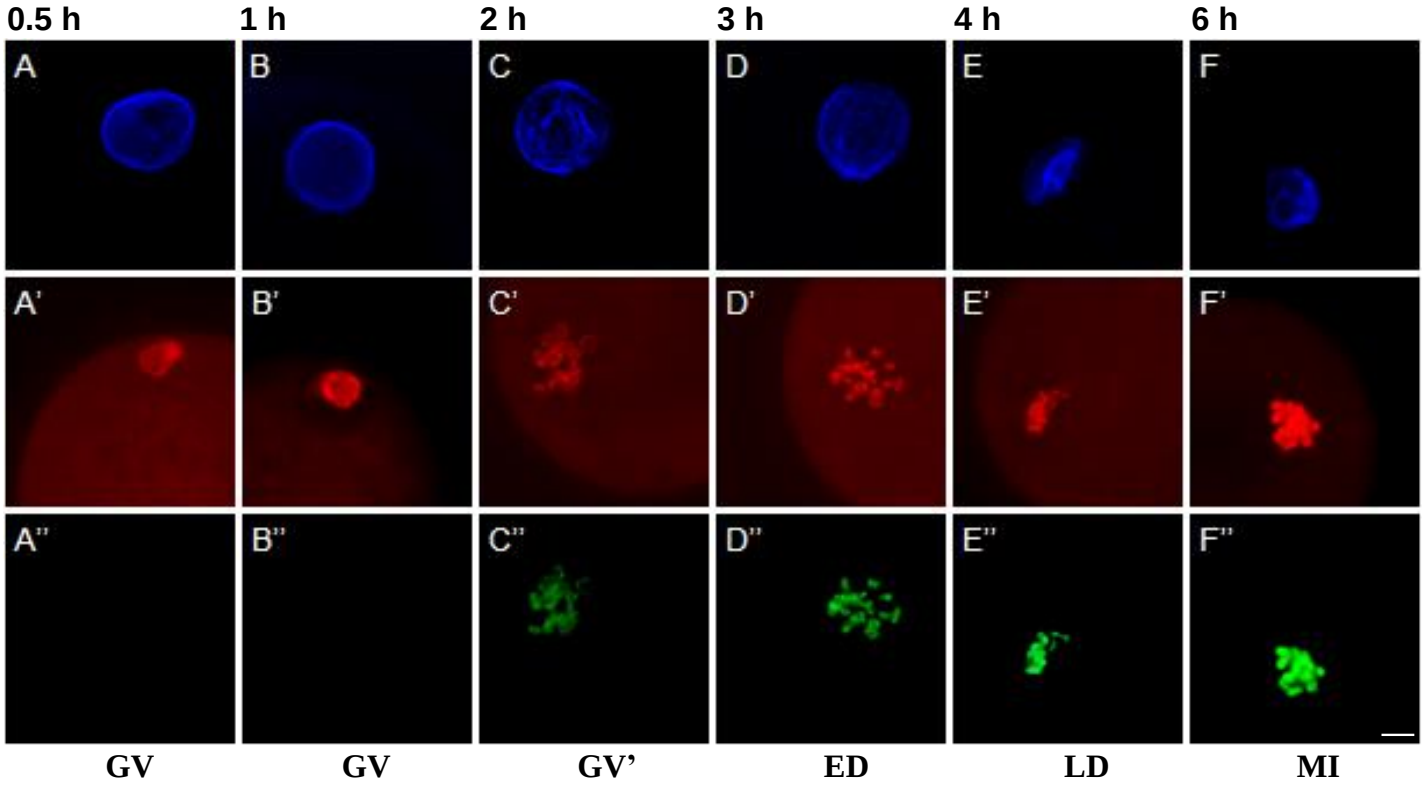

Fig. 2.6. Effect of calyculin A (CL-A) on histone H3 phosphorylation, chromosome configuration, and nuclear membrane morphology of pig oocytes. Each treated oocyte with different time was stained with anti-lamin A/C and Alexa 350-labeled antibodies for the nuclear membrane (blue), PI for the chromosome (red), and anti-phospho-histone H3-S10 and Alexa 488-labeled antibodies for phosphorylated histone H3 (green). **A**, **B**) Germinal vesicle stage (GV), **C**) Chromosomes starting to condense with phosphorylated histone H3 (GV'), **D**) Early diakinesis stage (ED), **E**) Late diakinesis stage (LD), and **F**) Chromosomes condensed like in metaphase I (MI). Scale bar = 10 μm.

Table 2.1. Effects of calyculin A on chromosome condensation in pig oocytes

Time of treatment (h)	CL-A (50 nM)	No. of oocytes examined	No. (%) of oocytes underwent GVBD	No. (%) of oocytes had phosphorylated histone H3	No. (%) of oocytes at stage of					No. (%) of oocytes degenerated
					GVI-IV	GV'	ED	LD	MI	
0		35	0 (0)[a]	0 (0)[a]	35 (100)[a]	0 (0)[a]	0 (0)[a]	0 (0)[a]	0 (0)[a]	0 (0)
0.5		27	0 (0)[a]	0 (0)[a]	27 (100)[a]	0 (0)[a]	0 (0)[a]	0 (0)[a]	0 (0)[a]	0 (0)
1		32	0 (0)[a]	0 (0)[a]	32 (100)[a]	0 (0)[a]	0 (0)[a]	0 (0)[a]	0 (0)[a]	0 (0)
2	–	30	0 (0)[a]	0 (0)[a]	29 (97)[a]	0 (0)[a]	0 (0)[a]	0 (0)[a]	0 (0)[a]	1 (3)
3		28	0 (0)[a]	0 (0)[a]	28 (100)[a]	0 (0)[a]	0 (0)[a]	0 (0)[a]	0 (0)[a]	0 (0)
4		33	0 (0)[a]	0 (0)[a]	33 (100)[a]	0 (0)[a]	0 (0)[a]	0 (0)[a]	0 (0)[a]	0 (0)
6		32	0 (0)[a]	0 (0)[a]	31 (97)[a]	0 (0)[a]	0 (0)[a]	0 (0)[a]	0 (0)[a]	1 (3)
0.5		28	0 (0)[a]	0 (0)[a]	28 (100)[a]	0 (0)[a]	0 (0)[a]	0 (0)[a]	0 (0)[a]	0 (0)
1		30	0 (0)[a]	0 (0)[a]	30 (100)[a]	0 (0)[a]	0 (0)[a]	0 (0)[a]	0 (0)[a]	0 (0)
2	+	27	0 (0)[a]	15 (56)[b]	12 (44)[b]	9 (33)[b]	3 (11)[a]	3 (11)[a]	0 (0)[a]	0 (0)
3		28	0 (0)[a]	25 (89)[c]	1 (4)[c]	4 (14)[ab]	10 (36)[b]	9 (32)[b]	2 (7)[ab]	2 (7)
4		30	0 (0)[a]	29 (97)[c]	0 (0)[c]	2 (7)[a]	4 (13)[a]	17 (57)[c]	6 (20)[b]	1 (3)
6		32	21 (66)[b]	32 (100)[c]	0 (0)[c]	0 (0)[a]	2 (6)[a]	4 (12)[a]	26 (81)[c]	0 (0)

Oocytes at the GV stage were cultured with or without calyculin A (CL-A) for different time. Histone H3 phosphorylation, chromosome configuration, and nuclear membrane morphology were evaluated by the fluorescent microscopy. GVI-IV, germinal vesicle I to IV stage as defined by Motlik and Fulka (1976). GV', chromosomes start to condense with phosphorylated histone H3. ED, early diakinesis stage. LD, late diakinesis stage. MI, chromosomes condensed like those at metaphase I.

[a-c)] Values with different superscripts in the same column differ significantly ($P<0.05$).

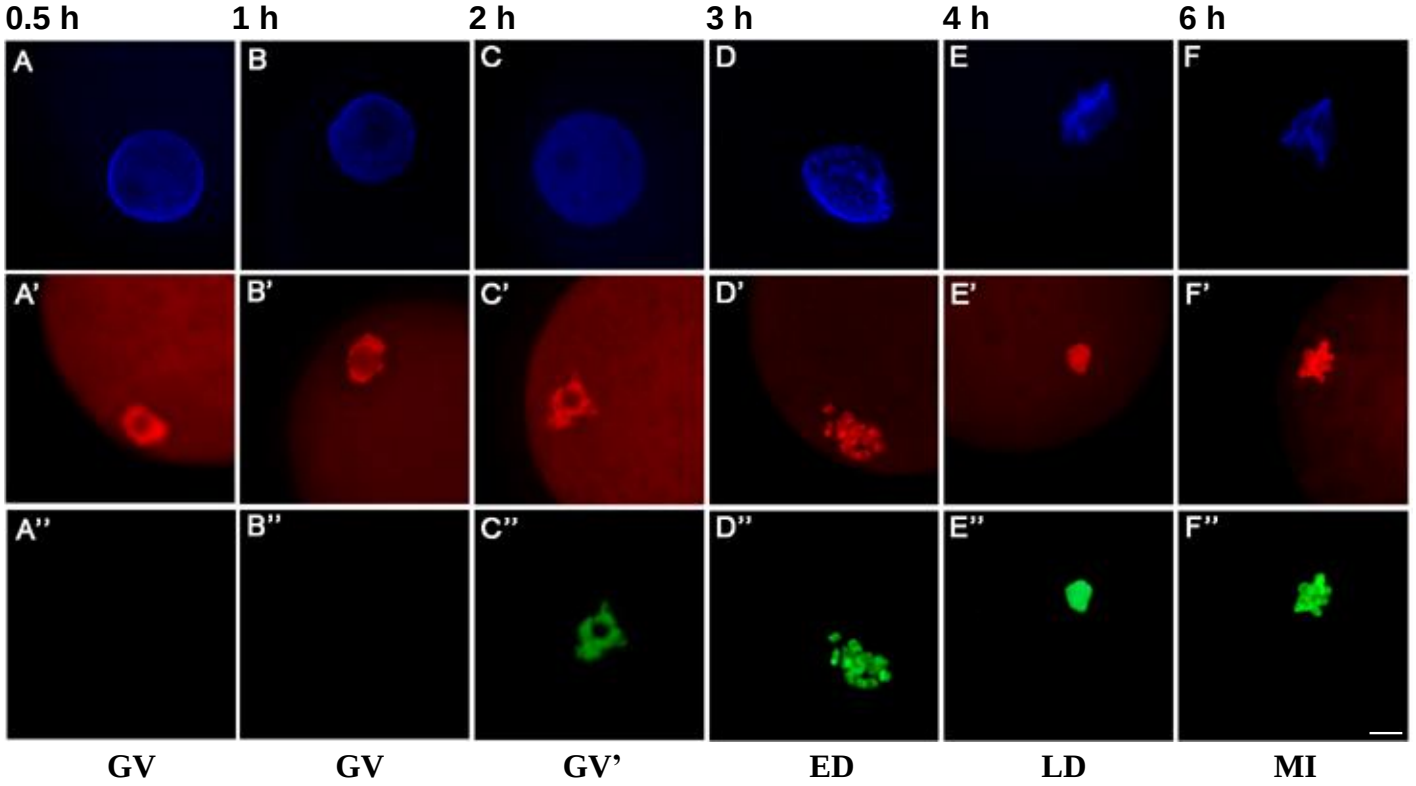

Fig. 2.7. Effect of okadaic acid (OA) on histone H3 phosphorylation, chromosome configuration, and nuclear membrane morphology of pig oocytes. Each treated oocyte with different time was stained with anti-lamin A/C and Alexa 350-labeled antibodies for the nuclear membrane (blue), PI for the chromosome (red), and anti-phospho-histone H3-S10 and Alexa 488-labeled antibodies for the phosphorylated histone H3 (green). Panels show the identical stages of oocytes as presented in the legend for Fig. 2.6. Scale bar = 10 μm.

Table 2.2. Effects of okadaic acid on chromosome condensation in pig oocytes

Time of treatment (h)	OA (2.5 μM)	No. of oocytes examined	No. (%) of oocytes underwent GVBD	No. (%) of oocytes had phosphorylated histone H3	No. (%) of oocytes at stage of					No. (%) of oocytes degenerated
					GVI-IV	GV'	ED	LD	MI	
0		32	0 (0)	0 (0)[a]	32 (100)[a]	0 (0)[a]	0 (0)[a]	0 (0)[a]	0 (0)[a]	0 (0)
0.5		33	0 (0)	0 (0)[a]	33 (100)[a]	0 (0)[a]	0 (0)[a]	0 (0)[a]	0 (0)[a]	0 (0)
1		31	0 (0)	0 (0)[a]	31 (100)[a]	0 (0)[a]	0 (0)[a]	0 (0)[a]	0 (0)[a]	0 (0)
2	–	34	0 (0)	0 (0)[a]	34 (100)[a]	0 (0)[a]	0 (0)[a]	0 (0)[a]	0 (0)[a]	0 (0)
3		36	0 (0)	0 (0)[a]	35 (97)[a]	0 (0)[a]	0 (0)[a]	0 (0)[a]	0 (0)[a]	1 (3)
4		30	0 (0)	0 (0)[a]	30 (100)[a]	0 (0)[a]	0 (0)[a]	0 (0)[a]	0 (0)[a]	0 (0)
6		32	0 (0)	0 (0)[a]	32 (100)[a]	0 (0)[a]	0 (0)[a]	0 (0)[a]	0 (0)[a]	0 (0)
0.5		31	0 (0)	0 (0)[a]	31 (100)[a]	0 (0)[a]	0 (0)[a]	0 (0)[a]	0 (0)[a]	0 (0)
1		30	0 (0)	0 (0)[a]	30 (100)[a]	0 (0)[a]	0 (0)[a]	0 (0)[a]	0 (0)[a]	0 (0)
2	+	30	0 (0)	28 (93)[b]	0 (0)[b]	21 (70)[b]	2 (7)[a]	3 (10)[ab]	2 (7)[a]	2 (7)
3		31	0 (0)	31 (100)[b]	0 (0)[b]	3 (10)[a]	10 (32)[b]	14 (45)[c]	4 (12)[a]	0 (0)
4		33	0 (0)	31 (94)[b]	0 (0)[b]	0 (0)[a]	1 (3)[a]	18 (54)[c]	12 (36)[b]	2 (6)
6		34	0 (0)	33 (97)[b]	0 (0)[b]	0 (0)[a]	1 (3)[a]	8 (23)[b]	24 (71)[c]	1 (3)

Oocytes at the GV stage were cultured with or without okadaic acids (OA) for different time. Histone H3 phosphorylation, chromosome configuration, and nuclear membrane morphology were evaluated by the fluorescent microscopy. The meiotic stages are same as presented in Table 2.1.

[a-c)] Values with different superscripts in the same column differ significantly ($P<0.05$).

was like that at MI (81% in the CL-A, and 71% in the OA treated oocytes).

Histone H3 started to be phosphorylated after 2 h in 56% and 93% of the CL-A and OA treated oocytes, respectively. After 3 h, most of the treated oocytes showed histone H3 phosphorylation, which was maintained during the course of treatment. In the non-treated oocytes, the chromosomes stayed in the GV, and no histone H3 phosphorylation was observed during the culture. In all of the CL-A and OA treated oocytes, an intact nuclear membrane was observed around the condensed chromosomes until 4 h. At 6 h, 66% of the CL-A treated oocytes underwent GVBD, while no OA treated oocytes underwent GVBD (Tables 2.1 and 2.2). However, 100% of the OA treated oocytes underwent GVBD after 8 h (data not shown).

2.3.3. Change in the Activities of Cdc2 Kinase, MAP Kinase, and Histone H3 Kinase during Chromosome Condensation in CL-A and OA Treated Oocytes

When the oocytes were treated with CL-A, both histone H3 kinase (shown by phosphorylation of histone H3 in Fig. 2.8A) and MAP kinase (shown by phosphorylation of MBP in Fig. 2.8A) were activated after 2 h, and the activities increased during the time of treatment. Cdc2 kinase (shown by phosphorylation of H1 in Fig. 2.8A) was not activated until 6 h. In the control non-treated oocytes, Cdc2 kinase, MAP kinase, and histone H3 kinase were not activated. The oocytes treated with OA also showed a similar result with the CL-A treated oocytes (data not shown). These results indicate that the PP1/PP2A inhibitors induce activation of both MAP kinase and histone H3 kinase, although they have no effect on Cdc2 kinase.

To investigate whether MAP kinase activation is required for the phosphorylation of histone H3, the oocytes were treated with CL-A in the presence of the MAP kinase inhibitor U0126. In the oocytes, MAP kinase was not activated, but the histone H3 kinase was still activated after 2 h of treatment (Fig. 2.8). There were no difference between the histone H3 kinase levels of oocytes treated with CL-A and CL-A+U0126. Histone H3 phosphorylation and chromosome condensation in the oocytes were also examined after 6 h of treatment (Table 2.3). The histone H3 phosphorylation and chromosome condensation in the oocytes treated with CL-A and CL-A+U0126 was similar. However, no GVBD was observed in the CL-A+U0126 treated oocytes.

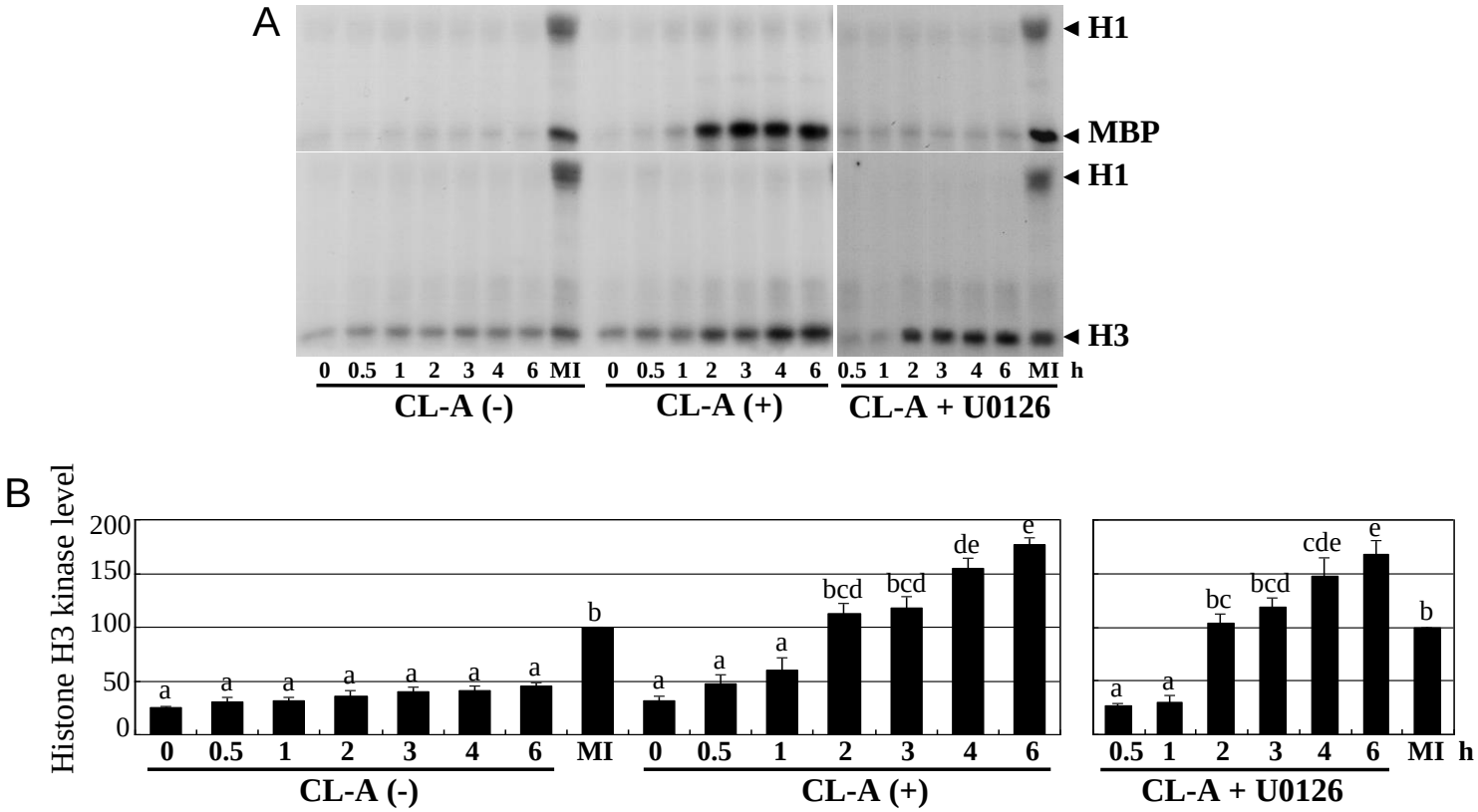

Fig. 2.8. A) Autoradiographs showing effects of calyculin A (CL-A) and MAP kinase inhibitor U0126 on the activities of Cdc2 kinase, MAP kinase, and histone H3 kinase in pig oocytes. Histone H1 (H1), myelin basic protein (MBP), and histone H3 (H3) were used for the substrates of Cdc2 kinase, MAP kinase, and histone H3 kinase, respectively. Samples were subjected to the double kinase assay of H1/MBP or H1/H3 to examine the change in the activities of Cdc2 kinase, MAP kinase, and histone H3 kinase in the oocytes treated with (+) or without (–) the CL-A, and CL-A and MAP kinase inhibitor U0126. **B**) The intensity of phosphorylated histone H3 was measured by densitometry analysis of blots. The activities of histone H3 kinase in MI oocytes were set to 100%. The data represent the histone H3 kinase activities as the mean ± SEM. Values with different superscripts are significantly different ($P<0.05$). The experiments were conducted three times with similar results.

Table 2.3. Effects of MAP kinase inhibitor, U0126 on chromosome condensation induced by calyculin A in pig oocytes

Treatment	No. of oocytes examined	No. (%) of oocytes underwent GVBD	No. (%) of oocytes had phosphorylated histone H3	No. (%) of oocytes at stage of					No. (%) of oocytes degenerated
				GVI-IV	GV'	ED	LD	MI	
-	60	0 (0)[a]	0 (0)[a]	60 (100)[a]	0 (0)[a]	0 (0)[a]	0 (0)[a]	0 (0)[a]	0 (0)
CL-A	57	34 (60)[b]	55 (96)[b]	1 (2)[b]	0 (0)[a]	3 (5)[a]	8 (15)[b]	44 (77)[b]	1 (2)
CL-A+U	59	0 (0)[a]	54 (91)[b]	3 (5)[b]	3 (5)[a]	1 (2)[a]	11 (18)[b]	39 (66)[b]	2 (3)

Oocytes at the GV stage were treated with calyculin A (CL-A) and U0126 (U) for 6 h. Histone H3 phosphorylation, chromosome configuration, and nuclear membrane morphology were evaluated by the fluorescent microscopy. The meiotic stages are same as presented in Table 2.1.

[a,b)] Values with different superscripts in the same column differ significantly ($P<0.05$).

2.4. DISCUSSION

The results showed that the phosphorylation of histone H3 at S10 occured in condensed chromosomes during maturation in pig oocytes. Furthermore, the chromosome condensation is correlated with histone H3 kinase activity, but not with Cdc2 kinase and MAP kinase activities.

Pig oocytes underwent GVBD in a similar time-course required to activate the Cdc2 kinase. Following the gonadotropic stimulation, pig oocytes start to accumulate cyclin B1 at 21 h, and Cdc2 kinase activity gradually increases around GVBD at 24 h and reaches a maximal level at MI at 27 h (Miyano and Lee, 2001). Pig oocytes have MAP kinase in the inactive form before the resumption of the meiosis, and the MAP kinase becomes phosphorylated and activated after GVBD (Inoue et al., 1998; Lee et al., 2000). It has been reported that the phosphorylation of histone H3 in the nucleosome is closely linked to mitotic chromosome condensation, and occurs at the S10 position in diverse organisms (Strahl and Allis, 2000; Hans and Dimitrov, 2001). I determined the phosphorylation of histone H3-S10 in maturing pig oocytes. There was no phosphorylation of histone H3 in the oocytes at the GV stage (G2 phase in cell cycle), and phosphorylation started in condensed chromosomes at the diakinesis stage. This observation differs from that of mitotic chromosomes in somatic cells, where phosphorylated histone H3-S10 is first detected in pericentromeric heterochromatin in the late G2 phase, spreads throughout the chromosomes, completes in late prophase and is maintained through metaphase (Hendzel et al., 1997). Thus, the meiotic phosphorylation of histone H3-S10 appears late at the time at which the chromosomes have become highly condensed. During the meiosis in the maize, the phosphorylation of histone H3-S10 also takes place at the diakinesis-metaphase I transition (Kaszas and Cande, 2000). In mitosis in animal cells and meiosis in the maize, histone H3-S10 phosphorylation is diminished in anaphase (AI in meiosis), and disappears at telophase (TI) (Hendzel et al., 1997; Kaszas and Cande, 2000). On the other hand, the phosphorylation of histone H3-S10 in pig oocytes was maintained until MII, even in AI and TI. The activity of histone H3 kinase in pig oocytes showed a similar change to the phosphorylation of histone H3-S10 in the present study. It increased the activity at the diakinesis stage, and maintained high activity until MII. This indicates the active histone H3 kinase perhaps phosphorylates histone H3 at the S10 residue in condensed chromosomes in pig oocytes during maturation.

PP1/PP2A is implicated in regulating meiosis in starfish and *Xenopus* oocytes (Picard et al., 1989; Rime et al., 1990). PP1/PP2A has recently been shown to exist in mouse oocytes, and their relocation and activity change are detected during oocyte maturation (Smith et al., 1998). PP1/PP2A has also been suggested to play a role in regulating chromosome condensation in mouse oocytes (Gavin et al., 1991) and mouse mammary cells (Guo et al., 1995). Histone H3 phosphorylation at both S10 and S28 are governed by Aurora-B kinase and PP1 in mammalian somatic cells (Murnion and Adams, 2001; Goto et al., 2002). In somatic cells, PP1 was reported to be phosphorylated and inactivated by Cdc2 kinase (Kwon et al., 1997). Goto et al. (2002) also suggested that Cdc2 kinase may play central roles in mitosis-specific chromosome condensation through the regulation of histone H3-S28 phosphorylation by the inactivation of PP1. The present study showed that activation of Cdc2 kinase was not required for either chromosome condensation or histone H3 phosphorylation in pig oocytes, since CL-A and OA induced chromosome condensation and histone H3 phosphorylation without the activation of Cdc2 kinase. This finding is consistent with the recent report showing that Cdc2 kinase is not required for chromosome condensation in pig oocytes treated with OA and butyrolactone I (an inhibitor of Cdks) (Kubelka et al., 2002).

It has been suggested that the MAP kinase cascade induces histone H3 phosphorylation at S10 (Sassone-Corsi et al., 1999). It has been shown that the ERKs-activated Rsk-2 kinase is directly involved in histone H3 phosphorylation in mouse (Chadee et al., 1999) and human fibroblasts (Sassone-Corsi et al., 1999). However, the involvement of MAP kinase in chromosome condensation is controversial. In mouse spermatocyte experiments, it was suggested that ERK1 was specifically activated during G2/M transition and was essential for chromosome condensation (Sette et al., 1999). In *Xenopus* oocyte experiments, it was suggested that histone H3 kinase activation which concerned chromosome condensation during oocyte meiotic maturation did not require Cdc2 kinase activation, but rather depended on activation of the MAPK/p90^{Rsk} pathway (Schmitt et al., 2002). Experiments in pig oocytes suggested that the inhibition of protein phosphatase promptly activated MAP kinase, which in turn induced premature chromosome condensation (Sun et al., 2002). In disagreement with these results, a recent study suggested that activation of the ERK1/p90^{Rsk} pathway was not necessary for the phosphorylation of H3 *in vivo* in mouse spermatocytes (Di Agostino et al., 2002). In fact,

PP1/PP2A inhibitors induce rapid chromosome condensation concomitantly with MAP kinase activation in mouse and pig oocytes (Lu et al., 2002; Sun et al., 2002). Numerous observations suggest that PP2A plays an important role in the downregulation of the Ras/MAP kinase pathway (Millward et al., 1999). PP2A dephosphorylates and inactivates MAP kinase kinase (MEK) and MAP kinase *in vitro* (Sontag et al., 1993). Therefore, OA or CL-A perhaps inhibited PP2A and induced MAP kinase activation in the present experiments. In a similar time course, CL-A and OA treated pig oocytes showed chromosome condensation accompanied by the activation of both MAP kinase and histone H3 kinase. However, even after the activity of MAP kinase was inhibited in the oocytes, the chromosomes condensed, histone H3-S10 was phosphorylated, and histone H3 kinase was activated. These results suggest that MAP kinase is not required for the chromosome condensation.

The disassembly of nuclear lamina is an essential prerequisite for GVBD (Gerace and Burke, 1988). Active Cdc2 kinase phosphorylates lamins on specific serine residues and causes nuclear lamina disassembly (Peter et al., 1990). It is thought that oocyte GVBD is induced by active Cdc2 kinase. When pig oocytes were treated with PP1/PP2A inhibitors in this experiment, the oocytes underwent GVBD after 6-8 h. Cdc2 kinase was not activated during the culture period, but MAP kinase was activated in the oocytes after 2 h of treatment. Since MAP kinase has a weak activity to phosphorylate nuclear lamins (Peter et al., 1992), MAP kinase is supposed to substitute for the role of Cdc2 kinase in GVBD in the oocytes. Actually, when oocytes were treated with an MEK inhibitor and CL-A, MAP kinase activation was completely inhibited. In the oocytes, CL-A did not induce GVBD at all, while chromosome condensation occurred in the GV. Under our normal maturational conditions, the Cdc2 kinase of oocytes was still inactive at the diakinesis stage, and these oocytes had a nuclear membrane. However, the chromosomes were highly condensed with their histone H3 phosphorylation, and histone H3 kinase was activated in the diakinesis stage. Together with the above results, these data suggest that the activation of Cdc2 kinase is required for nuclear membrane breakdown, but not for chromosome condensation in the pig oocytes.

In the present study, the change in histone H3 kinase activity accurately corresponded with histone H3 phosphorylation at S10 in pig oocytes and chromosome condensation. Histone H3 phosphorylation was detected in the clump of condensed chromosomes at the diakinesis stage and

maintained during maturation of the oocytes. Histone H3 was also phosphorylated in condensed chromosomes in the inhibitor-treated oocytes. Furthermore, the chromosome condensation occurred without GVBD in the absence of the activation of both Cdc2 kinase and MAP kinase, but was accompanied by histone H3 kinase activation. Although we did not identify histone H3 kinase in pig oocytes, accumulating data reveal that Aurora-B is required for mitotic histone H3-S10 phosphorylation in *Drosophila* and mammals (Giet and Glover, 2001; Crosio et al., 2002), and Aurora-B is a mitotic histone H3 kinase in humans (Sugiyama et al., 2002). Goto et al. (2002) reported that Aurora-B phosphorylated histone H3 at both S10 and S28 during mitosis in mammalian somatic cells. In both yeasts and nematodes, the reduction of PP1 activity is responsible for histone H3 phosphorylation interacting with Aurora kinase (Hsu et al., 2000). Sugiyama et al. (2002) have suggested that human Aurora-B is a mitotic histone H3 kinase which associated protein phosphatases (PP1 or PP2A) as negative regulators of kinase activation. Moreover, chromatin-associated PP1 regulates Aurora-B activity and histone H3 phosphorylation (Murnion et al., 2001). Based on these findings and the present results, I propose that a balance of histone H3 kinase and PP1/PP2A activities regulates the meiotic phosphorylation of histone H3, and that the PP1/PP2A inhibition induces histone H3 phosphorylation, leading to chromosome condensation in pig oocytes.

Chapter 3. Histone H3 Modifications during Oocyte Growth, Maturation, and Activation

3.1. INTRODUCTION

As revealed in Chapter 2, histone H3-S10 is phosphorylated in condensed chromosomes in pig oocytes during maturation. The chromosome condensation is correlated with the histone H3 kinase activity, but not with Cdc2 kinase and MAP kinase activities. In addition, it was suggested that the histone modifications affect chromatin structure directly. A body of recent findings showing how histone modifications exert their biological effects lead to the theory in which site-specific histone modifications might influence chromatin function through two mechanisms: first, by affecting nucleosome-nucleosome interactions that control the folding of nucleosomal arrays; second, by recruiting and interacting with docking proteins or complexes that remain to be identified (Strahl and Allis 2000; Jaskelioff and Peterson, 2003). Thus, histone modifications provide means to recruit enzymes that disrupt chromatin structure or to recruit proteins, such as heterochromatin protein 1 (HP1), that further package the chromatin fiber into inaccessible states. It is necessary to elucidate how the histone modifications were involved in chromatin/ chromosome morphology during oocyte growth, maturation and activation of mammalian oocytes.

The sites for post-translational modifications are clustered within the first 30 amino acids of core histones. Histone H3 is acetylated at lysines (K) 9, 14, 18, and 23, phosphorylated at serines (S) 10 and 28, and methylated at K4 and K9 (Cheung et al., 2000a). The juxtaposition of these sites provides potential cross regulation of different modificational events. Several reports have described that modification at one site can influence modification of the second site. For example, histone H3 phosphorylation at S10 facilitates acetylation of K14 (Cheung et al., 2000b), but inhibits methylation of K9 *in vitro* (Lachner et al., 2001). Vice versa, methylation of H3 at K9 prevents phosphorylation of S10 (Rea et al., 2000).

Methylation of H3 at K9 creates a high-affinity binding site for the HP1 (Lachner et al., 2001). Heterochromatin mediates diverse functions in the cell nuclei, including centromere

function, gene silencing and nuclear organization. The decision to silence or active heterochromatic genes appears to be the result of a balance between negative factors that promote the formation of the condensed higher-order chromatin structure, and positively acting transcription factors that bind to regulatory sequences to active gene expression. Histone H3-K9 methylation is associated with long-term transcriptional repression as a stable modification through recruitment of HP1 (Jaskelioff and Peterson, 2003; Mateescu et al., 2004). There is growing evidence that HP1 protein can associate with the DNA methyltransferase activity (Bachman et al., 2001). In the mammalian oogenesis, a set of imprinted genes become methylated. Lucifero et al. (2004) showed that the DNA methylation acquisition was related to oocyte growth and coincided with the accumulation of methyltransferase transcripts in the mouse and human. However, there is no evidence for histone methylation during growing stage in mammalian oocytes.

Pig oocytes in primordial follicles are 30 μm in diameter and grow to their final size of 120-125 μm. Non-growing oocytes in primordial follicle are transcriptionally quiescent. When the oocytes enter the growth phase, transcription is initiated and ribosome-synthesizing nucleoli are established. Towards the end of the oocyte growth phase, these biological processes cease, and oocytes acquire the full meiotic competence to mature and to be fertilized (Fair et al., 1997). Chromatin in growing oocytes from early antral follicle is filamentous. Chromatin becomes thicker and with stringy configuration, then forms a condensed chromatin ring around the nucleolus. However, little is known about the molecular changes in oocyte chromatin during the growth phase. It has been shown in somatic cells that acetylation of histones is important in both the chromatin remodeling and transcription. Histone acetylation has been proposed as a potential inherited epigenetic marker, as the acetylation of histone H3 and H4 persists during the mitotic phase (Kruhlak et al., 2001). When histones become deacetylated, the chromatin is packed, and the packing of chromatin probably limits the accessibility of many regulatory factors to DNA sequence. On the contrary, histone acetylation promotes transcription factor access to nucleosomal DNA (Struhl et al., 1998). Therefore, acetylation status of histones not only alters the transcriptional activity, but also affects the configuration of chromatin. Although it has been suggested that histone acetylation plays important roles during mitosis, little is known about its involvement in meiosis. In addition, there is no evidence of histone acetylation in growing

oocytes that have the intense transcriptional activity.

The mitotic cell cycle-dependent phosphorylation of histone H3 at S10 is conserved in eukaryotes. This dynamic post-translational modification has been linked to transcriptional activation (Sassone-Corsi et al., 1999) and to chromosome condensation and segregation (Hans and Dimitrov, 2001). It is suggested that in mammals, mitotic phosphorylation of histone H3-S10 initiates in pericentromeric heterochromatin in late G2 interphase cells (Hendzel et al., 1997; Van Hooser et al., 1998). On the other hand, meiotic phosphorylation of H3-S10 was first detected in a clump of condensed chromosomes at early prometaphase and not in the condensing chromosome in pig oocytes (in Chapter 2). This implies that other histone modifications possibly occurs when the chromosomes start to condense in the oocytes. It has been reported that during mitosis in mammals histone H3 is phosphorylated not only at S10 but also at S28, and that Aurora-B kinase directly phosphorylates H3 at both serine positions (Goto et al., 2002; Sugiyama et al., 2002). Goto et al. showed that histone H3-S28 phosphorylation occurred in prophase but not during the late G2 phase. It has not been known whether H3-S28 modification occurs during maturation in mammalian oocytes and how it is involved in the chromosome condensation.

After maturation, oocytes are arrested at metaphase of the second meiosis. Upon fertilization, oocytes resume meiosis and complete the second meiotic division. The second polar body extrudes, the female chromosome and sperm chromatin decondense, and two pronuclei are formed. Shortly after their formation, DNA replication is initiated in the pronuclei. Therefore, it needs to clarify whether the changes in histone H3 modifications such as dephosphorylation, methylation, and acetylation occurs during the chromatin/chromosome decondensation and initiation of DNA replication after activation of pig oocytes.

Generally, histone modifications in relation to the change of chromatin/chromosome morphology during meiosis of mammalian oocytes have not been understood. Especially, there is no evidence of the relationship between histone modifications and chromatin morphology during growth phase of mammalian oocytes. In this chapter, the focus was to find out the correlation between morphology of chromatin/chromosome and histone H3 phosphorylation, acetylation, and methylation in pig oocytes. For that purpose, first, chromatin and nucleolus morphology and histone H3 modifications were examined in growing pig oocytes. Next, histone H3 modifications were examined during oocyte maturation, and then change in chromatin/chromosome

morphology in relation to histone H3 modifications was examined in electro-activated MII oocytes. Finally, the relation of different types of histone H3 modifications during meiosis of pig oocytes will be discussed.

2. MATERIALS AND METHODS

3.2.1. Collection of Growing Pig Oocytes

Growing oocytes were collected from follicles at various diameters in pig ovaries. Follicles 3-6 mm in diameter were collected in the same manner described in Section 2.2.1. To collect small follicles between 0.1-3 mm in diameter, cortical slices (0.5-3 mm thickness) were cut from ovarian surface by using a surgical blade (No. 21) and a pair of forceps. Under a microscope, preantral and antral follicles were dissected from the cortices and the tissues surrounding the follicles were torn off. Follicles with different sizes were classified into five groups according to their diameter: I: 0.1-0.2 mm, II: 0.5-1 mm, III: 1-2 mm, IV: 2-3 mm, V: 3-4 mm, and VI: 4-6 mm. From the follicles of 0.1-3 mm in each class, oocytes-granulosa cell complexes were collected with a pair of fine forceps and a needle (25G) in 25 mM HEPES buffered TCM-199 containing 0.1% (w/v) PVA (HEPES-199). From the each class of follicles larger than 3 mm, oocyte-cumulus complexes were collected as described in Section 2.2.1. Oocytes from different sized follicles were denuded of cumulus cells or granulosa cells by a small-bore pipet. Then the diameters of the oocytes (excluding zona pellucida) were measured with an ocular micrometer (Olympus, Tokyo, Japan) attached to an inverted microscope.

Some oocytes in each follicle class were mounted on slides, fixed in acetic alcohol (acetic acid: ethanol = 1: 3), and stained with 1% orcein. The chromatin and nucleolar morphology of oocytes were examined under a differential interference microscope (Optiphoto; Nikon, Tokyo, Japan). Other oocytes were used for immunostaining and kinase assay.

3.2.2. Oocyte Maturation and Activation

Oocyte-cumulus-granulosa cell complexes (OCGCs) collected from follicles 4-6 mm in diameter were cultured for various time as described in Section 2.2.1 to obtain oocytes at the

germinal vesicle I (0 h), germinal vesicle II-IV (9-15 h), diakinesis (18 h), metaphase I (27 h), anaphase I and telophase I (30-33 h), and metaphase II (42 h) stages. After culturing, 200 μl of 0.1% (w/v) hyaluronidase (Type I-S; Sigma Chemical Co.) in PBS-PVA was added to 2 ml of the maturation medium. Several minutes later, the oocytes were denuded of cumulus cells completely by pipetting.

After maturation culture of 42 h, some oocytes were activated using a protocol that was described previously (Nguyen et al., 2003). The oocytes were denuded of cumulus cells completely by hyaluronidase and gentle pipetting as describe above. Denuded oocytes were transferred to new drops of HEPES-199 to rinse off the hyaluronidase solution. The extrusion of the first polar body was inspected under an inverted microscope to assess oocyte maturation. The oocytes with the first polar body were washed three times in a field solution that was composed of 0.3 mM mannitol, 0.1 mM $MgSO_4$, and 0.05 mM $CaCl_2$ and 0.01% (w/v) PVA. Each group of less than 20 oocytes was transferred to 100 μl of the field solution between two parallel stainless electrodes in a chamber (FTC-03; Shimadzu Co. Ltd., Kyoto, Japan). A single direct-current pulse of 1,500 V/cm for 100 μsec was supplied from an Electro Cell Manipulator (ECM 2000; BTX Inc., Sandiego, CA). Electro-activated oocytes were washed 3 times in HEPES-199 to rinse off the mannitol solution. Then they were cultured for 2, 4, 6, and 8 h in bicarbonate-buffered TCM-199 supplemented with 10% (v/v) heat-treated fetal calf serum, 0.1 mg/ml sodium pyruvate, 0.08 mg/ml kanamycin sulphate, and 2.2 mg/ml sodium bicarbonate. The activated oocytes were cultured under the same temperature and gas phase as the oocyte maturation. After culturing, the oocytes were used for immunostaining and kinase assay.

3.2.3. Classification of Nuclear Morphology

Nuclear morphology of GV-stage oocytes were classified into the following 6 categories as described by Motlik and Fulka (1976) and Hirao et al. (1995).

Filamentous chromatin stage (FC): Decondensed filamentous chromatin is distributed throughout the germinal vesicle, and the nucleolus is stained by orcein and has many vacuoles.

Stringy chromatin stage (SC): Chromatin has begun to condense forming thick chromatin strings in the germinal vesicle, and the nucleolus is not stained by orcein.

Germinal vesicle I stage (GV I): Intact germinal vesicle is characterized by a distinct nuclear envelope and by the chromatin which is stained only around the nucleolus.

Germinal vesicle II stage (GV II): Chromatin arranges around the nucleolus and a few orcein-positive zones (chromocenters) appear near the nuclear membrane.

Germinal vesicle III stage (GV III): Nucleoplasm loses its granulation, but the nuclear membrane still remains distinct. Filamentous bivalents appear around the nucleolus.

Germinal vesicle IV stage (GV IV): Nuclear membrane becomes less distinct and the nucleolus disappears completely. Individual filamentous bivalents are distinguishable.

After germinal vesicle breakdown, the meiotic stages of oocytes were classified as follows; diakinesis (D), metaphase I (MI), anaphase I (AI), telophase I (TI), metaphase II (MII), anaphase II (AII), telophase II (TII), and pronucleus stage (PN).

3.2.4. Immunofluorescent Microscopy

The method is described in Section 2.2.2 in Chapter 2. The first antibodies used here were rabbit polyclonal anti-phospho-histone H3 at serine 10 (Cell Signaling Technology Inc., MA), rabbit polyclonal anti-phospho-histone H3 at serine 28 (Upstate, Cell Signaling Solutions, VA), rabbit polyclonal anti-trimethyl-histone H3 at lysine 9 (Abcam, Cambridge, UK), rabbit polyclonal anti-acetyl-histone H3 at lysine 9 (Upstate), rabbit polyclonal anti-acetyl-histone H3 at lysine 14 (Upstate), and rabbit polyclonal anti-acetyl-histone H3 at lysine 18 (Upstate) antibodies. To determine the integrity of the nuclear membrane and meiotic stages, mouse monoclonal anti-lamin A/C (Santa Cruz Biotechnology Inc) and mouse monoclonal anti-α tubulin antibodies (Sigma Chemical Co.) were used. The conjugated second antibodies used here were Alexa Fluor 488-labeled goat anti-rabbit IgG (Molecular Probes Inc.) and Alexa Fluor 568-labeled goat anti-mouse IgG (Molecular Probes Inc.). The chromosomes were stained with propidium iodide (400 µg/ml; Sigma Chemical Co.) or 4,6-diamidino-2-phenylindole (DAPI) (2 µg/ml; Molecular Probes Inc.). The oocytes were observed under a fluorescent microscope (U-LH100HGAPO, Olympus Optical Co.) or a confocal scanning laser microscope (Bio-Rad Radiance 2100). In the negative control, oocytes were reacted with nonimmune rabbit serum instead of rabbit polyclonal first antibody, or with mouse IgG instead of mouse monoclonal antibodies.

3.2.5. Kinase Assay

The activities of Cdc2 kinase and histone H3 kinase in the oocytes during growth phase, maturation, and after electro-activation were measured using the method described in Section 2.2.3 in Chapter 2.

The typical patterns of filamentous chromatin (FC), stringy chromatin (SC), and germinal vesicle I (GVI) stages were found in the oocytes from follicles 0.1-0.2, 2-3, and 4-6 mm in diameter corresponding to oocyte diameters of 70, 108, and 122 μm, respectively (Fig. 3.1). Therefore, oocytes in follicles 0.1-0.2, 2-3, and 4-6 mm in diameter were chosen to measure the kinase activity of growing oocytes at FC, SC, and GVI stages, respectively.

Stages of electro-activated oocytes were determined before they were transferred into Eppendorf tubes by staining with 12 μg/ml Hoechst 33342 (Polysciences Inc.) for 20 min followed by observation under a fluorescent microscope.

3.2.6. Statistical Analysis

At least 40 immunostained oocytes were examined for each antibody against modified histone H3 and in each meiotic stage. Each kinase assay experiment was performed at least 3 replicates. Statistical differences in the activities of the kinases in autoradiographs were analysed by one-way ANOVA (F1-test) followed by the Tukey's multiple range test. Other values were analysed using the chi-square test. P values less than 0.05 were considered statistically significant.

3.3. RESULTS

3.3.1. Chromatin and Nucleolus Morphology of Growing Oocytes

The mean diameters of oocytes isolated from various sized follicles, classes I (0.1-0.2 mm), II (0.5-<1 mm), III (1-<2 mm), IV (2-<3 mm), V (3-<4 mm), and VI (4-6 mm), were 70.0±3.2 (n=75), 89.7±2.5 (n = 70), 108.2±2.6 (n = 64), 115.3±3.0 (n = 69), 119.8±2.7 (n = 71), and 122.1±2.2 μm (n = 79), respectively.

Nuclear morphology of the oocytes is summarized in Fig. 3.1A. Oocytes in class I contained

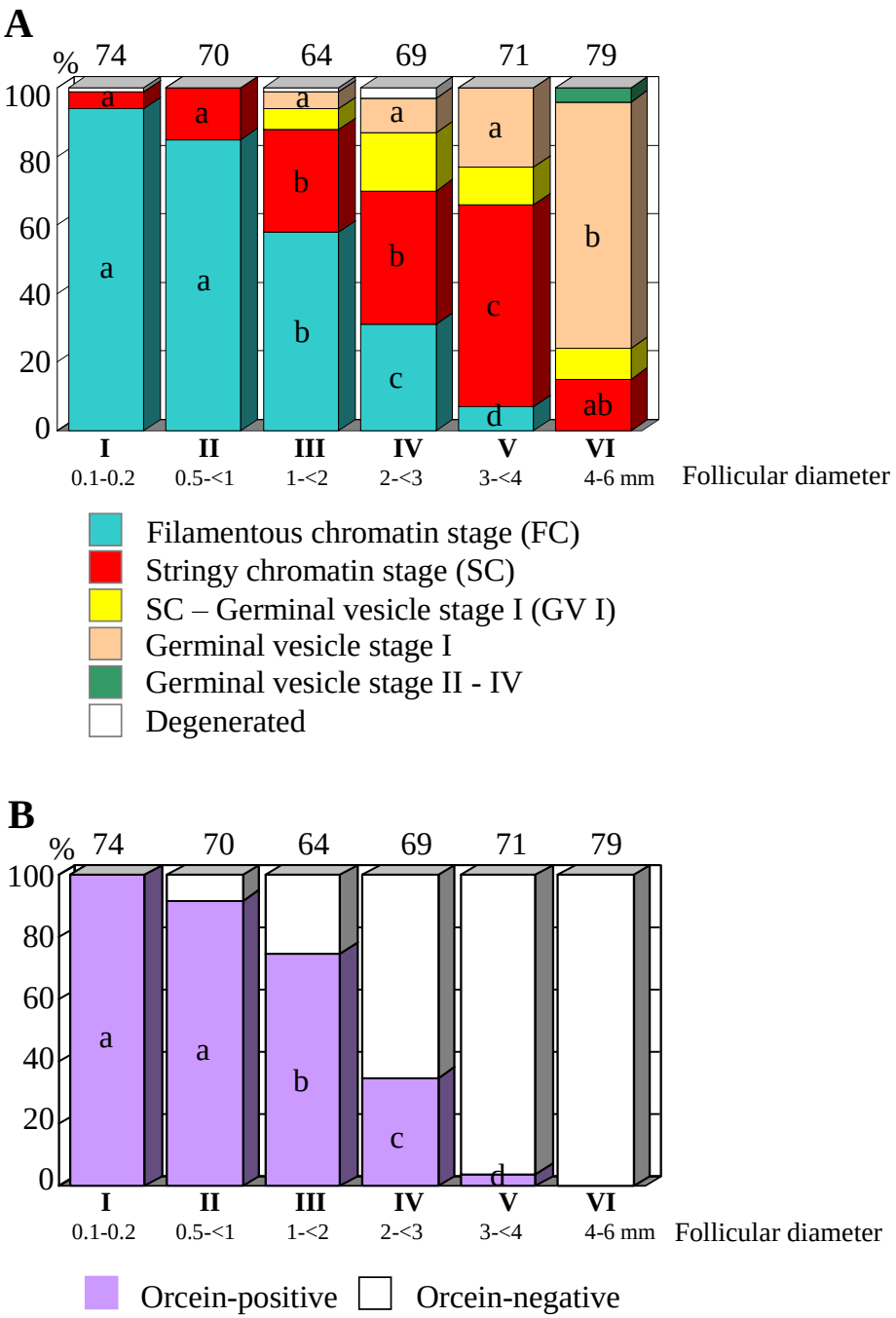

Fig. 3.1. A) Chromatin configuration of pig oocytes from various sized follicles. **B**) Nucleolus morphology of oocytes from various sized follicles. Figure above each colum shows the number of oocytes examined. a-d: P<0.05.

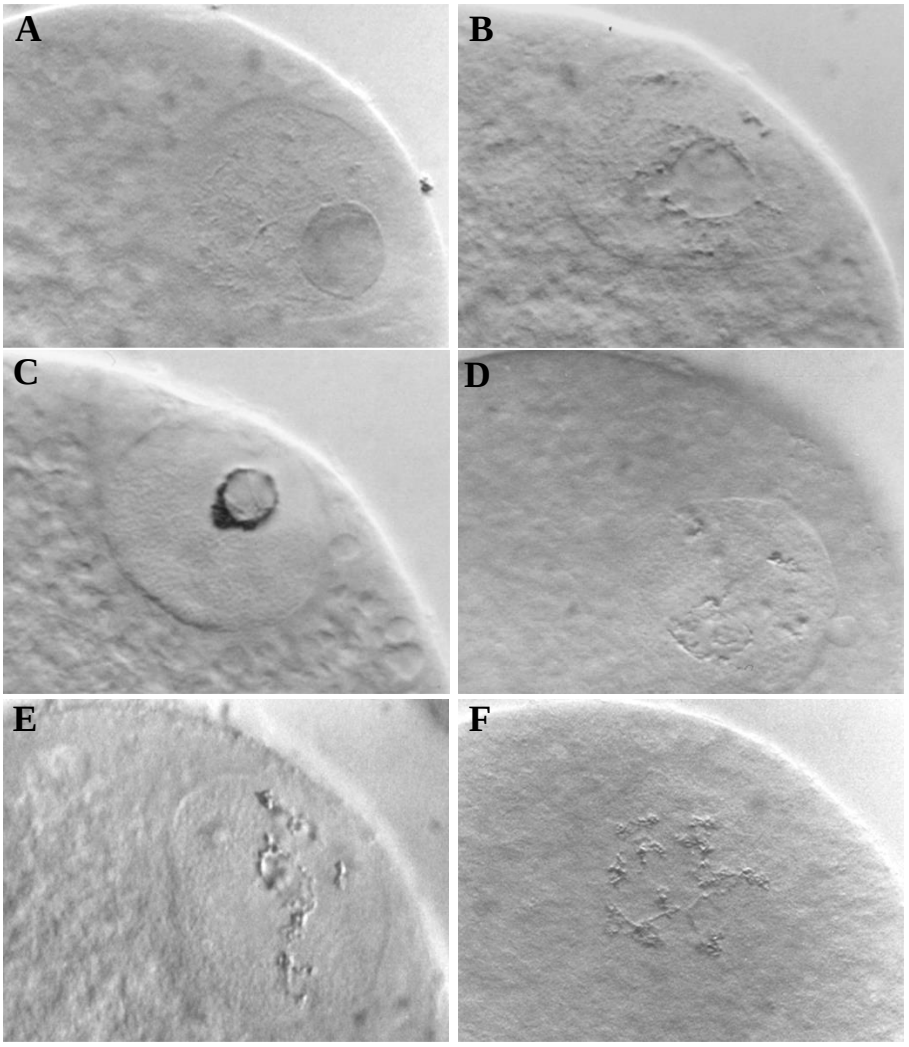

Fig. 3.2. Chromatin configurations in germinal vesicles of pig oocytes. Oocytes collected from various sized follicles were fixed in acetic alcohol (1/3, v/v), stained with 1% orcein, and examined under a differential interference microscope. Chromatin configurations of oocytes at the germinal vesicle stage were classified into 6 categories as described by Motlik and Fulka (1976) and Hirao et al. (1995). **A**) Filamentous chromatin stage, **B**) Stringy chromatin stage, **C)**. Germinal vesicle stage I, **D**) Germinal vesicle stage II, **E**) Germinal vesicle stage III, and **F**) Germinal vesicle stage IV.

decondensed-filamentous chromatin (FC) (Fig. 3.2A). As oocytes grew from class II to class V, chromatin became thicker and formed stringy configuration (SC) (Fig. 3.2B). Finally, a high frequency of oocytes in class VI formed a condensed chromatin rim around the nucleolus (GV I) (Fig. 3.2C).

All of the oocytes examined in this experiment had a single nucleolus. However, there were significant differences in the frequency of nucleoli stained with orcein among different follicle classes (Fig. 3.1B). Almost all of the nucleoli in the oocytes in class I were stained with orcein (99%). The frequencies of oocytes with orcein positive nucleolus decreased to 83% and 75% in class II and III, respectively. In class IV, 65% of oocytes had an orcein-negative nucleolus, and most of the oocytes in classes V and VI had an orcein-negative nucleolus (96% and 100%, respectively).

3.3.2. Histone H3 Modifications during Oocyte Growth

The phosphorylation of histone H3 at serine 10 (P-H3-S10) and serine 28 (P-H3-S28) were not detected in any oocytes during the growth phase, and oocytes reaching the final size (Fig. 3.3). The changes in the activities of Cdc2 kinase and histone H3 kinase during oocyte growth were measured. Both of Cdc2 kinase and histone H3 kinase were inactive during oocyte growth (Fig. 3.4).

The acetylation levels of various lysine residues on histone H3 were examined by immunocytochemistry with specific antibodies against acetylated lysines 9, 14, and 18. Acetylation of histone H3 at lysines 9 (Ac-H3-K9), 14 (Ac-H3-K14), and 18 (Ac-H3-K18) were detected in oocytes at the filamentous chromatin stage in secondary follicles of 0.1-0.2 mm diameter (Figs. 3.5, 3.6 and 3.7). The fluorescent signals of acetylation of H3-K14 and H3-K18 extended throughout the whole chromatin. Acetylation level of H3-K9 was highest in oocytes from secondary follicles, thereafter it decreased as oocytes grew. The acetylation levels of all lysines examined appeared high in growing oocytes and were diminished in the fully-grown oocytes at the GVI stage.

The methylation levels of histone H3 were examined by the antibody that specifically recognized the trimethylated form of H3 at lysine 9 (Me-H3-K9). The fluorescent signal was not detected in oocytes at the filamentous chromatin stage in secondary follicles (Fig. 3.8).

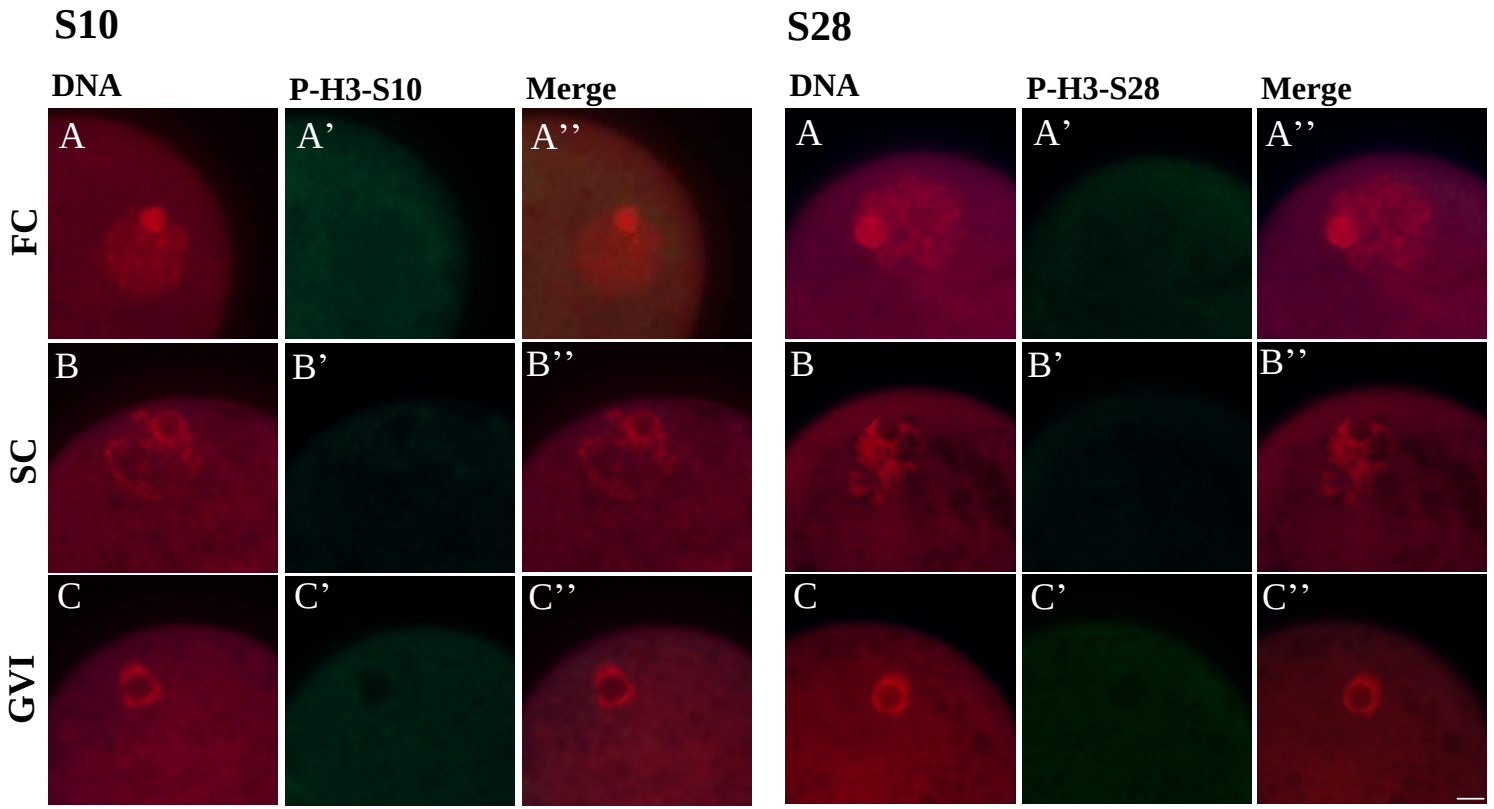

Fig. 3.3. Immunofluorescent localization of phosphorylated histone H3-S10 (S10) and H3-S28 (S28) during oocyte growth. PI stained the chromosome (red), anti-phospho-histone H3-S10 and Alexa 488-labeled antibodies or anti-phospho-histone H3-S28, and Alexa 488-labeled antibodies stained the phosphorylated histone H3 (green) in the same oocyte. The meiotic stages are **FC:** Filamentous chromatin stage, **SC:** Stringy chromatin stage, and **GVI:** Germinal vesicle stage I. Scale bar = 10 µm.

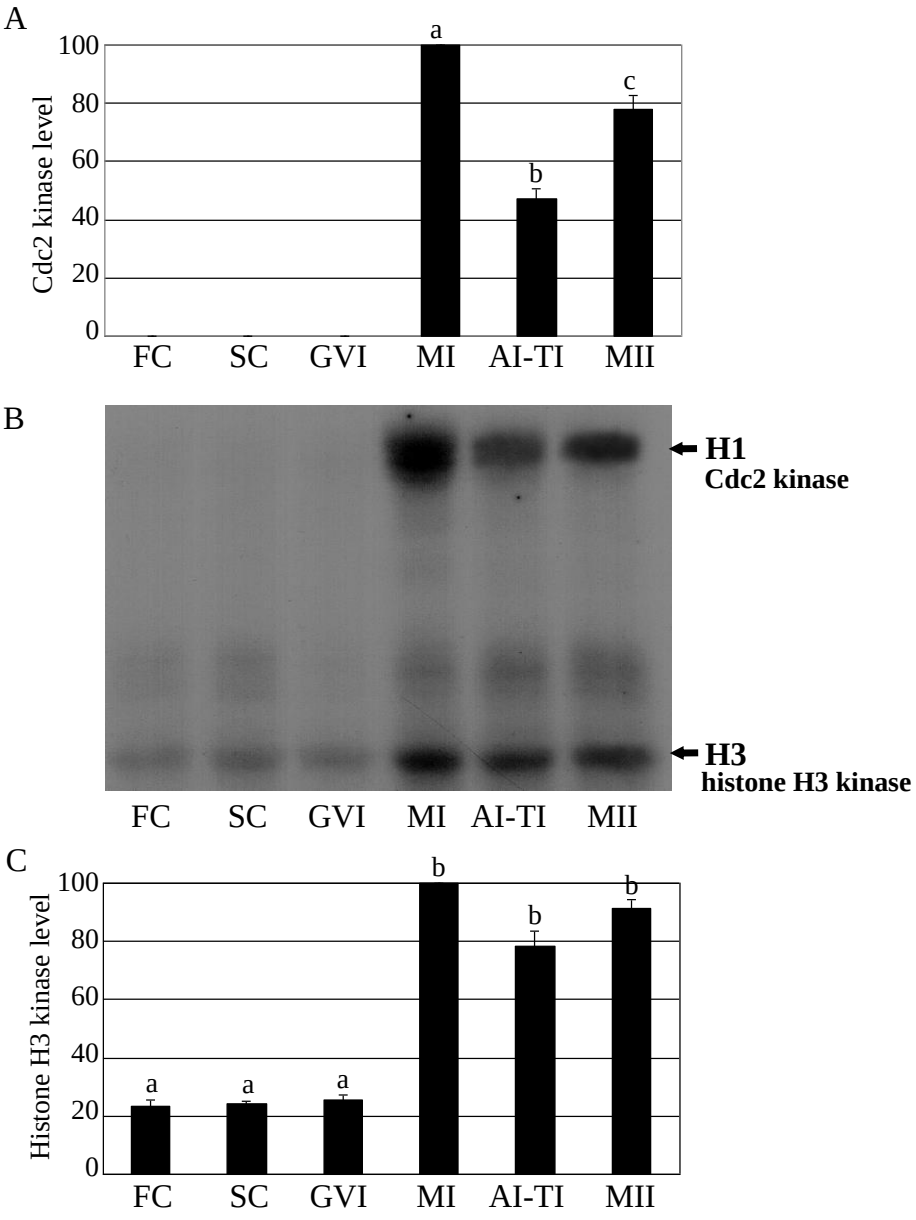

Fig. 3.4. The autoradiograph showing the changes in Cdc2 kinase and histone H3 kinase activities of pig oocytes during the growth and maturation. Histone H1 (H1) and histone H3 (H3) were used for the substrates of Cdc2 kinase and histone H3 kinase, respectively. The meiotic stages are **FC**: Filamentous chromatin stage, **SC**: Stringy chromatin stage, **GVI:** Germinal vesicle stage I, **MI**: Metaphase I, **AI:** Anaphase I, **TI:** Telophase I, and **MII:** Metaphase II.

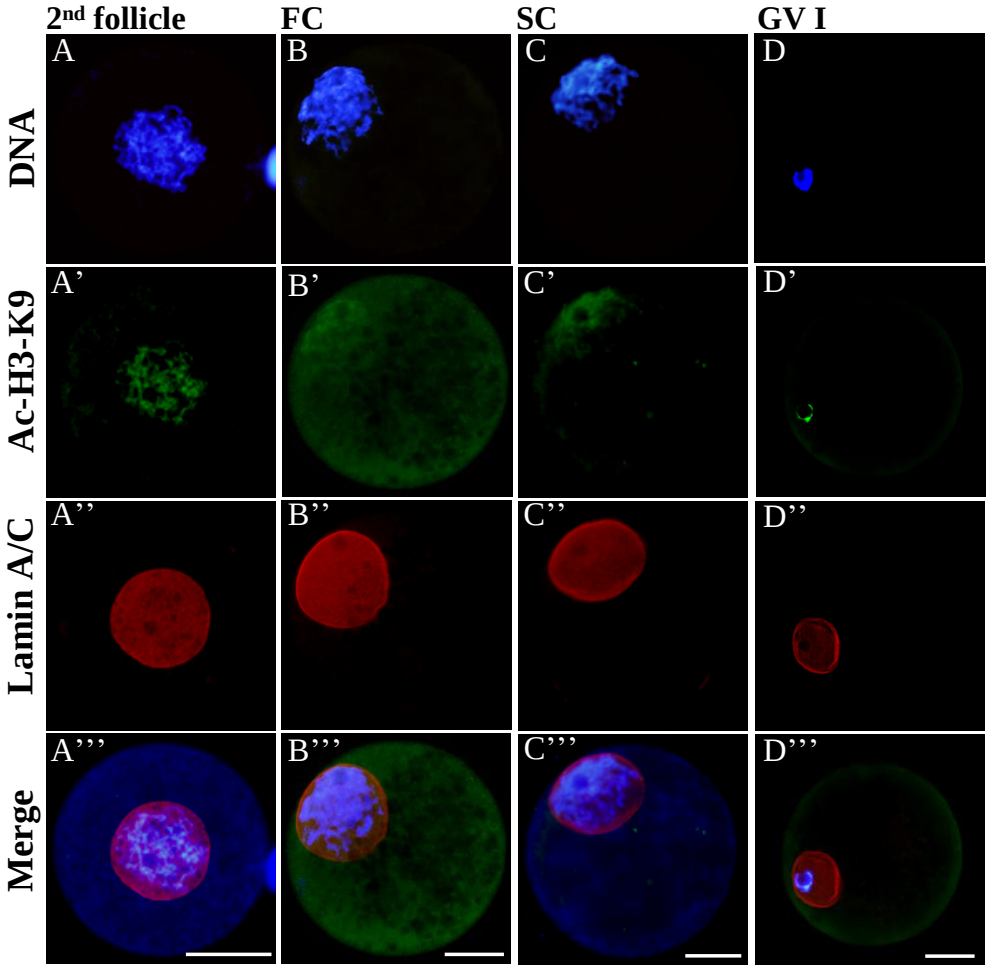

Fig. 3.5. Acetylation of histone H3-K9 (Ac-H3-K9) in growing pig oocytes. DAPI stained the chromosome (blue), anti-acetyl-histone H3-K9 and Alexa 488-labeled antibodies stained the acetylated H3-K9 (green), and anti-lamin A/C and Alexa 568-labeled antibodies stained the nuclear membrane (red) in the same oocyte. The meiotic stages are **A)** Filamentous chromatin stage of an oocyte collected from secondary follicle (2nd follicle), **B)** Filamentous chromatin stage of an oocyte from early antral follicle (FC), **C)** Stringy chromatin stage (SC), and **D)** Germinal vesicle stage I (GVI). Scale bar = 30 µm.

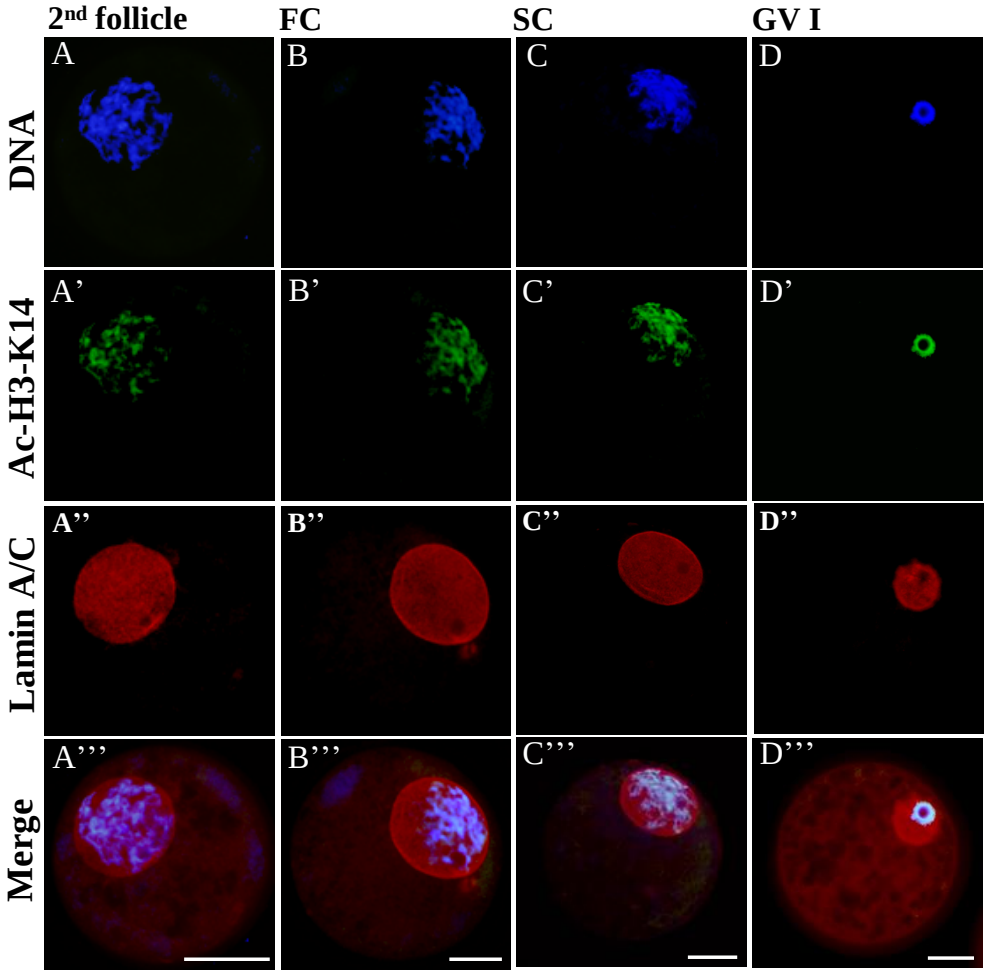

Fig. 3.6. Acetylation of histone H3-K14 (Ac-H3-K14) in growing pig oocytes. DAPI stained the chromosome (blue), anti-acetyl-histone H3-K14 and Alexa 488-labeled antibodies stained the acetylated H3-K14 (green), and anti-lamin A/C and Alexa 568-labeled antibodies stained the nuclear membrane (red) in the same oocyte. The meiotic stages are **A)** Filamentous chromatin stage of an oocyte collected from secondary follicle (2nd follicle), **B)** Filamentous chromatin stage of an oocyte from early antral follicle (FC), **C)** Stringy chromatin stage (SC), and **D)** Germinal vesicle stage I (GVI). Scale bar = 30 µm.

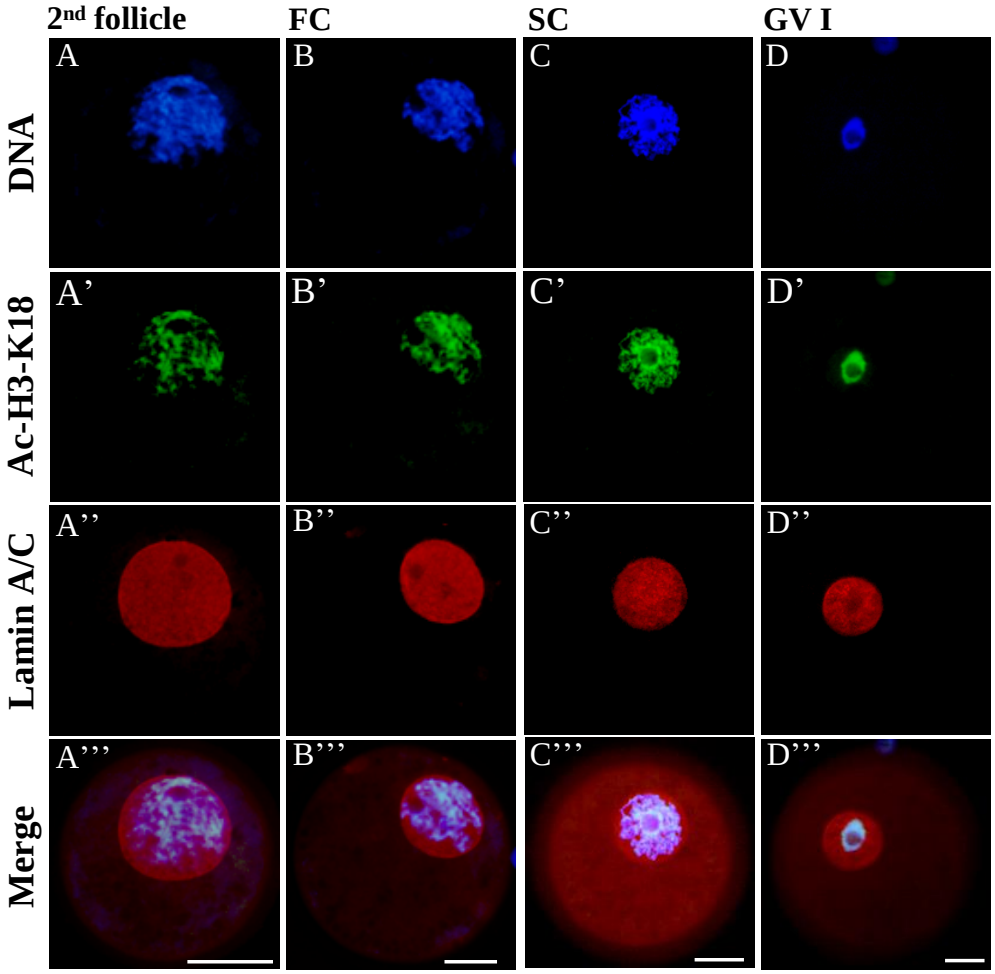

Fig. 3.7. Acetylation of histone H3-K18 (Ac-H3-K18) in growing pig oocytes. DAPI stained the chromosome (blue), anti-acetyl-histone H3-K18 and Alexa 488-labeled antibodies stained the acetylated H3-K18 (green), and anti-lamin A/C and Alexa 568-labeled antibodies stained the nuclear membrane (red) in the same oocyte. The meiotic stages are **A)** Filamentous chromatin stage of an oocyte collected from secondary follicle (2nd follicle), **B)** Filamentous chromatin stage of an oocyte from early antral follicle (FC), **C)** Stringy chromatin stage (SC), and **D)** Germinal vesicle stage I (GVI). Scale bar = 30 µm.

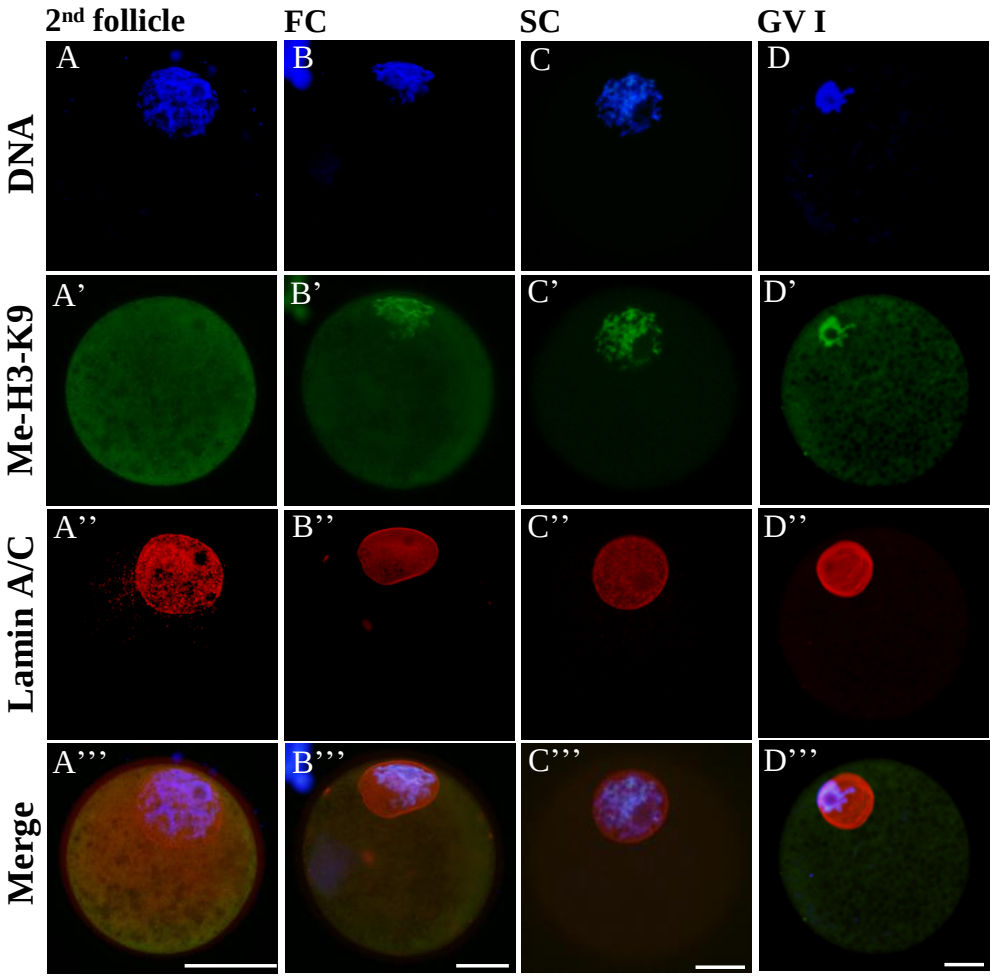

Fig. 3.8. Methylation of histone H3-K9 (Me-H3-K9) in growing pig oocytes. DAPI stained the chromosome (blue), anti-methyl-histone H3-K9 and Alexa 488-labeled antibodies stained the methylated H3-K9 (green), and anti-lamin A/C and Alexa 568-labeled antibodies stained the nuclear membrane (red) in the same oocyte. The meiotic stages are **A)** Filamentous chromatin stage of an oocyte collected from secondary follicle (2nd follicle), **B)** Filamentous chromatin stage of an oocyte from early antral follicle (FC), **C)** Stringy chromatin (SC) stage, and **D)** Germinal vesicle stage I (GVI). Scale bar = 30 µm.

Methylation of H3-K9 started to appear in chromatin knobs in growing oocytes when follicles increased from 0.5 to 1 mm in diameter. The staining of Me-H3-K9 was weak in oocytes at the FC and SC stages from follicles 1-2 mm in diameter. The methylation of histone H3-K9 extended throughout the whole chromatin in the oocytes at the SC stage in 2-4 mm follicles. Finally, the methylation became observed at the entire condensed heterochromatin ring when oocytes reached to the GVI stage with the final size (Fig 3.8).

3.3.3. Chromosome Morphology and Histone H3 Modifications during Oocyte Maturation

As shown in Chapter 2, phosphorylation of histone H3-S10 (P-H3-S10) was first detected in the clump of condensed chromosomes at the diakinesis stage after 18 h of culture, and thereafter the phosphorylation was maintained during oocyte maturation. Fluorescent signal of P-H3-S28 was seen first around the nucleolus in oocytes at GVII-IV stages after 9 h of culture (Fig. 3.9B). The phosphorylation of H3-S28 extended throughout the whole condensing chromosomes in oocytes at GVII-IV stages after 15 h of culture. Thereafter, the phosphorylation of H3-S28 was maintained during oocyte maturation. The kinase assay showed that histone H3 kinase was activated after 9 h and the activity increased during meiotic maturation of pig oocytes (Fig. 3.10). The Cdc2 kinase became active at 24 h and reached the maximum level at 27 h.

All of acetylation of H3 at K9, K14 and K18 were detected in oocytes at GVI stage before maturation culture. Intensity of fluorescent signal of acetylation of H3-K9 completely disappeared at the diakinesis stage (Fig. 3.11). On the other hand, acetylation of H3-K14 and H3-K18 decreased in the clump of condensed chromosomes at this stage (Figs. 3.12 and 3.13). The signals of acetylation of H3-K14 disappeared while acetylation H3-K18 still remained at a low level at the late diakinesis stage when nuclear membrane brokedown but the membrane fragments still remained. Then, Ac-H3-K18 completely disappeared at MI.

Fluorescent signal of Ac-H3-K9 was detected again with a low level at TI. Similary, acetylation of H3-K14 was temporarily appeared around AI and TI. Finally, all of these signals completely disappeared again when oocytes reached MII (Figs. 3.11 and 3.12). However, the deacetylation of H3-K18 was maintained until MII stage.

Methylation of H3 at K9 was detected in oocytes at GV I stage, and it was maintained throughout meiotic maturation of pig oocytes (Fig. 3.14).

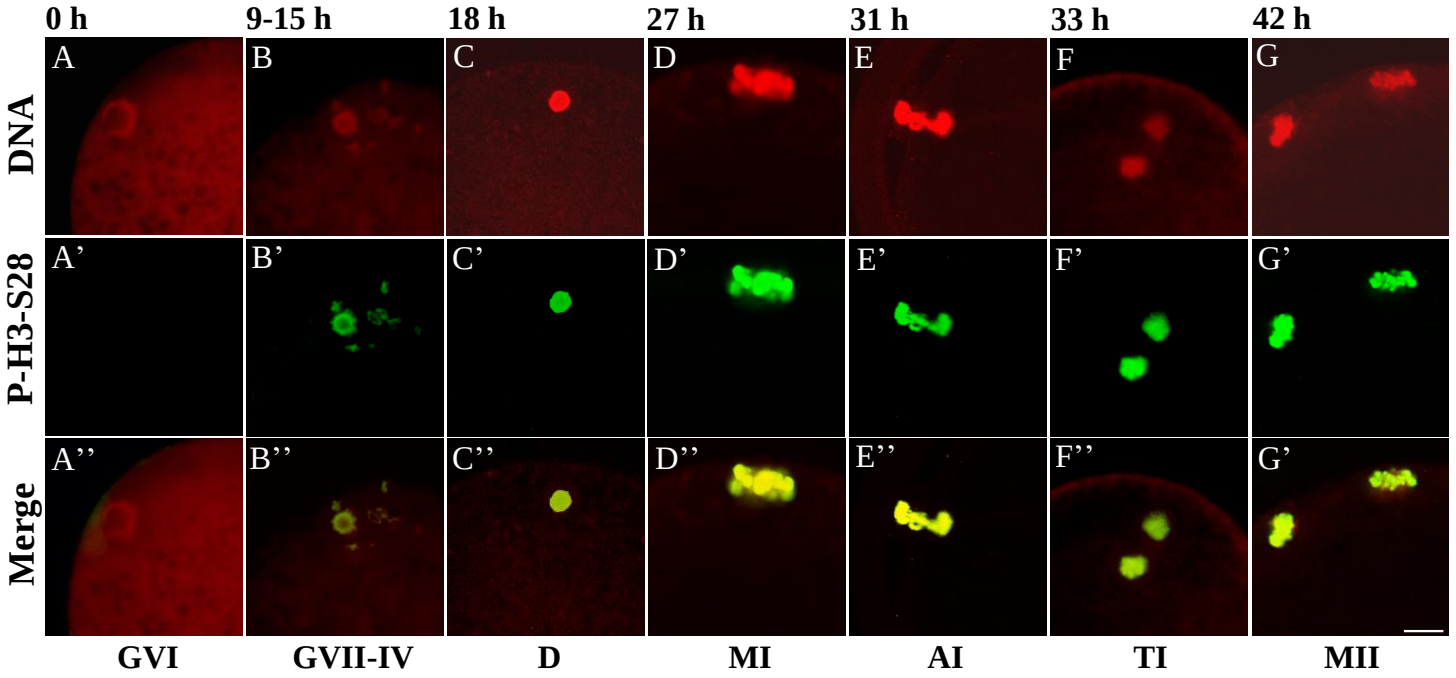

Fig. 3.9. Immunofluorescent localization of phosphorylated histone H3-S28 (P-H3-S28) during maturation of pig oocytes. PI stained the chromosome (red), and anti-phospho-histone H3-S28 and Alexa 488-labeled antibodies stained the phosphorylated H3-S28 (green) in the same oocyte. The meiotic stages are **A**) Germinal vesicle stage I (GVI), **B**) Germinal vesicle stage II-IV (GVII-IV), **C)** Diakinesis (D), **D)** Metaphase I (MI), **E)** Anaphase I (AI), **F)** Telophase I (TI), and **G)** Metaphase II (MII). Scale bar = 10 µm.

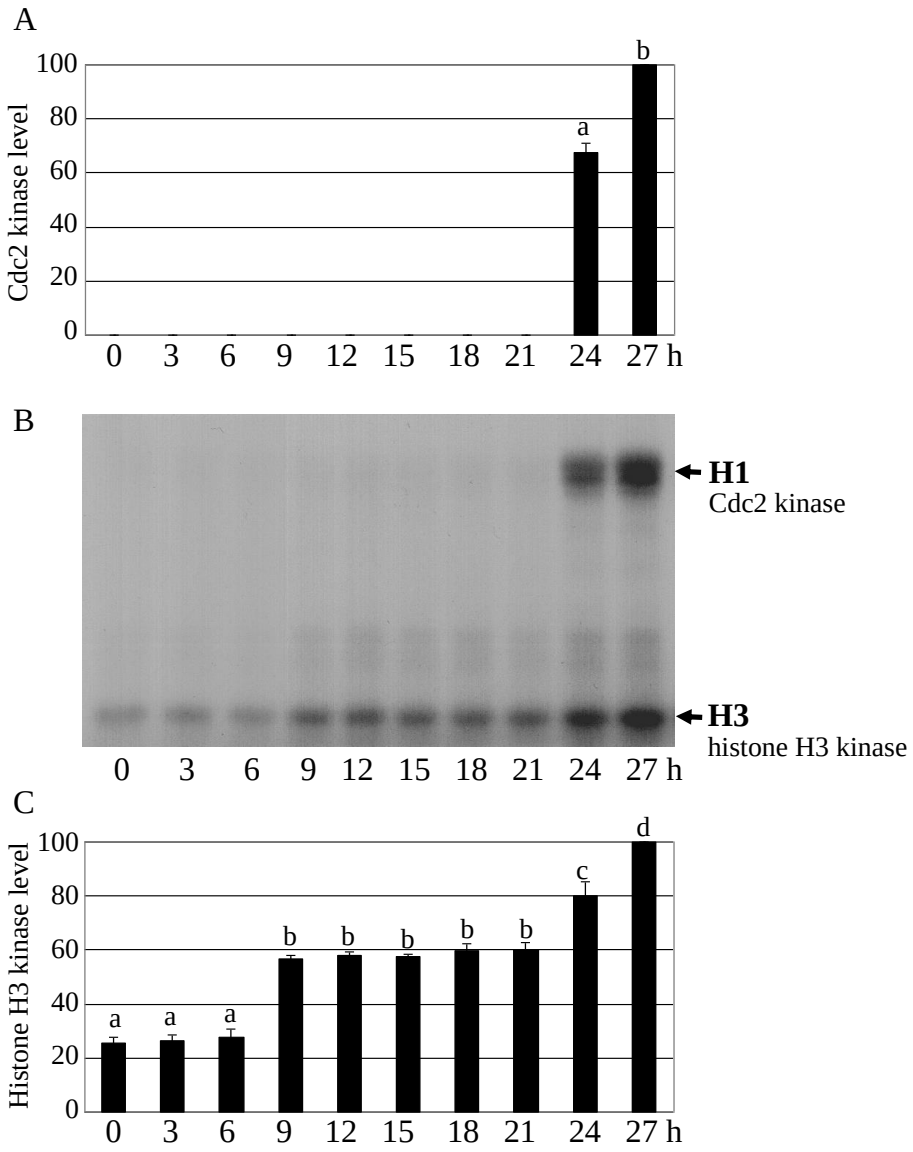

Fig. 3.10. An autoradiograph showing the changes in Cdc2 kinase and histone H3 kinase activities during meiotic maturation of pig oocytes. Histone H1 (H1) and histone H3 (H3) were used for the substrates of Cdc2 kinase and histone H3 kinase, respectively. The lower figures represent the hours of maturation culture.

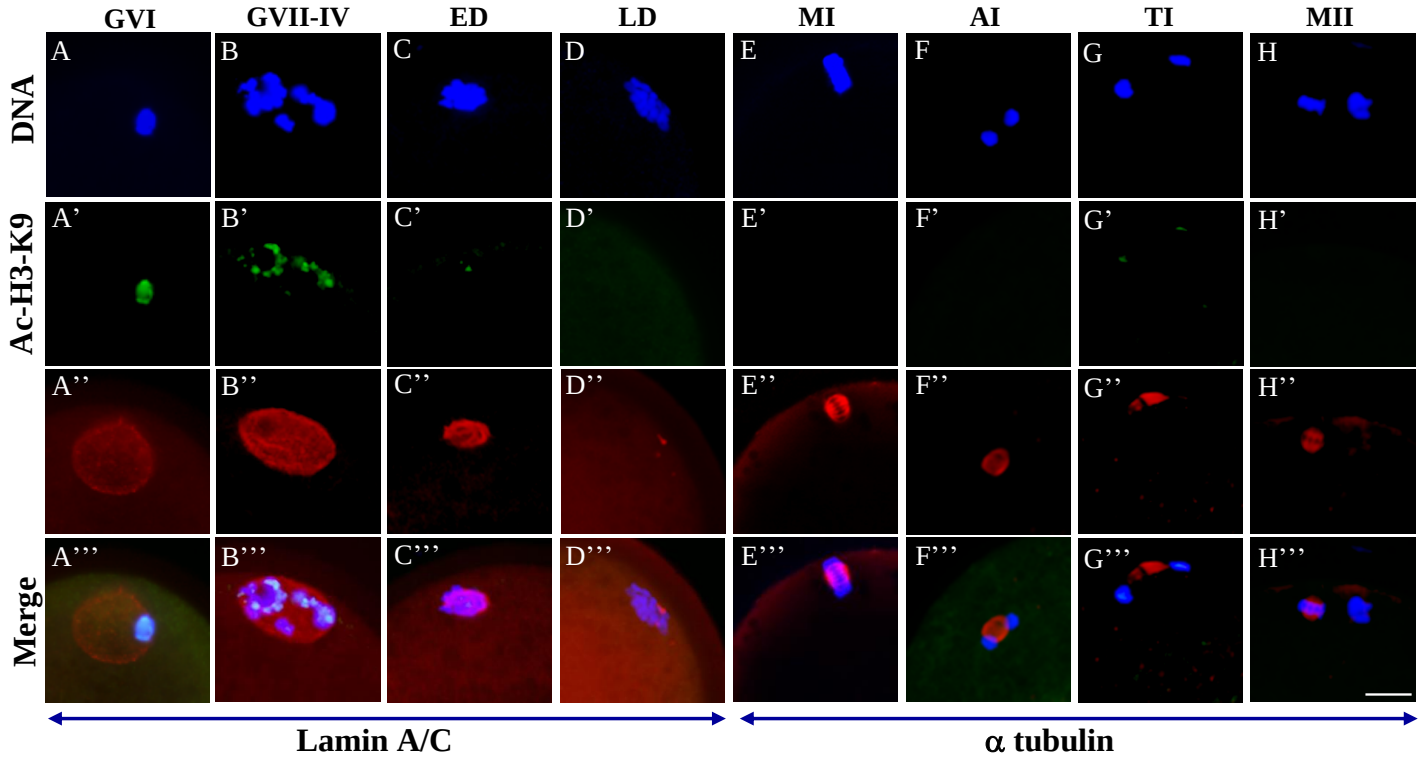

Fig. 3.11. Immunofluorescent localization of acetylated histone H3-K9 (Ac-H3-K9) during maturation of pig oocytes. DAPI stained the chromosome (blue), anti-acetyl-histone H3-K9 and Alexa 488-labeled antibodies stained the Acetylated H3-K9 (green), and anti-lamin A/C and Alexa 568-labeled antibodies stained the nuclear membrane (red, A''- D''), or anti-αtubulin and Alexa 568-labeled antibodies stained the microtubule (red, E''- H''), in the same oocyte. The meiotic stages are **A**) Germinal vesicle stage I (GVI), **B**) Germinal vesicle stage II-IV (GVII-IV), **C**) Early diakinesis (ED), **D**) Late diakinesis (LD), **E)** Metaphase I (MI), **F)** Anaphase I (AI), **G)** Telophase I (TI), and **H)** Metaphase II (MII). Scale bar = 20 µm.

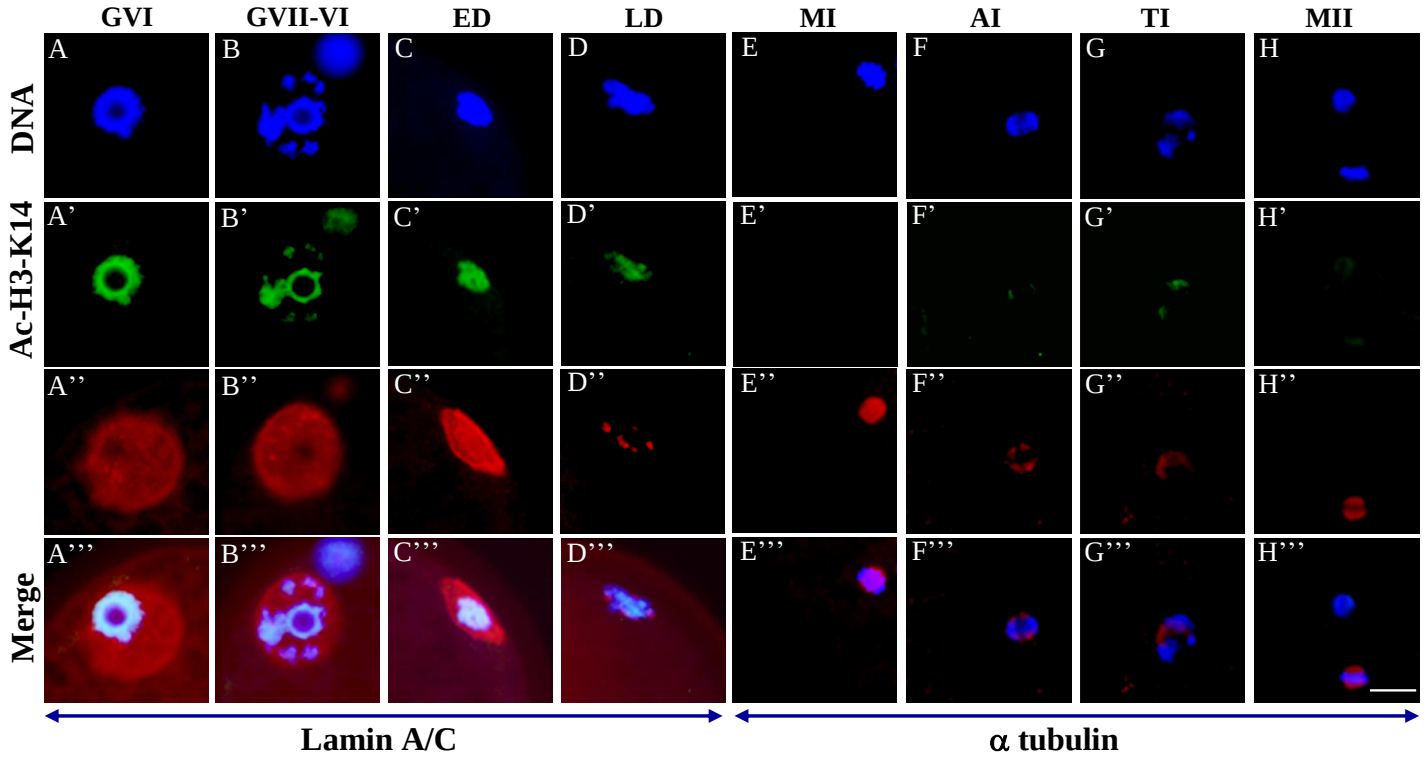

Fig. 3.12. Immunofluorescent localization of acetylated histone H3-K14 (Ac-H3-K14) during maturation of pig oocytes. DAPI stained the chromosome (blue), anti-acetyl-histone H3-K14 and Alexa 488-labeled antibodies stained the acetylated H3-K14 (green), and anti-lamin A/C and Alexa 568-labeled antibodies stained the nuclear membrane (red, A''- D''), or anti-αtubulin and Alexa 568-labeled antibodies stained the microtubule (red, E'' - H''), in the same oocyte. The meiotic stages are **A**) Germinal vesicle stage I (GVI), **B**) Germinal vesicle stage II-VI (GVII-IV)), **C**) Early diakinesis (ED), **D**) Late diakinesis (LD), **E**) Metaphase I (MI), **F**) Anaphase I (AI), **G**) Telophase I (TI), and **H**) Metaphase II (MII). Scale bar = 20 µm.

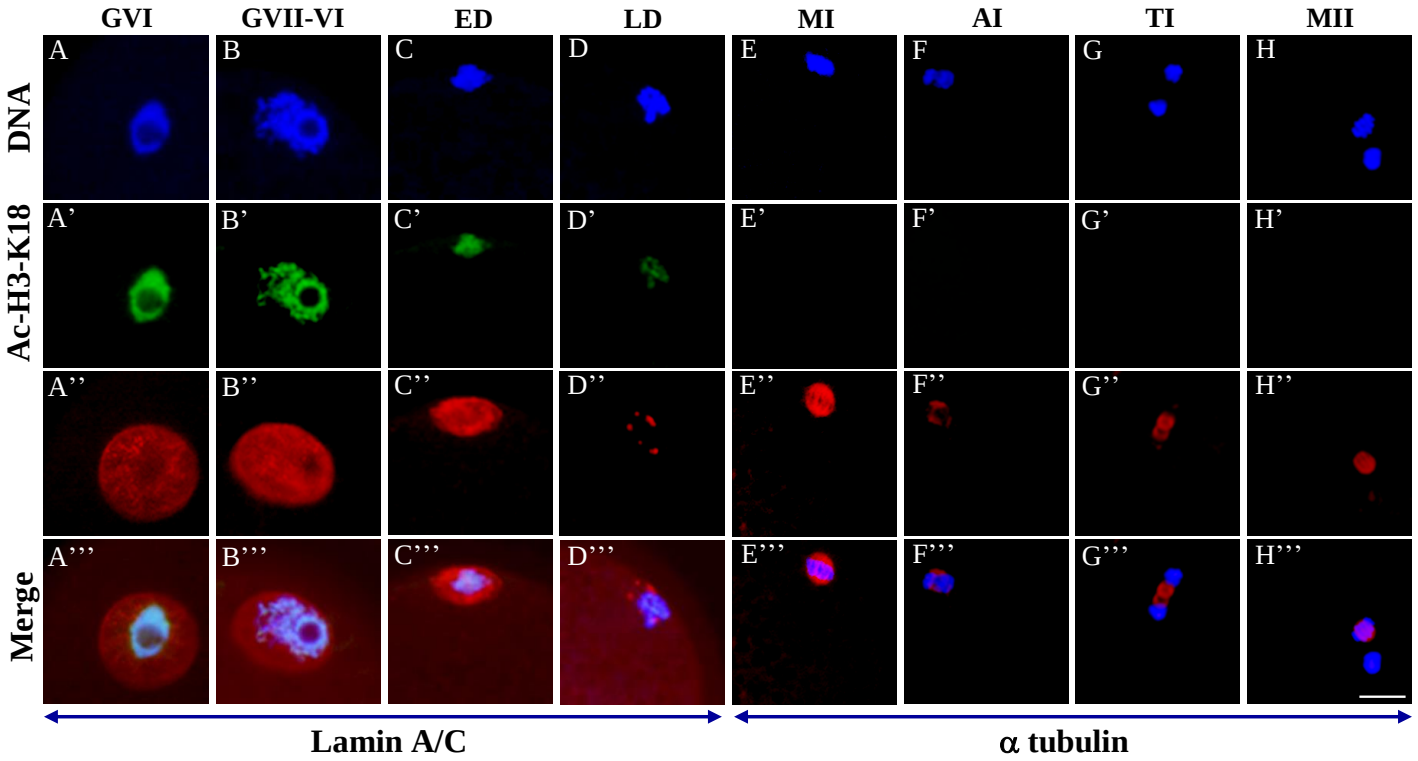

Fig. 3.13. Immunofluorescent localization of acetylated histone H3-K18 (Ac-H3-K18) during maturation of pig oocytes. DAPI stained the chromosome (blue), anti-acetyl-histone H3-K18 and Alexa 488-labeled antibodies stained the acetylated H3-K18 (green), and anti-lamin A/C and Alexa 568-labeled antibodies stained the nuclear membrane (red, A'' - D''), or anti-αtubulin and Alexa 568-labeled antibodies stained the microtubule (red, E'' - H''), in the same oocyte. The meiotic stages are **A**) Germinal vesicle stage I (GV I), **B**) Germinal vesicle stage II-VI (GVII-IV)), **C**) Early diakinesis (ED), **D**) Late diakinesis (LD), **E**) Metaphase I (MI), **F**) Anaphase I (AI), **G**) Telophase I (TI), and **H**) Metaphase II (MII). Scale bar = 20 µm.

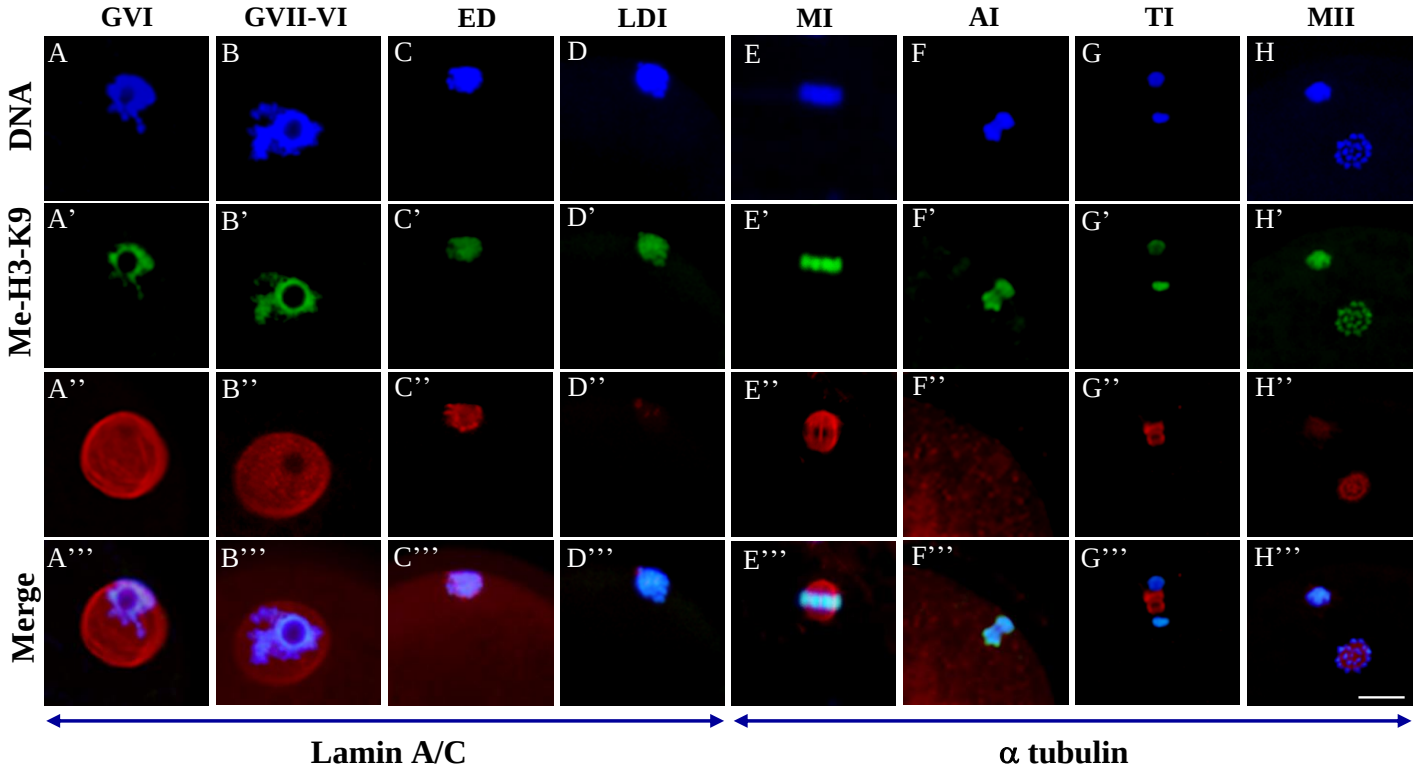

Fig. 3.14. Immunofluorescent localization of methylated histone H3-K9 (Me-H3-K9) during maturation of pig oocytes. DAPI stained the chromosome (blue), anti-methyl-histone H3-K9 and Alexa 488-labeled antibodies stained the methylated H3-K9 (green), and anti-lamin A/C and Alexa 568-labeled antibodies stained the nuclear membrane (red, A'' - D''), or anti-αtubulin and Alexa 568-labeled antibodies stained the microtubule (red, E''- H'') in the same oocyte, The meiotic stages are **A**) Germinal vesicle stage I (GVI), **B**) Germinal vesicle stage II-VI (GVII-VI), **C**) Early diakinesis (ED), **D**) Late diakinesis (LD), **E**) Metaphase I (MI), **F**) Anaphase I (AI), **G**) Telophase I (TI), and **H**) Metaphase II (MII). Scale bar = 20 µm.

3.3.4. Chromosome Morphology and Histone H3 Modifications after Electro-activation

The typical meiotic stage of oocytes 2 h after electro-activation was AII or TII. After 4 h, most of oocytes reached TII and some of them started to form a female pronucleus (PN). Chromosomes completely decondensed to form a PN 6-8 h after activation. Activities of histone H3 kinase was high in MII oocytes and started to decrease at AII-TII stages (Fig. 3.15). Both kinases became inactive in the PN stage 6 h after activation.

The phosphorylation levels of histone H3 at both S10 and S28 were high in oocytes at MII (Figs. 3.16 and 3.17). It still remained at AII and started to decrease at TII. Phosphorylation of H3-S10 completely disappeared at the PN stage. On the other hand, phosphorylation of H3-S28 was still maintained around the nucleoli in the PN (Fig. 3.17) and completely disappeared at the 2 cells stage (data not shown).

The fluorescent signals of all of the acetylated lysines were absent in oocytes at MII. However, the signals of acetylation of H3-K14 and H3-K9 reappeared in oocytes at TII 2 h after electro-activation (Figs. 3.18 and 3.19). The signals of acetylation of H3-K18 reappeared in the PN of activated oocytes (Fig. 3.20). After that, the acetylation of all the lysines 9, 14, and 18 was maintained in the oocytes that were examined until the 2-cell stage (data not shown).

The methylation of H3-K9 was detected in the chromosomes at MII. Even after electro-activation, the signals were maintained in oocytes at AII, TII, and the PN stage (Fig. 3.21).

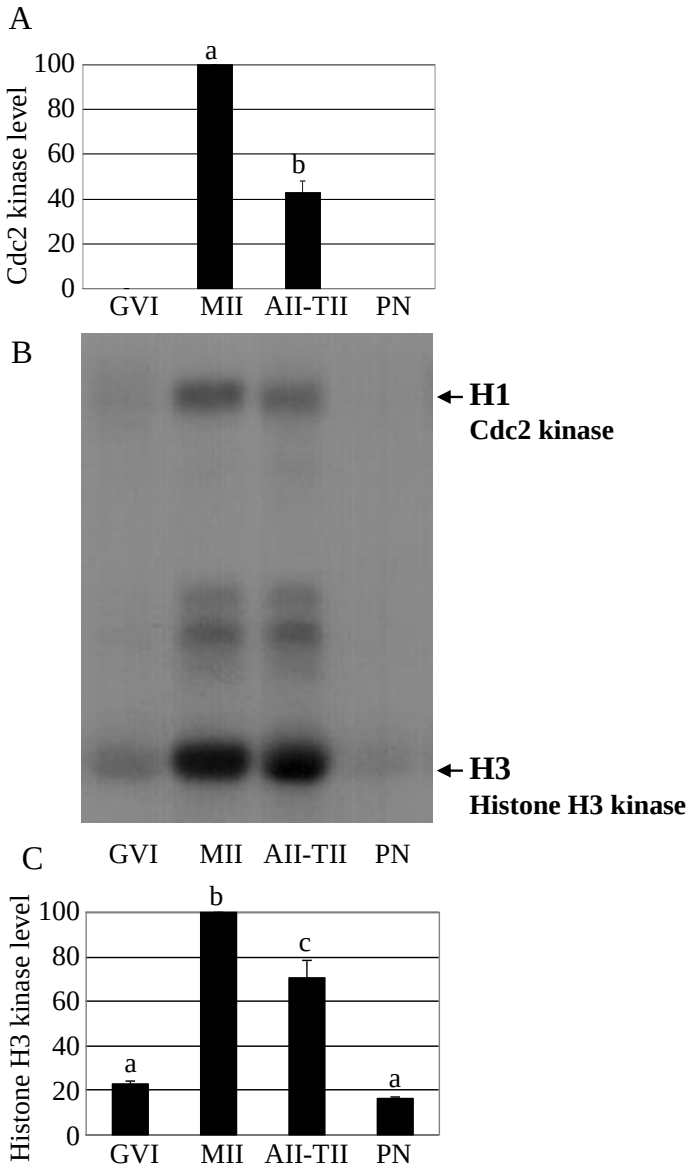

Fig. 3.15. The autoradiograph showing the changes in Cdc2 kinase and histone H3 kinase activities in pig oocytes after electro-activation. Histone H1 (H1) and histone H3 (H3) were used for the substrates of Cdc2 kinase and histone H3 kinase, respectively. The meiotic stages are: Germinal vesicle stage I (GVI); Metaphase II (MII); Anaphase II - Telophase II (AII-TII), and the pronucleus stage (PN**)**.

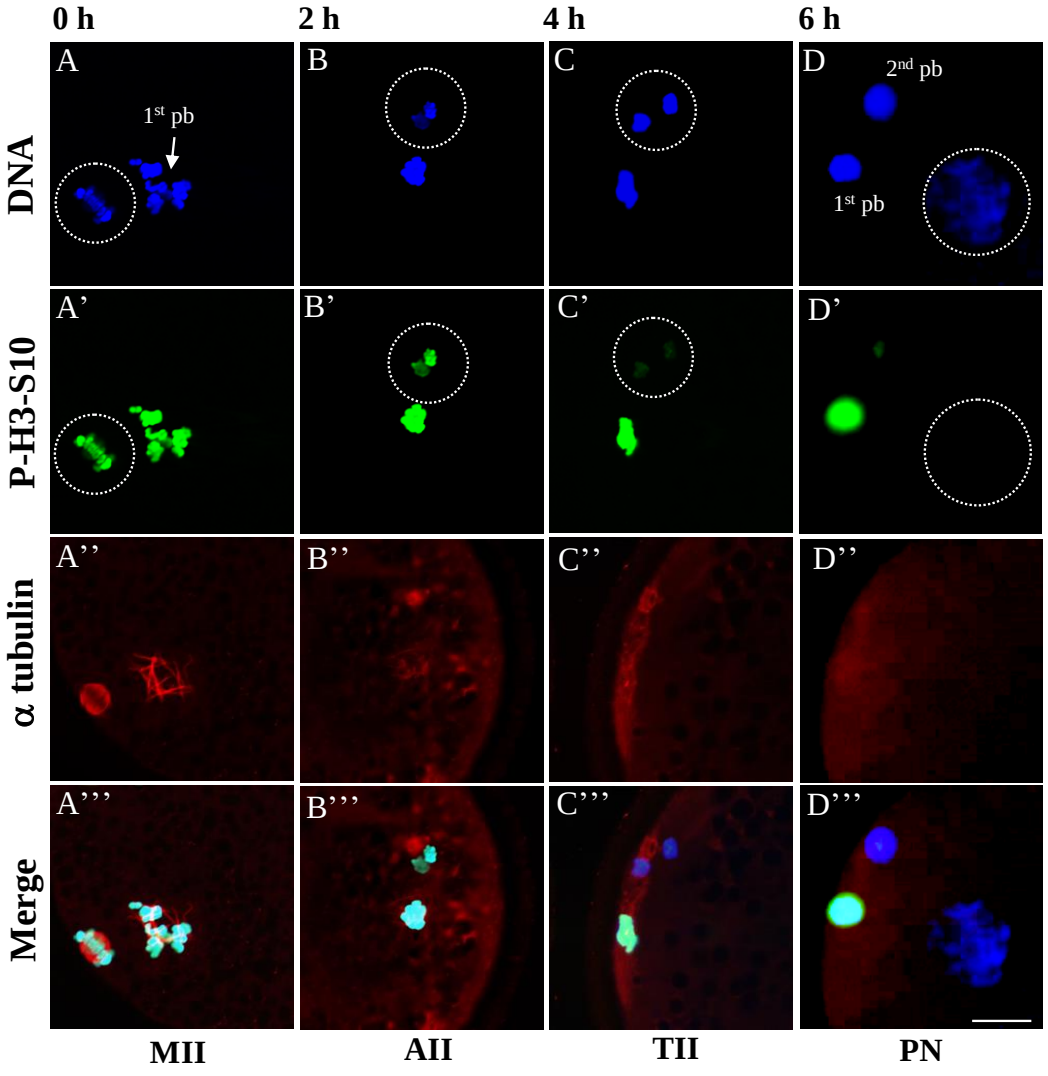

Fig. 3.16. Histone H3-S10 dephosphorylation in electro-activated pig MII-oocytes. Oocytes were cultured for maturation for 42 h, and then electro-activated. Oocytes were examined after 2, 4, and 6 h by immunostaining with anti-phospho-histone H3-S10 and Alexa 488-labeled antibodies for the phosphorylated histone H3 (P-H3-S10, green), and anti-αtubulin and Alexa 568-labeled antibodies for the microtubule (red). The chromosome was counterstained by DAPI (blue). The meiotic stages are **A-A'")** Metaphase II (MII), **B-B'")** Anaphase II (AII), **C-C'")** Telophase II (TII), and **D-D'")** Pronucleus stage (PN**)**. 1st pb: 1st polar body, 2nd pb: 2nd polar body. Scale bar = 20 µm.

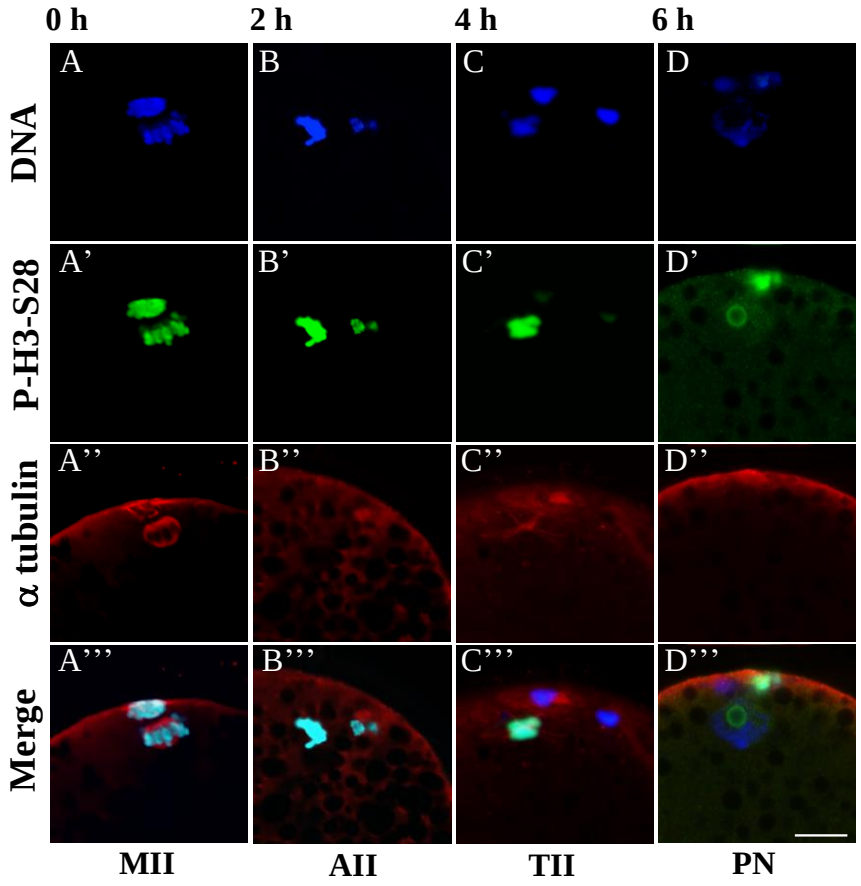

Fig. 3.17. Histone H3-S28 dephosphorylation in electro-activated pig MII-oocytes. Oocytes were cultured for maturation for 42 h, and then electro-activated. Oocytes were examined after 2, 4, and 6 h by immunostaining with anti-phospho-histone H3-S28 and Alexa 488-labeled antibodies for the phosphorylated histone H3 (P-H3-S28, green), and anti-αtubulin and Alexa 568-labeled antibodies for the microtubule (red). The chromosome was counterstained by DAPI (blue). The meiotic stages are **A-A''')** Metaphase II (MII), **B-B''')** Anaphase II (AII), **C-C''')** Telophase II (TII), and **D-D''')** Pronucleus stage (PN**)**. Scale bar = 20 μm.

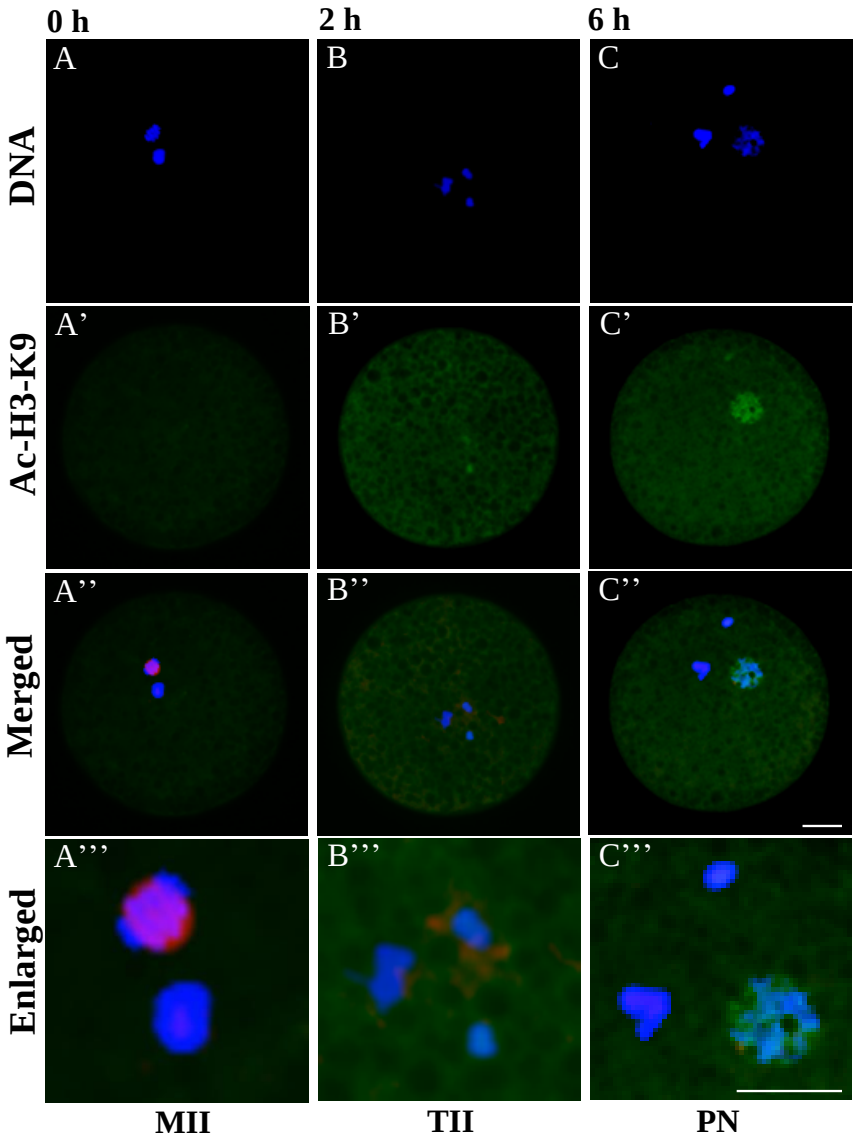

Fig. 3.18. Histone H3-K9 reacetylation (Ac-H3-K9) in electro-activated pig MII-oocytes. Oocytes were cultured for maturation for 42 h, and then electro-activated. Oocytes were examined after 0, 2, and 6 h by immunostaining with anti-acetyl-histone H3-K9 and Alexa 488-labeled antibodies for Ac-H3-K9 (green), and anti-α tubulin and Alexa 568-labeled antibodies for the microtubule (red). The chromosome was counterstained by DAPI (blue). The meiotic stages are **A-A'''**) Metaphase II (MII), **B-B'''**) Telophase II (AII), and **C-C'''**) Pronucleus stage (PN**)**. Scale bar = 20 μm.

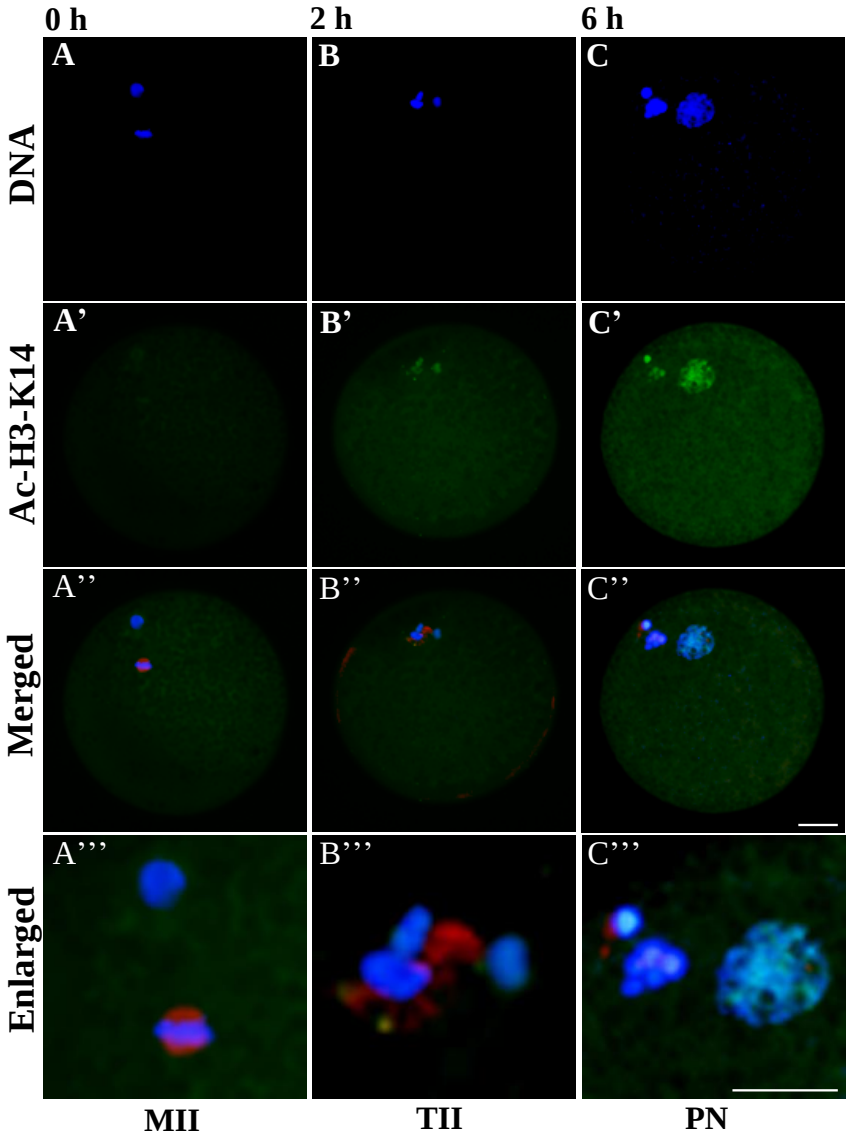

Fig. 3.19. Histone H3-K14 reacetylation (Ac-H3-K14) in electro-activated pig MII-oocytes. Oocytes were cultured for maturation for 42 h, and then electro-activated. Oocytes were examined after 0, 2, and 6 h by immunostaining with anti-acetyl-histone H3-K14 and Alexa 488-labeled antibodies for Ac-H3-K14 (green), and anti-α tubulin and Alexa 568-labeled antibodies for the microtubule (red). The chromosome was counterstained by DAPI (blue). The meiotic stages are **A-A'")** Metaphase II (MII), **B-B'")** Telophase II (AII), and **C-C'")** Pronucleus stage (PN**)**. Scale bar = 20 μm.

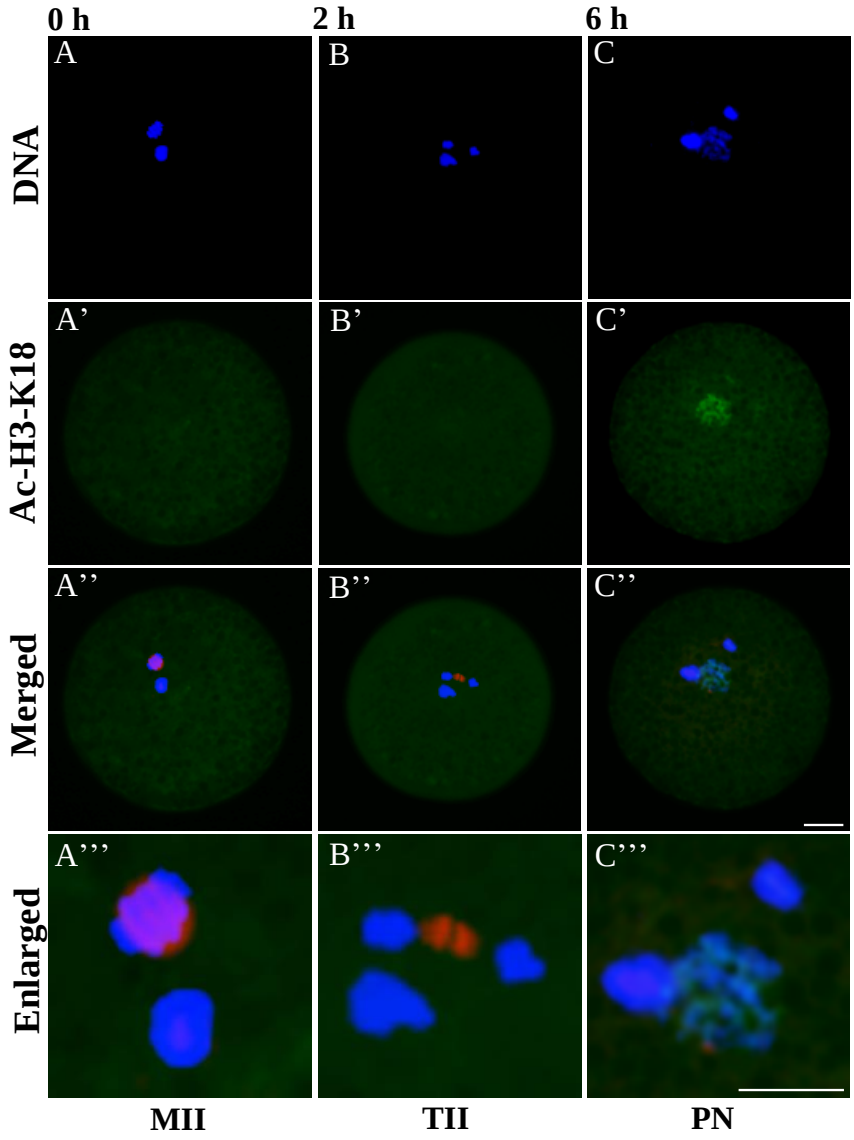

Fig. 3.20. Histone H3-K18 reacetylation (Ac-H3-K18) in electro-activated pig MII-oocytes. Oocytes were cultured for maturation for 42 h, and then electro-activated. Oocytes were examined after 0, 2, and 6 h by immunostaining with anti-Acetyl-histone H3-K18 and Alexa 488-labeled antibodies for Ac-H3-K18 (green), and anti-α tubulin and Alexa 568-labeled antibodies for the microtubule (red). The chromosome was counterstained by DAPI (blue). The meiotic stages are **A-A'')** Metaphase II (MII), **B-B'')** Telophase II (AII), and **C-C'')** Pronucleus stage (PN**)**. Scale bar = 20 μm.

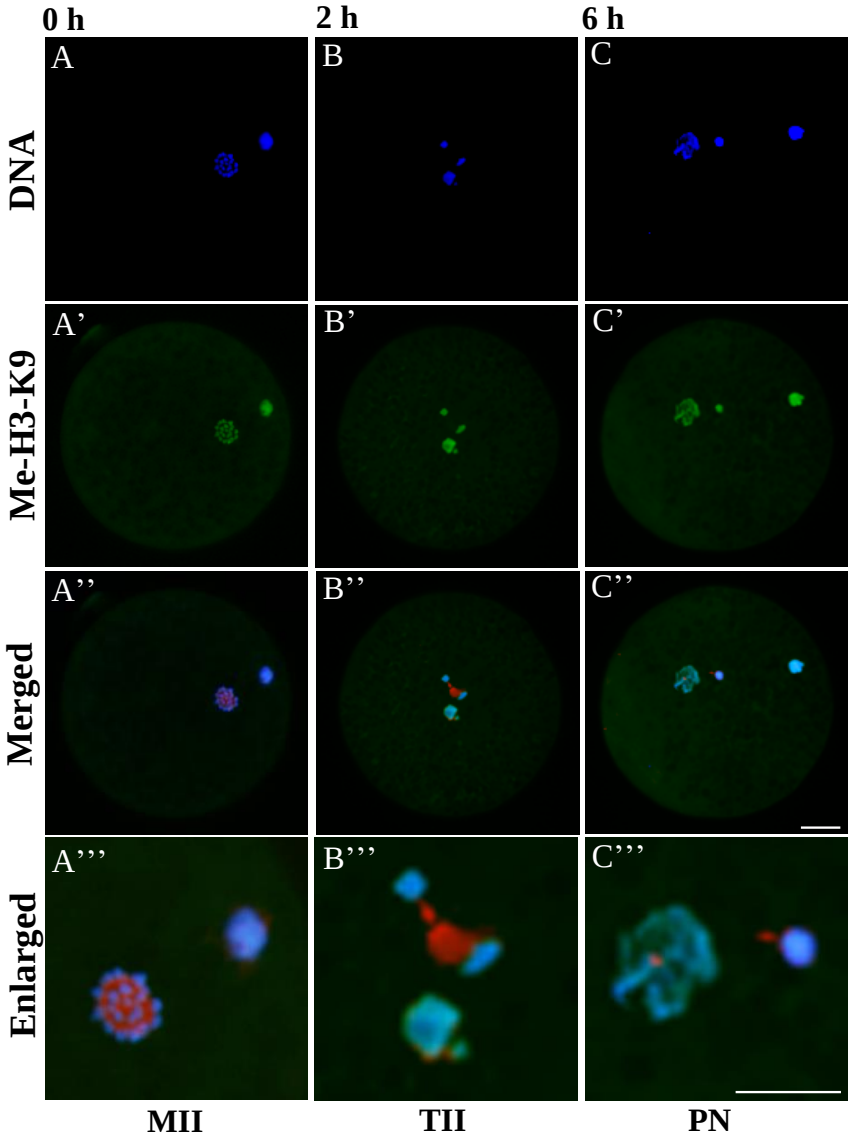

Fig. 3.21. Histone H3-K9 methylation (Me-H3-K9) in electro-activated pig MII-oocytes. Oocytes were cultured for maturation for 42 h, and then electro-activated. Oocytes were examined after 0, 2, and 6 h by immunostaining with anti-methyl-histone H3-K9 and Alexa 488-labeled antibodies for Me-H3-K9 (green), and anti-α tubulin and Alexa 568-labeled antibodies for the microtubule (red). The chromosome was counterstained by DAPI (blue). The meiotic stages are **A-A'")** Metaphase II (MII), **B-B'")** Telophase II (AII), and **C-C'")** Pronucleus stage (PN**)**. Scale bar = 20 μm.

3.4. DISCUSSION

In this study, the correlation between morphology of chromatin/chromosome and histone H3 phosphorylation, acetylation, and methylation throughout oocyte growth, maturation, and activation was investigated. The findings suggest that the morphological change in growing oocyte chromatin is probably regulated by acetylation of histone H3, and that the chromosome condensation during oocyte maturation is regulated by phosphorylation of histone H3 at two serine residues, S10 and S28. After oocyte activation, acetylation and dephosphorylation of histone H3 correlate to the decondensation of chromosomes. The data also indicate that histone acetylation and phosphorylation are reversible, whereas histone methylation has the energetic stability and is established during the oocyte growth phase.

Follicle development in pig is associated with the growth of oocytes in which progressive change in nuclear organization occurs. The nuclear morphology of growing oocytes was characterized by decondensed chromatin with a vacuolated nucleolus. It has been known that pig oocytes acquire the meiotic competence as the chromatin changes from the decondensed state to condensed state (Hirao et al., 1995). It has also been known that there is a concomitant change in the patterns of heterochromatin and the nucleoli progressively from transcriptionaly active to inactive state in pig oocytes (Motlik et al., 1984). Chromatin of the oocytes in secondary follicles was distributed in patches over the nucleoplasm and did not appear to be condensed in the present experiment. As the oocyte diameter increased, orcein-positive nucleoli became orcein-negative and the chromatin became more heterogeneous, in part heavily condensed to form heterochromatin rim around the nucleolus. When oocytes reached the final size, the nucleoli were observed to be encapsulated by highly condensed heterochromatin. These observations correspond to the findings by Hirao et al. (1995). Compaction of nucleolus during oocyte growth results in the extrusion of the granules into the central vacuole or the surrounding nucleoplasm (Fair et al., 1996). Fibrous nucleoli are not stained by orcein. It has been thought that RNA is synthesized in granular component in nucleoli (Fiil 1976; Kopecny et al., 1996). Therefore, the morphological change of orcein-stained nucleoli to orcein-negative one perhaps reflects the transcriptional inactivation. The acetylation of nuclear core histones has been shown to play an important role in the regulation of gene expression by producing conformational changes in

chromatin structure, which render the DNA accessible to transcription factors during interphase (Turner et al., 1998). The acetylation of H3-K9, H3-K14, and H3-K18 was detected in chromatin patches spreading over the nucleoplasm of the growing pig oocytes at the filamentous chromatin stage in secondary follicles at 0.1-0.2 mm in diameter. The modulation pattern of chromatin configurations from decondensed to peri-nucleolar heterochromatin sheath involved transition of the histone H3 status from hyper-acetylation to hypo-acetylation of histone H3 at K9, K14, and K18. This indicates that deacetylation of histone H3 reflects the chromatin remodeling with the decrease of the transcription activity in pig oocytes.

Studies in fungi and plants have revealed a relationship between DNA methylation and histone H3-K9 methylation, and have suggested that DNA methylation acts downstream of histone H3-K9 methylation (Tamaru and Selker, 2001). In the present experiments, any methylation signal of histone H3-K9 was found in the pig oocytes from secondary follicles. The methylation of H3-K9 appeared in chromatin knobs in growing oocytes from the antral follicles increasing in size from 1 to 2 mm. Then, towards the end of the growth phase, H3-K9 became highly methylated. The result of histone H3 methylation in this study appears to correspond to the reports in DNA methylation of oocytes. DNA methylation is proposed to be the imprinting signal (Wutz et al., 1997). Non-growing mouse oocyte is lack of maternal imprinting (Obata et al., 1998) and the imprinting is established during the oocyte growth (Obata and Kono, 2002). Recently, a report in mice suggested that the DNA methylation acquirement takes place in every imprinted gene correlative with oocyte size. In the present experiments, histone H3 methylation at K9 was acquired in the oocytes about 90 μm in diameter. The growth stage corresponds to the stage where oocytes showed the decrease in acetylation at H3-K9. Moreover, this stage is thought that oocytes have the initiation of transcriptional repression (De La Fuente and Eppig 2001). Therefore, oocytes acquire the histone H3 methylation as the change from transcriptionaly active to inactive. In addition, the present result showed that the methylation became high in the entire condensed heterochromatin ring at GVI stage when oocytes reached the final size. This may indicate that the complete acquisition of histone H3 methylation corresponds to the formation of heterochromatin in fully-grown oocytes.

Cdc2 kinase and histone H3 kinase were inactive in growing pig oocytes. Histone H3 phosphorylation of S10 and S28 was negative in these oocytes. The results suggest that there is

no histone H3 phosphorylation in growing pig oocytes, and that the phosphorylation is not involved in the change in the chromatin morphology and perhaps in the transcriptional activity. These findings are quite different from somatic cells where histone H3-S10 is phosphorylated in both interphase and mitosis (Cheung et al., 2000a).

There are many events that specifically occur during meiotic cell cycle. For example, two rounds of nuclear divisions follow a single round of DNA replication. Moreover, the oocyte genome must be reprogrammed during maturation, which is followed by fertilization to allow the remarkable transformation from differentiated oocytes into the totipotent embryos of the next generation (Schultz et al., 1999). Therefore, the gene expression patterns of immature oocytes need to be reprogrammed, and the new program is established before fertilization. In the present experiment, methylation of histone H3-K9 was actually maintained during oocyte maturation perhaps for preserving the meternal genomic imprinting. On the other hand, all of histone H3 acetylation levels decreased dramatically during oocyte maturation. It indicates that the deacetylation may be involved in genome remodeling by erasing the epigenetic markers for active genes in the oocytes, and renovating the gene expression pattern. In addition, it has been suggested that histone acetylation is associated with DNA replication (Jeppesen and Turner 1993; Zhang et al., 2002). Meiotic maturation of oocytes has two successive M phases without intervening DNA replication. Thus, histone H3 deacetylation is possible to be a prerequisite for the absence of DNA replication during oocyte maturation. In the present experiment, all of the acetylation of H3-K9, H3-K14, and H3-K18 completely disappeard around GVBD and the deacetylated status was maintained during oocyte maturation. However, histone H3-K9 and H3-K14 were temporarily acetylated around the MI/MII transition. A low level of acetylation of H3-K9 reappeared at TI and disappeared again at MII. Similarly, the acetylation of H3-K14 temporarily appeared around AI and TI, and disappeared at MII. Since there is no transcriptional activity during oocyte maturation (Bachvarova, 1985), the change in histone acetylation would not be associated with gene expression. Histone acetylation is a dynamic process that is regulated by two kinds of enzymes, histone acetyltransferases (HATs) and histone deacetylases (HDACs). It has been suggested that during mitosis, HATs and HDACs are unable to acetylate or deacetylate histones because the enzymes are spatially reorganized and displaced from condensing chromosomes (Kruhlak et al., 2001). In contrast, Kim et al. (2003) have indicated that

HDACs are able to deacetylate histones and HATs are inactivated specifically during maturation of mouse oocytes. Thus, there are some differences in the regulation of histone deacetylation in mitosis and meiosis. During MI/MII transition of oocytes, Cdc2 kinase activity fell at AI-TI as shown in Chapter 2. This oscillation pattern of Cdc2 kinase activity coincides with the temporal acetylation of histone H3-K9 and H3-K14 at MI/MII transition. Thus, it is likely that the histone H3 acetylation is dependent on the Cdc2 kinase activity directly or indirectly.

Histone H3-S10 was phosphorylated in condensed chromosomes in pig oocytes during maturation as shown in the previous chapter. In addition, the phosphorylation of H3-S28 was detected earlier in condensing chromosomes in pig oocytes at GVII-IV stage after 9 h of maturation culture. Since chromosome condensation began at this point, the observations led to the idea that phosphorylation of H3-S28 might be one of the key events initiating meiotic chromosome condensation. The activity of histone H3 kinase increased in oocytes after 9 h of culture. The activation occurred at the similar time course to that of phosphorylation of histone H3-S28. The fluorescent signal of H3-S28 was seen first around the nucleolus in the germinal vesicle after 9 h, and it extended throughout the whole chromosomes after 15 h. The phosphorylation of histone H3-S10 occurred after 18 h (in Chapter 2) which was later than the activation of H3 kinase.

The histone code hypothesis predicts that specific combinations of histone modifications provide regulatory information through changes in the structure of chromatin (Strahl and Allis, 2000; Jenuwein and Allis, 2001). In this hypothesis, modification of one residue in a histone may affect the type and frequency of modifications at other sites. Since chromosome condensation in pig oocytes takes a long time, it is possible to dissect the each step of histone modification. In the first step, after 9 h of culture, H3 kinase was activated and histone H3-S28 started to be phosphorylated while H3 acetylation was still maintained. In the second step, after 18 h, acetylation of histone H3 started to decrease, especially Ac-H3-K9 completely disappeared concomitant with the appearance of phosphorylation of H3-S10 at this stage. This suggests that deacetylation of H3-K9 and phosphorylation of H3-S10 possibly affect on each other. This corresponds to the reports in budding yeasts and nematodes where the decrease in acetylation of H3-K9 level was observed when the H3-S10 phosphorylation level increased (Hsu et al., 2000). Beside that, histone acetylation levels of H3-K14 and H3-K18 decreased remarkably at the

diakinesis stage when H3-S10 started to be phosphorylated. This is opposite to the change in somatic cells where histone H3-S10 phosphorylation facilitates the acetylation of H3-K14 (Cheung et al., 2000b). The metaphase chromosomes in pig oocytes were always found to be heavily phosphorylated at both S10 and S28 but to be deacetylated at H3-K9, H3-K14, and H3-K18. However, histone H3 phosphorylation at S28 started earlier than S10. It has been reported that in mitotic chromosome condensation, Aurora-B kinase directly phosphorylates histone H3-S10 and H3-S28 in mammals (Goto et al., 2002). Because S28 position is farer from K9, K14, and K18 than S10, the phosphorylation at S28 is possibly not under the influence of interactions between phosphorylation and acetylation of other residues.

The data showed that the methylation of histone H3-K9 was maintained during oocyte maturation regardless of the phosphorylation of H3-S10 and H3-S28, and deacetylation at H3-K9, H3-K14, and H3-K18. The methylation level of H3-K9 was still high after activation of oocytes until the pronucleus stage. It has been suggested that there is a direct link between histone methylation and DNA methylation pathways (Tamaru and Selker 2001). This idea is supported by the present results, which suggest that methylation of histone H3-K9 is involved in the propagation of genomic function through the preservation of stable methylation during maturation and after activation of oocytes. The energetic stability of histone methylation may have a role in enhancing epigenetic stability. The methylation level of H3-K9 was high regardless the reappearance of acetylation of H3-K9, H3-K14, and H3-K18 at TII, AII, and the pronucleus stages after electro-activation. These observations were similar to the recent report where the methylated H3-K9 was detected in chromosomes in MII mouse oocytes and in the female pronucleus of one-cell embryos (Liu et al., 2004). Aoki and Schultz (1999) suggested that during the one-cell stage, DNA replication occurred asynchronously between the two pronuclei, in that the female pronucleus required a longer time to complete replication. Moreover, methylated H3-K9 recruits HP1, an essential protein constituting hetrochromatin (Bannister et al., 2001), and this protein is accumulated only in the female pronucleus in mouse embryos at the 1 cell stage (Arney et al., 2002). The present results showed that the methylation of H3-K9 was similarly maintained after activation until pronucleus stage in pig oocytes.

After electro-activation of pig oocytes, acetylation of H3-K14 reappeared at AII. The histone H3 at S10 and S28 were dephosphorylated at TII. The reappearance of acetylation of H3-K9 was

concomitant with the drop of phosphorylation of H3-S10 and H3-S28. This result reinforces the suggestion described above that the histone phosphorylation/dephosphorylation coincides with the wave of the acetylation. Chromosomes were completely decondensed and H3-S10 was completely dephosphorylated at the time of pronucleus formation. Fluorescent signals of Ac-H3-K9 increased at the same time. These data are supported by the results indicating that phosphorylation of histone H3-S10 antagonizes acetylation of H3-K9 in yeast (Edmondson et al., 2002). Transcription is initiated in the one-cell stage embryos (Aoki et al., 1997). The reappearance of acetylation at H3-K14 and H3-K9 at AII and TII, and H3-K18 at the pronucleus stage appeared to prepare for the transcription.

In conclusion, the findings in this chapter suggest that chromatin morphology and chromosome condensation/decondensation of pig oocytes are regulated by acetylation/ deacetylation and phosphorylation/dephosphorylation of histone H3. It is also shown that the oocytes in secondary follicles lack of histone H3-K9 methylation and the methylation is established correlative with oocyte growth. Although histone acetylation and phosphorylation are reversible, the stable methylation of H3-K9 is maintained through oocyte maturation. Furthermore, it is suggested that the ordered phosphorylation of histone H3 at S10 and S28 is thought to be influenced by other modifications, namely acetylation of neighboring lysines in the histone H3 molecule.

Chapter 4. Chromosome Condensation and Decondensation of the Somatic Cell Nuclei Injected into Mature Oocytes

4.1. INTRODUCTION

Recent successes in mammalian cloning with differentiated adult nuclei strongly indicate that oocyte cytoplasm contains unidentified reprogramming activities with the capacity to erase the previous memory of cell differentiation (Wilmut et al., 1997; Wakayama et al., 1998). The breakthrough of animal cloning by using adult somatic cells has opened new ways of investigation in basic cell biology, and reproductive sciences. Mammalian cloning has been achieved by introducing the nucleus of a donor cell into an enucleated mature oocyte. It makes possible to study on the interaction of the donor nucleus with the oocyte cytoplasm after embryo reconstruction. Following nuclear transfer, nuclear reprogramming a process of returning a differentiated somatic nucleus to a topitotent stage is a prerequisite for the clonal development of reconstructed embryos.

The early reprogramming consists of morphological remodeling of the donor nucleus which includes nuclear membrane breakdown, initial chromatin condensation, spindle assembly, and pronuclear formation after activation. It is suggested that a high level of Cdc2 kinase activity in the enucleated MII oocytes induces breakdown of the nuclear membrane of the transferred nucleus, resulting in chromosome condensation within the cytoplasm of the ooplast (Campbell et al., 1996; Tani et al., 2001). When a stimulus for activation is applied, activity of Cdc2 kinase decreases, resulting in chromosome decondensation and formation of a pronucleus-like structure. As revealed in Chapters 2 and 3, histone H3-S10 and H3-S28 are phosphorylated in condensed chromosomes in pig oocytes during maturation, and the chromosome condensation is correlated with histone H3 kinase activity. Therefore, it needs to elucidate whether histone H3 phosphorylation is involved in the change in chromosome morphology of transferred somatic nuclei as it does in oocyte chromosomes.

The timing of oocyte activation after nuclear transfer is considered to be an important factor

in the efficiency of cloned embryo production (Fulka et al., 2001). The time of oocyte activation reported has varied among species, for example, immediately to 10 h after nuclear transfer in cattle (Wells et al., 1999; Kato et al., 2000; Kasinathan et al., 2001), immediately to 4 h in pigs (Onishi et al., 2000; Polejaeva et al., 2000; De Sousa et al., 2002; Walker et al., 2002), and immediately to 6 h in mice (Wakayama et al., 1998). The effect of activation timing on the development of cloned embryos may be largely through modulation of the degree of nuclear reprogramming achieved. The timing of nuclear transformation depends on donor cell types, cell-cycle stage, and species. However, it is suggested that the length of direct exposure time of chromosomes of somatic cells to the ooplasm is important in reprogramming of the chromatin to support embryo development (Wakayama and Yanagimachi, 2001).

The methylation and acetylation of histones H3 are thought to play important roles in the regulation of gene expression and to be essential for normal development in cloned embryos. Histone H3 in somatic cells for the nuclear transfer may be differently phosphorylated, methylated, and acetylated, and the modifications would change under the influence of ooplasm. Moreover, histone H3 phosphorylation and acetylation of the oocyte itself also change during decondensation of chromosomes after electro-activation as described in Chapter 3. It has to be elucidated whether such processes occur in a similar way in the chromosomes of the somatic cells transferred into oocytes.

The study in this chapter was carried out to determine the involvement of histone H3 phosphorylation, acetylation, and methylation in the change in chromosome morphology of the somatic nucleus transferred into *in vitro* matured pig oocytes. Next, injected pig oocytes with somatic cell nucleus were electro-activated, and the chromosome morphology of the oocytes and injected somatic cell nucleus were examined in correlation with their histone modifications in the same oosplasm.

4.2. MATERIALS AND METHODS

4.2.1. Collection and Maturation Culture of Oocytes

OCGCs from follicles 4-6 mm in diameter were collected from pig ovaries and cultured in

the same manner described in Section 2.2.1. OCGCs were cultured for 45 h for maturation. After culture, oocytes were denuded from cumulus cells completely by hyaluronidase and gentle pipetting, and used for nuclear transfer experiments.

4.2.2. Collection and Culture of Somatic Cells

Healthy pig antral follicles of 4-6 mm in diameter were everted in HEPES-199 to collect mural granulosa cells using two pairs of fine forceps. Granulosa cells were dispersed by vigorously aspirating them in and out of a pipet, and then the suspention was transferred into a 1.5 ml tube. After centrifugation at 500 *g* for 3 min, the pellet was resuspended in PBS. This treatment was repeated 2 times. The resulting pellet of granulosa cells was resuspended in a small amount of Dulbecco's modified Eagle's medium (DMEM, Sigma Chemical Co.) supplemented with 10% fetal bovine serum, and the cells were seeded in the dish whose bottom had been covered by 0.1 % gelatin (Sigma Chemical Co.). Then 2 ml of DMEM was added into the culture dish. The granulosa cells were cultured in an atmosphere of 5% CO_2 in humidified air at 38.5^{o}C for 2 days. After culture, the granulosa cells were collected by trypsinization. Briefly, the culture medium was removed and the cells were rinsed thoroughly with PBS two times. Trypsin solution (Sigma Chemical Co.) was added to cover the cultured granulosa cells for 1 min, and then 2 ml of serum containing DMEM was added. Granulosa cells were dispersed and transferred into a tube. After three times washes and centrifugations in PBS, granulosa cells were suspended in HEPES-CZB (Chatot et al., 1989) (Fig. 4.1A).

4.2.3. Nuclear Transfer and Oocyte Activation

Nuclear transfer of granulosa cells was carried out using a piezo-actuated micromanipulator system (Prime Tech, Tsuchiura, Japan). Matured pig MII oocytes were placed in droplets (10 μl) of HEPES-CZB in a micro-manipulation chamber. The process of injection of somatic cell nuclei into MII oocytes is shown in Figs. 4.1B-E. Trypsinzed granulosa cells were transferred into droplets of HEPES-CZB containing 12% polyvinyl pyrrolidone (PVP, M_r 360 kDa; Wako, Japan). Plasma membrane of granulosa cell was removed using an injection pipet (6-8 μm in inner diameter) with several piezo pulses, and a single nucleus was injected into an oocyte near the

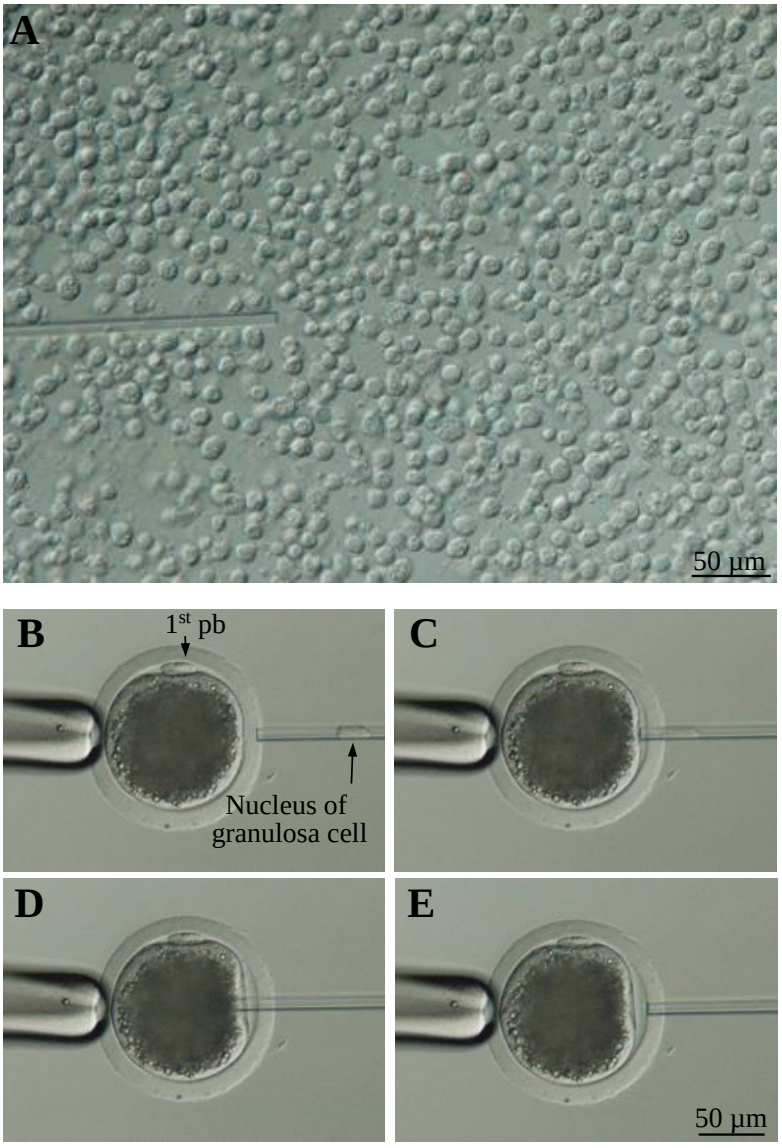

Fig. 4.1. A) Trypsinized pig granulosa cells after culture in DMEM for 2 days. **B-E)** Procedure of nuclear injection into pig oocytes by using a piezo-actuated micromanipulator system. **B)** Granulosa cell membrane was removed using an injection pipet (6-8 µm in diameter) with several piezo pulses and drew in and out of the injection pipet. 1st pb: 1st polar body. **C)** Opening hole on zona pelucida by piezo-action. **D)** Injection of a granulosa nucleus into an oocyte. **E)** Withdrawing the injection pipet from the oocyte.

holding pipet. After nuclear injection, oocytes were cultured in bicarbonate-buffered TCM-199 supplemented with 10% (v/v) heat-treated FCS, 0.1 mg/ml sodium pyruvate, 0.08 mg/ml kanamycine sulphate, and 2.2 mg/ml sodium bicarbonate. After culture for 1, 2, 3, 4, and 5 h, oocytes were fixed for the immunofluorescent microscopy.

Another group of injected oocytes were cultured in the same medium for 2 h before electro-activation. Oocytes were activated by the method described in Section 3.2.2. Oocytes were fixed for the immunofluorescent microscopy at 2, 4, 6, and 8 h after electro-activation.

4.2.4. Immunofluorescent Microscopy

The method for immunofluorescent staining of oocytes was described in Section 2.2.2 and 3.2.4. The first antibodies used here were rabbit polyclonal anti-phospho-histone H3 at serine 10 (Cell Signaling Technology Inc.), rabbit polyclonal anti-phospho-histone H3 at serine 28 (Upstate), rabbit polyclonal anti-trimethyl-histone H3 at lysine 9 (Abcam), rabbit polyclonal anti-acetyl-histone H3 at lysine 9 (Upstate), rabbit polyclonal anti-acetyl-histone H3 at lysine 14 (Upstate), and rabbit polyclonal anti-acetyl-histone H3 at lysine 18 (Upstate) antibodies. To determine the integrity of the nuclear membrane and the meiotic stage, mouse monoclonal antibody against anti-lamin A/C (Santa Cruz Biotechnology Inc.) and mouse monoclonal anti-αtubulin (Sigma Chemical Co.) antibodies were used. The conjugated second antibodies used here were Alexa Fluor 488-labeled goat anti-rabbit IgG (Molecular Probes Inc.) and Alexa Fluor 568-labeled goat anti-mouse IgG (Molecular Probes Inc.). The chromosomes were stained with propidium iodide (400 μg/ml; Sigma Chenical Co.) or 4, 6-diamidino-2-phenylindole (DAPI) (2 μg/ml; Molecular Probes Inc.). In the negative control, oocytes were reacted with nonimmune rabbit serum instead of rabbit polyclonal first antibodies, or with mouse IgG instead of mouse monoclonal anti-lamin A/C and anti-αtubulin antibodies.

4.2.5. Statistical Analysis

At least 40 immunostained oocytes were examined by the immunofluorescent microscopy in each group. The values were analysed using the chi-square test. P values less than 0.05 were considered statistically significant.

4.3. RESULTS

4.3.1. Chromosome Morphology and Histone H3 Modifications of Somatic cell Nuclei after Injection into Mature Oocytes

Pig oocytes maintained their MII stage for 5 h after nuclear transfer of granulosa cells (Tables 4.1 and 4.2). Histone H3 phosphorylation at S10 and S28 in the oocyte chromosomes was also maintained during the culture period.

Phosphorylation of histone H3-S10 and H3-S28 was not detected in any somatic nuclei immediately after injection (Fig. 4.2). Chromatin of injected somatic nuclei started to condense to make a single clump of chromosomes, as like the diakinesis stage of oocyte maturation, 0.5 h after nuclear transfer (Tables 4.1 and 4.2). In the clump of condensed chromosomes, histone H3 started to be phosphorylated at both positions S10 and S28 with 49% and 55%, respectively. Some of the somatic nuclei showed the metaphase-like stage but the percentage was low after 1 h. At this time, intensity of the fluorescent signal of phosphorylation of histone H3 was low at both S10 and S28. After 2 h, proportion of somatic cells showing metaphase-like chromosomes increased about 80%, thereafter the high proportion was maintained until 5 h after nuclear transfer. The highly phosphorylation of H3-S10 and H3-S28 in the condensed chromosomes of somatic cells was observed in more than 90% of oocytes between 2 and 5 h after nuclear transfer.

There were some differences between the morphologies of metaphase chromosomes of oocyte nuclei and somatic ones. The oocyte chromosomes were located in the metaphase plate of spindle, whereas somatic chromosomes were located on spindle poles or dispersed chaotically on the spindle. In addition, there were 20% of oocytes in which some chromosomes of somatic cells dispersed in ooplasm, out of the spindle (Fig. 4.3A). There were 10-15% of oocytes having somatic nuclei at the diakinesis-like stage even 2 h after nuclear transfer. In the oocytes, histone H3-S10 and H3-S28 were phosphorylated in the clumps of condensed chromosomes (Fig. 4.3).

Fluorescent signals were detected for all of the Ac-H3-K9, Ac-H3-K14, and Ac-H3-K18 in the somatic nuclei immediately after nuclear transfer (Figs. 4.4, 4.5, and 4.6). Intensity of the signal of Ac-H3-K9 decreased to a low level at 0.5 h and disappeared 1 h after nuclear transfer. The signals of Ac-H3-K14 and Ac-H3-K18 decreased after 1 h and disappeared after 2 h.

Table 4.1. Chromatin configurations and phosphorylation of histone H3-S10 in somatic cell nuclei transferred into pig MII-oocytes

Time after injection (h)	No. of oocytes injected	State of nuclei after injection into MII oocytes									
		Somatic nucleus						Oocyte nucleus			
		Int	D	M	P-H3-S10			MII	P-H3-S10		
					+	+/-	-		+	+/-	-
0.5	47	24 (51)[a]	23 (49)[a]	0 (0)[a]	9 (19)[a]	14 (30)[a]	24 (51)[a]	47 (100)	47 (100)	0 (0)	0 (0)
1	43	19 (44)[a]	20 (47)[a]	4 (9)[a]	8 (19)[a]	16 (37)[a]	19 (44)[a]	43 (100)	43 (100)	0 (0)	0 (0)
2	46	3 (7)[b]	7 (15)[b]	36 (78)[b]	42 (91)[b]	1 (2)[b]	3 (7)[b]	46 (100)	46 (100)	0 (0)	0 (0)
3	45	2 (5)[b]	6 (13)[b]	37 (82)[b]	43 (95)[b]	0 (0)[b]	2 (5)[b]	45 (100)	45 (100)	0 (0)	0 (0)
4	49	1 (2)[b]	6 (12)[b]	42 (86)[b]	47 (96)[b]	1 (2)[b]	1 (2)[b]	49 (100)	49 (100)	0 (0)	0 (0)
5	47	0 (0)[b]	5 (11)[b]	42 (89)[b]	47 (100)[b]	0 (0)[b]	0 (0)[b]	47 (100)	47 (100)	0 (0)	0 (0)

Somatic nuclei were injected into pig MII-oocytes. Oocytes were examined after 0, 1, 2, 3, 4, and 5 h for the chromosome morphology and histone phosphorylation (P-H3-S10) by the fluorescent microscopy. Int: Interphase, D: Diakinesis stage, and M: Metaphase. Levels of phosphorylation were classified into (+): hight levels of P-H3-S10, (+/-): low levels of P-H3-S10; and (-) : no P-H3-S10.

[a,b)] Values with different superscripts in the same column differ significantly ($P<0.05$).

Table 4.2. Chromatin configurations and phosphorylation of histone H3-S28 in somatic cell nuclei transferred into pig MII-oocytes

Time after injection (h)	No. of oocytes injected	State of nuclei after injection into MII oocytes									
		Somatic nucleus						Oocyte nucleus			
		Int	D	M	P-H3-S28			MII	P-H3-S28		
					+	+/-	-		+	+/-	-
0.5	40	18 (45)[a]	22 (55)[a]	0 (0)[a]	8 (20)[a]	14 (35)[a]	18 (45)[a]	40 (100)	40 (100)	0 (0)	0 (0)
1	41	15 (36)[a]	21 (51)[a]	5 (13)[b]	10 (24)[a]	16 (39)[a]	15 (37)[a]	41 (100)	41 (100)	0 (0)	0 (0)
2	47	3 (7)[b]	6 (12)[b]	38 (81)[c]	43 (91)[b]	1 (2)[b]	3 (7)[b]	47 (100)	47 (100)	0 (0)	0 (0)
3	44	1 (2)[b]	6 (13)[b]	37 (85)[c]	41 (94)[b]	2 (4)[b]	1 (2)[b]	44 (100)	44 (100)	0 (0)	0 (0)
4	43	0 (0)[b]	5 (11)[b]	38 (89)[c]	42 (98)[b]	1 (2)[b]	0 (0)[b]	43 (100)	43 (100)	0 (0)	0 (0)
5	48	0 (0)[b]	4 (9)[b]	44 (91)[c]	48 (100)[b]	0 (0)[b]	0 (0)[b]	48 (100)	48 (100)	0 (0)	0 (0)

Somatic nuclei were injected into pig MII-oocytes. Oocytes were examined after 0, 1, 2, 3, 4, and 5 h for the chromosome morphology and histone phosphorylation (P-H3-S28) by the fluorescent microscopy. Int: Interphase, D: Diakinesis stage, and M: Metaphase. Levels of phosphorylation were classified into (+): hight levels of P-H3-S28; (+/-): low levels of P-H3-S28, and (-) : no P-H3-S28.

[a-c)] Values with different superscripts in the same column differ significantly ($P<0.05$).

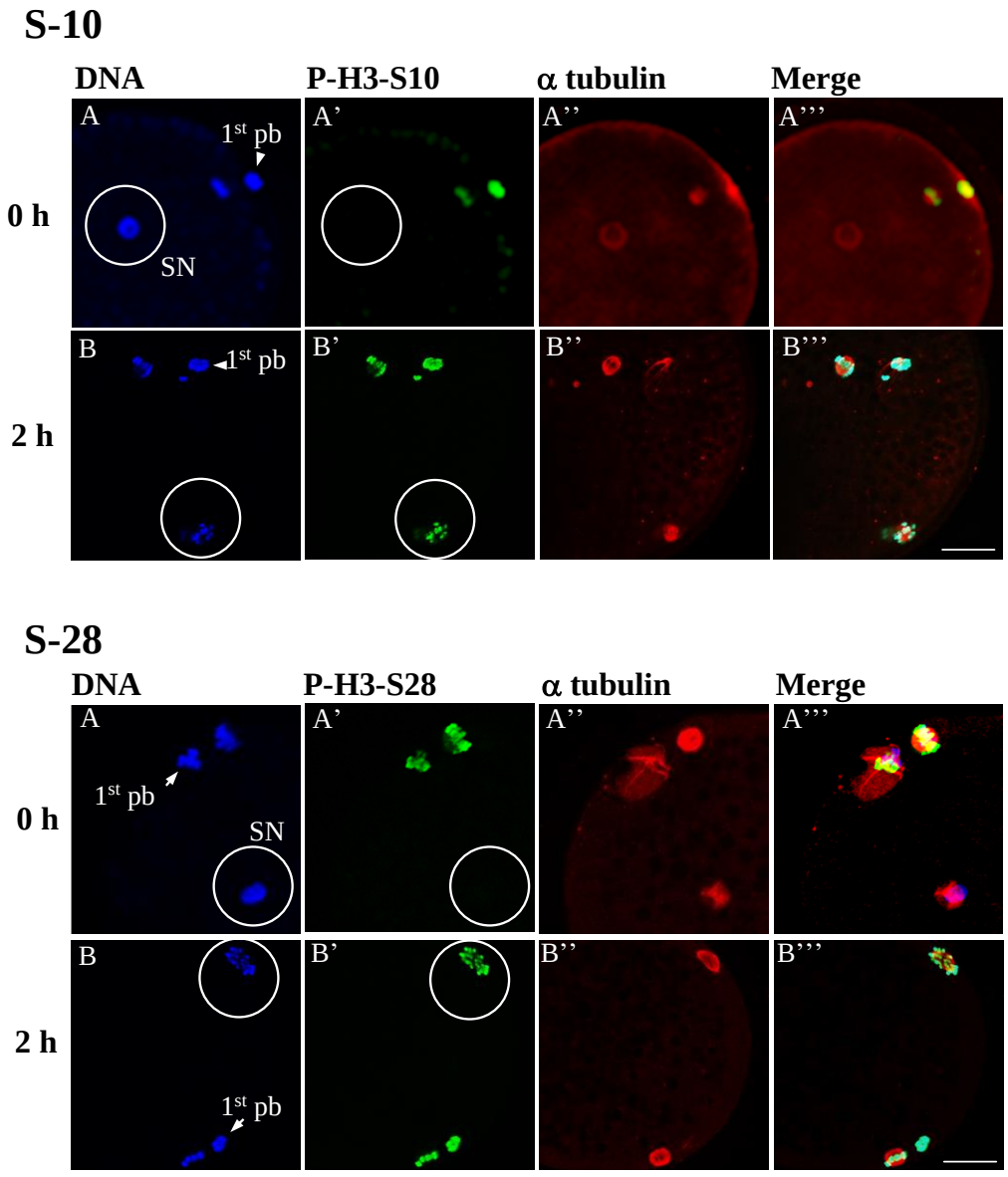

Fig. 4.2. Histone H3-S10 (S10) and H3-S28 (S28) phosphorylation of somatic nuclei transferred into pig MII-oocytes. Nuclei of pig granulosa cells were injected into MII oocytes. Oocytes were examined after 0 and 2 h by immunostaining with anti-phospho-histone H3-S10 and Alexa 488-labeled antibodies for the phosphorylated histone H3-S10, or anti-phospho-histone H3-S28 and Alexa 488-labeled antibodies for the phosphorylated histone H3-S28 (green), and anti-α tubulin and Alexa 568-labeled antibodies for the microtubules (red). The chromosome was counterstained by DAPI (blue). SN: somatic nucleus, 1st pb: first polar body. Scale bar = 20 μm.

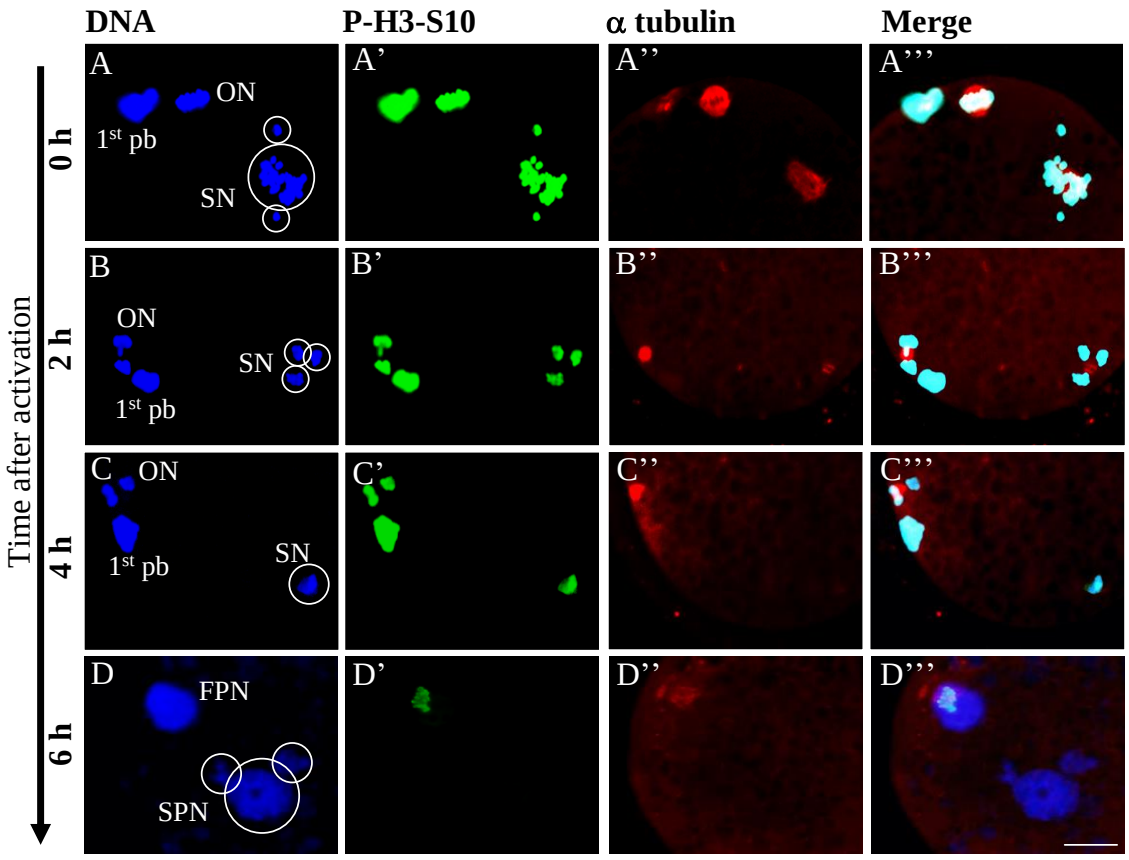

Fig. 4.3. Somatic cell chromosomes showing different morphologies in pig MII-oocytes. Nuclei of pig granulosa cells were injected into MII oocytes. Subsequently, the oocytes were cultured for 2 h and then electro-activated. Oocytes were examined after 2, 4, and 6 h by immunostaining with anti-phospho-histone H3-S10 and Alexa 488-labeled antibodies for the phosphorylated histone H3-S10 (green), and anti-α tubulin and Alexa 568-labeled antibodies for the microtubule (red). The chromosome was counterstained by DAPI (blue). ON: Oocyte nucleus, SN: Somatic nucleus, FPN: Female pronucleus, SPN: Somatic pronucleus. Scale bar = 20 μm.

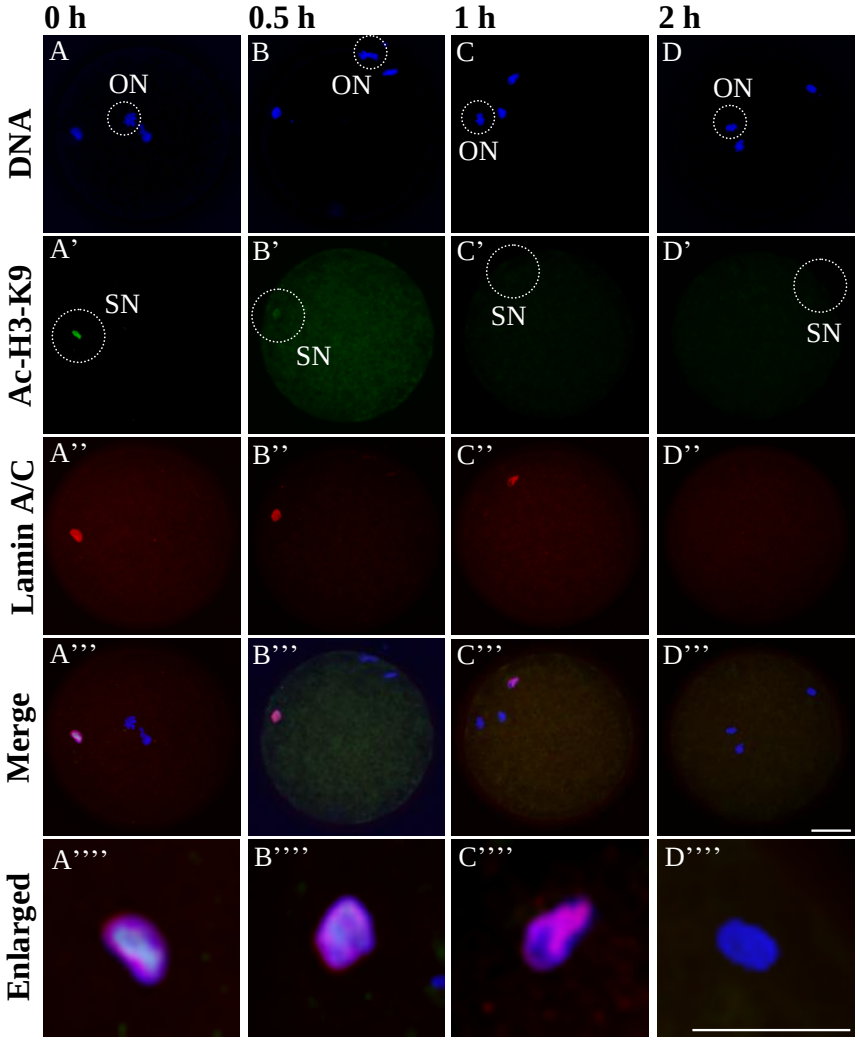

Fig. 4.4. Active deacetylation of histone H3-K9 (Ac-H3-K9) in somatic cell nuclei after injection into pig MII-oocytes. DAPI stained the chromosome (blue), anti-acetyl-H3-K9 and Alexa 488-labeled antibodies stained the acetylated H3-K9 (green), and anti-lamin A/C and Alexa 568-labeled antibodies stained the nuclear membrane (red). Oocytes injected with somatic cell nuclei were fixed at 0, 0.5, 1, and 2 h after nuclear transfer. ON: Oocyte nucleus, SN: Somatic nucleus. Scale bar = 30 µm.

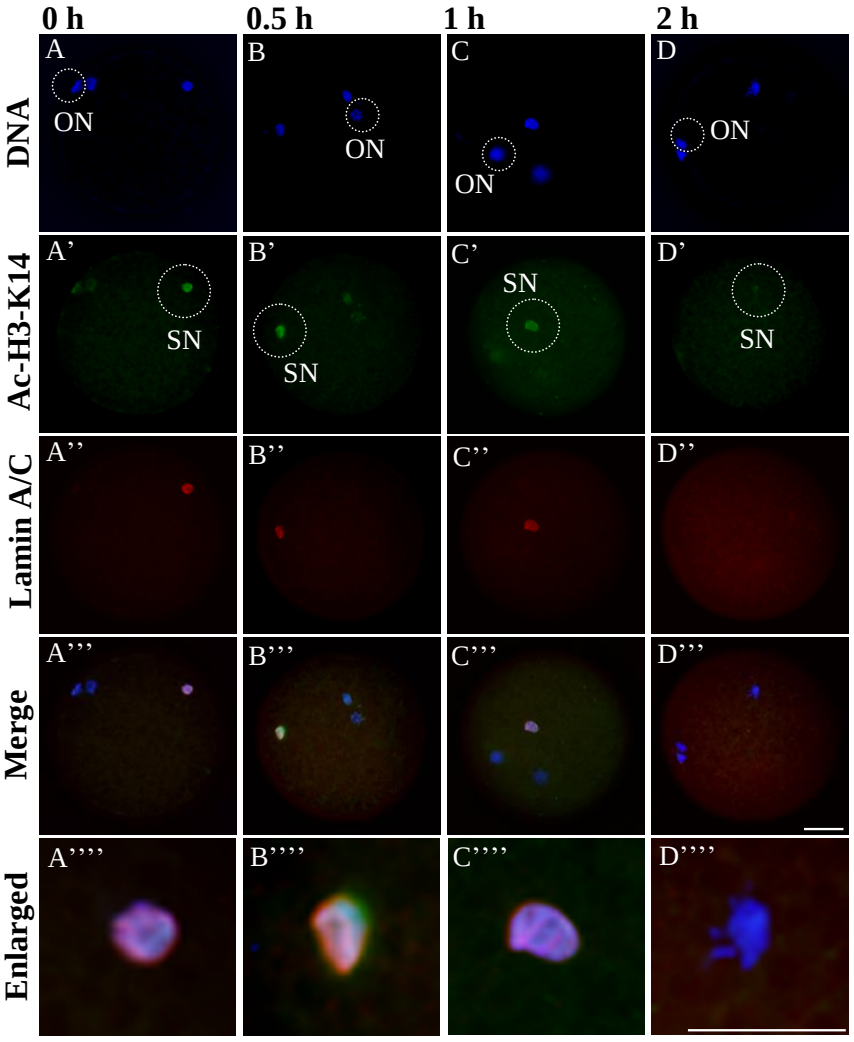

Fig. 4.5. Active deacetylation of histone H3-K14 (Ac-H3-K14) in somatic cell nuclei after injection into pig MII-oocytes. DAPI stained the chromosome (blue), anti-acetyl-H3-K14 and Alexa 488-labeled antibodies stained the acetylated H3-K14 (green), and anti-lamin A/C and Alexa 568-labeled antibodies stained the nuclear membrane (red). Oocytes injected with somatic cell nuclei were fixed at 0, 0.5, 1, and 2 h after nuclear transfer. ON: Oocyte nucleus, SN: Somatic nucleus. Scale bar = 30 μm.

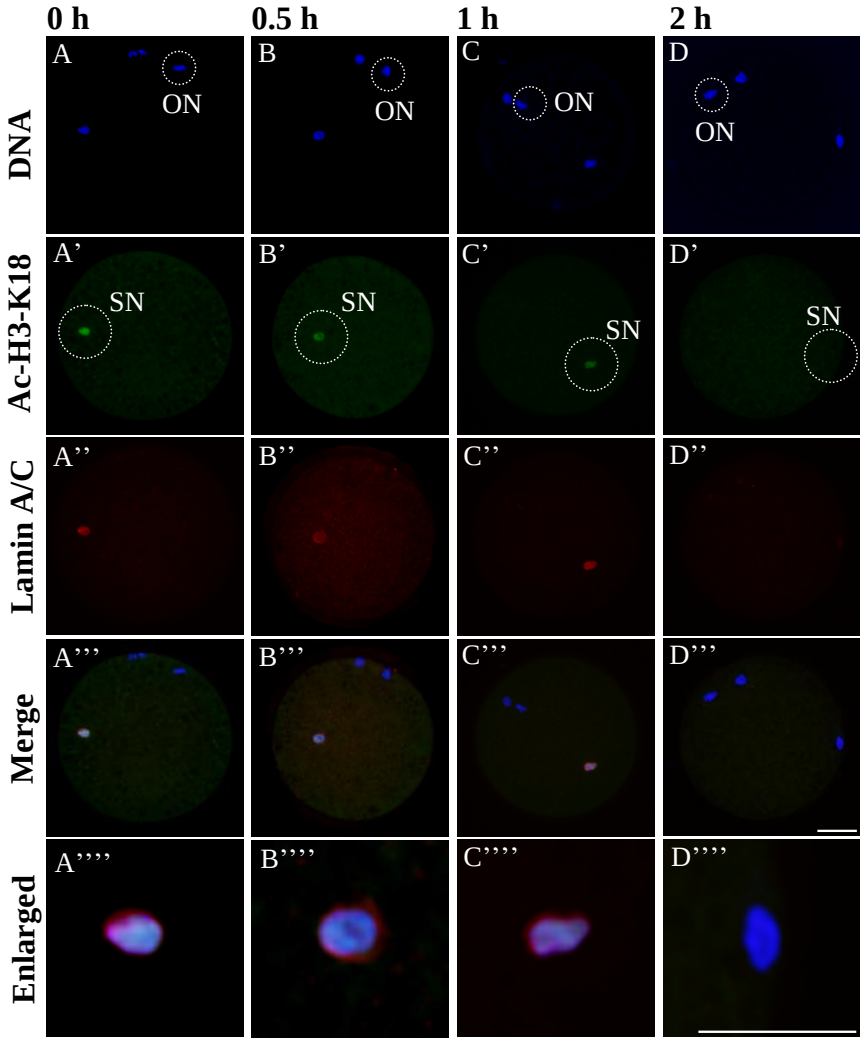

Fig. 4.6. Active deacetylation of histone H3-K18 (Ac-H3-K18) in somatic cell nuclei after injection into pig MII-oocytes. DAPI stained the chromosome (blue), anti-acetyl-H3-K18 and Alexa 488-labeled antibodies stained the acetylated H3-K18 (green), and anti-lamin A/C and Alexa 568-labeled antibodies stained the nuclear membrane (red). Oocytes injectied with somatic cell nuclei were fixed at 0, 0.5, 1, and 2 h after nuclear transfer. ON: Oocyte nucleus, SN: Somatic nucleus. Scale bar = 30 μm.

Integrity of the nuclear membrane of injected somatic cell nuclei was monitored by immunostaining with the anti-lamin A/C antibody. After 0.5 h, the antibody recognized the entire contour of somatic cell nuclei. After 1 h, the breakdown of nuclear membrane was observed in some somatic cell nuclei. After 2 h, most of the nuclear membranes had been completely disassembled (Figs. 4.4, 4.5, and 4.6).

The signal from the antibody that recognized the trimethylated form of H3-K9 was detected in somatic nuclei immediately after injection. The methylation was maintained until 2 h (Fig. 4.7).

4.3.2. Chromosome Morphology and Histone H3 Modifications of Injected Somatic Cell Nuclei after Electro-activation of Ooocytes

Proportion of somatic cell nuclei showing metaphase-like chromosomes increased 2 h after nuclear transfer and there was no statistical difference in the proportions after 2 h or later. Therefore, injected oocytes were electro-activated 2 h after injection of somatic cell nuclei to examine the changes in chromosome morphology and their histone modifications after oocyte activation.

Two hours after activation, about 90% of oocytes were at anaphase II/telophase II (AII-TII), and chromosomes of somatic cell nuclei in 50% of oocytes showed anaphase/telophase (A-T)-like morphology (Figs. 4.8, 4.9, and 4.10). The proportion increased to about 70% at 4 h after activation (Fig. 4.8). At this time, the decondensation of chromosomes started in some oocytes. After 6-8 h, oocyte chromosomes completely decondensed to form a female pronucleus, and somatic chromosomes also formed pronucleus-like structure.

After 2 h of electro-activation, the phosphorylation levels of H3-S10 and H3-S28 started to decrease in both oocyte and somatic chromosomes. The phosphorylation level of somatic chromosomes decreased earlier than that of oocyte chromosomes (Figs. 4.9 and 4.10). However, 4 h after electro-activation, the proportion of histone H3 dephosphorylated oocyte chromosomes was similar to that in somatic chromosomes. The phosphorylation of H3-S10 completely disappeared when the chromosomes decondensed in both female pronucleus and somatic pronucleus 6-8 h after electro-activation. However, the phosphorylation of histone H3-S28 was still maintained at the periphery of the nucleoli in both pronuclei.

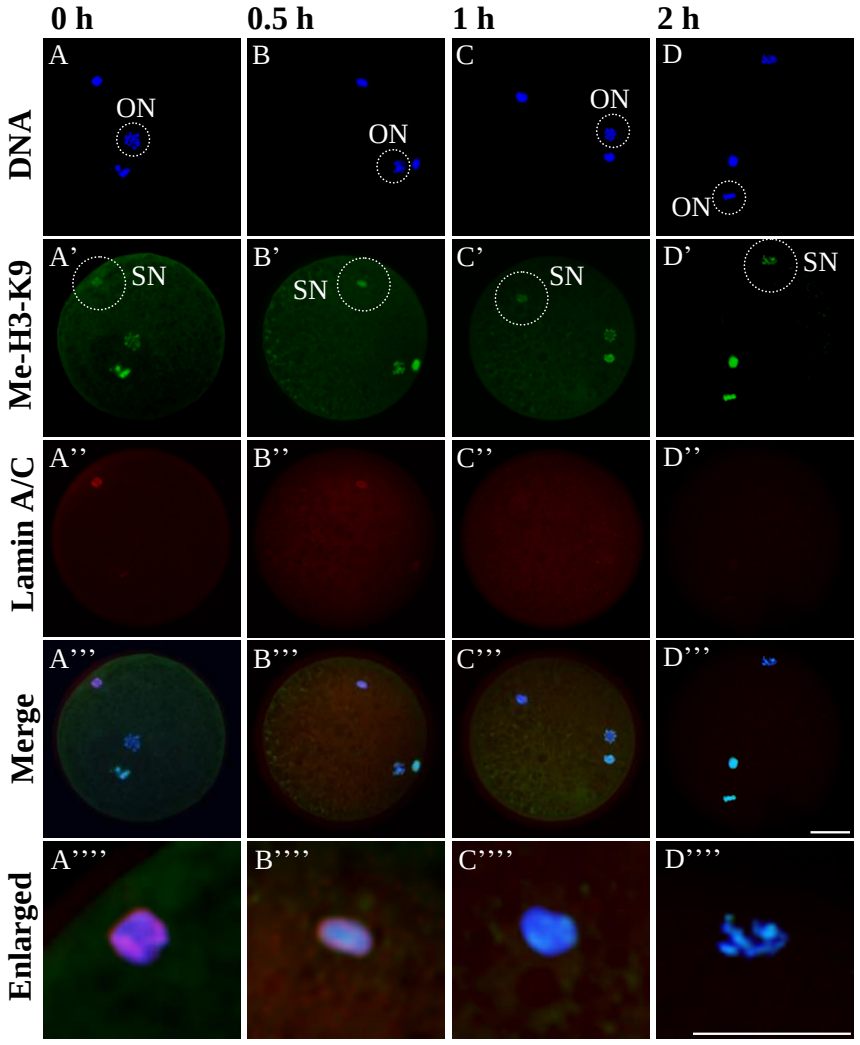

Fig. 4.7. Methylation of histone H3-K9 (Me-H3-K9) in somatic cell nuclei after injection into pig MII-oocytes. DAPI stained the chromosome (blue), anti-methyl-H3-K9 and Alexa 488-labeled antibodies stained the methylated H3-K19 (green), and anti-lamin A/C and Alexa 568-labeled antibodies stained the nuclear membrane (red). Oocytes injected with somatic nuclei were fixed at 0, 0.5, 1, and 2 h after nuclear transfer. ON: Oocyte nucleus, SN: Somatic nucleus. Scale bar = 30 μm.

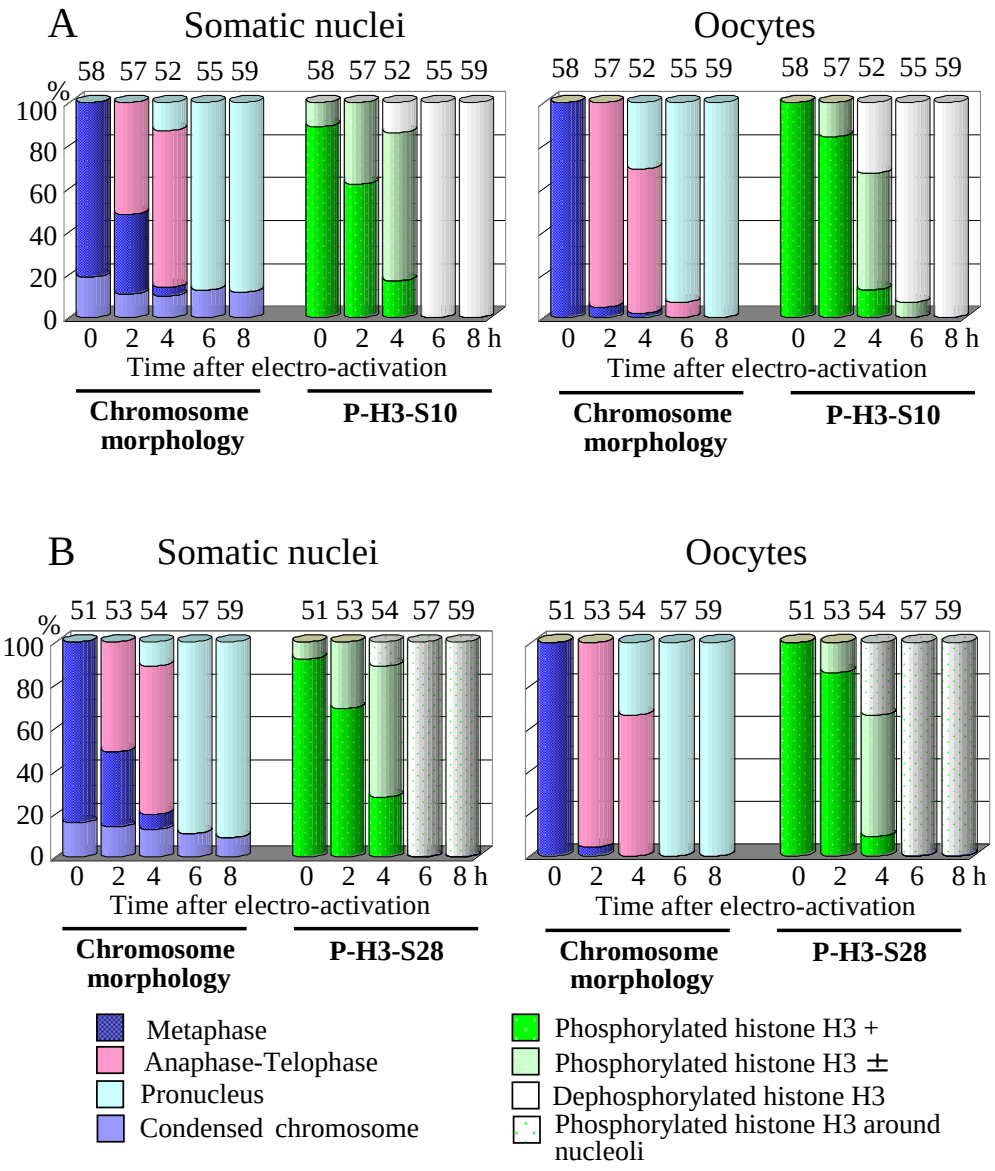

Fig. 4.8. Chromosome morphology and histone H3-S10 (A) and histone H3-S28 (B) phosphorylation of oocytes and injected somatic cell nuclei after electro-activation. Somatic nuclei were injected into pig MII-oocytes. Subsequently, the oocytes were cultured for 2 h and then electro-activated. Oocytes were examined after 0, 2, 4, 6, and 8 h. Figures above each colum shows number of oocytes examined. This experiment was repeated 5 times.

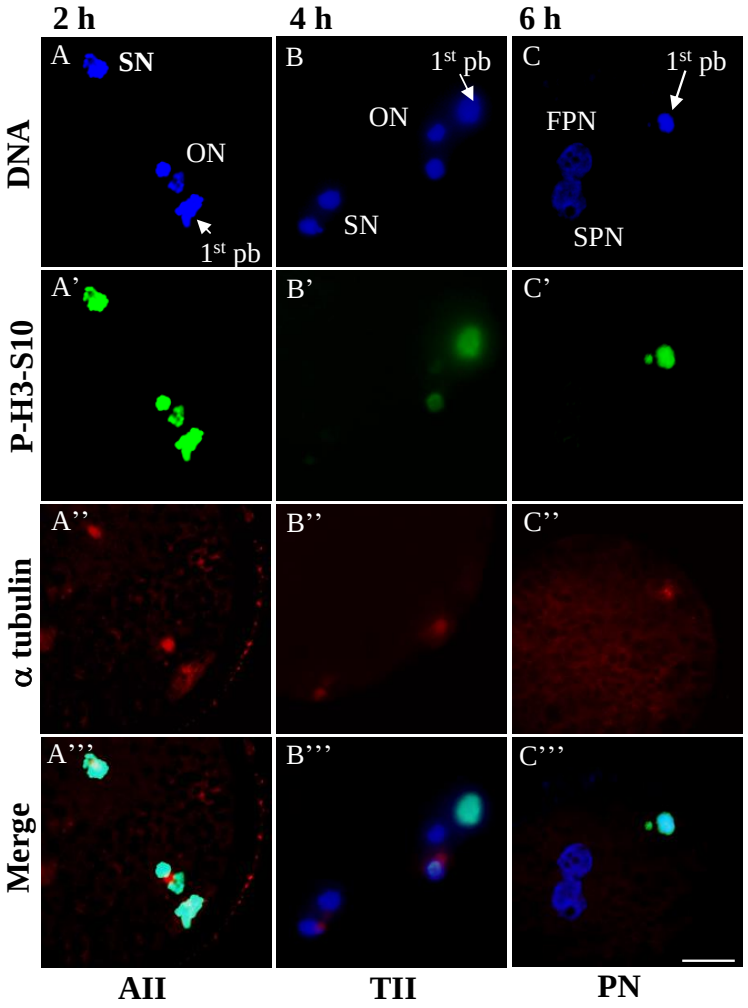

Fig. 4.9. Histone H3-S10 dephosphorylation of somatic cell chromosomes in electro-activated pig MII-oocytes. Oocytes were injected with pig granulosa cells. Subsequently, the oocytes were cultured for 2 h and then electro-activated. Oocytes were examined after 0, 2, 4, 6, and 8 h by immunostaining with anti-phospho-histone H3-S10 and Alexa 488-labeled antibodies for phosphorylated histone H3 (P-H3-S10, green), and anti-α tubulin and Alexa 568-labeled antibodies stained the microtubule (red). The chromosome was counterstained by DAPI (blue). SN: Somatic cell nucleus, ON: Oocyte nucleus, SPN: Somatic cell pronucleus, FPN: Female pronucleus. Meiotic stages are AII: Anaphase II, TII: Telophase II, and PN: Pronucleus stage. Scale bar = 20 μm.

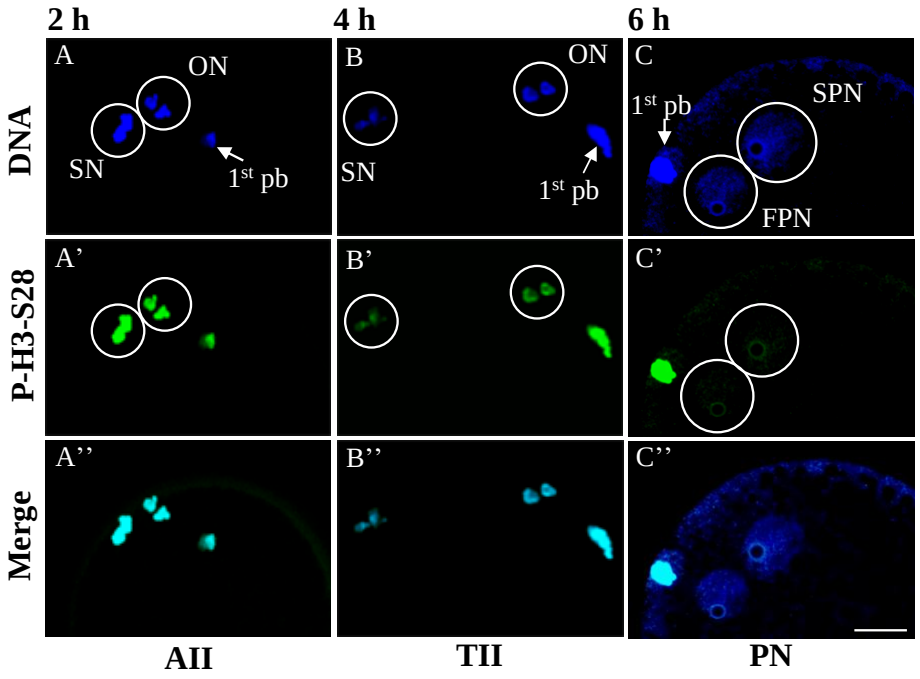

Fig. 4.10. Histone H3-S28 dephosphorylation of somatic cell chromosomes in electro-activated pig MII-oocytes. Oocytes were injected with pig granulosa cells. Subsequently, the oocytes were cultured for 2 h and then electro-activated. Oocytes were examined after 0, 2, 4, 6, and 8 h by immunostaining with anti-phospho-histone H3-S28 and Alexa 488-labeled antibodies for the phosphorylated histone H3 (P-H3-S28, green). The chromosome was counterstained by DAPI (blue). SN: Somatic cell nucleus, ON: Oocyte nucleus, SPN: Somatic pronucleus, FPN: Female pronucleus. Meiotic stages are AII: Anaphase II, TII: Telophase II, and PN: Pronucleus stage. Scale bar = 20 µm.

Generally, the somatic cell chromosomes showed similar morphological change to those of oocytes. In some cases, the meiotic stage of oocytes proceeded, whereas somatic chromosomes retained the clump shape (Fig. 4.3C). However, the phosphorylation and dephosphorylation of histone H3-S10 and H3-S28 in the somatic chromosomes changed in the similar manner to those of oocyte chromosomes.

The fluorescent signals of all acetylated lysines were absent in oocytes chromosomes and injected somatic nuclei 2 h after nuclear transfer (0 h of activation). The acetylation of H3-K14 reappeared in oocyte chromosomes at AII, then acetylation of H3-K9 appeared at TII. Thereafter, acetylation of H3-K18 appeared in oocytes at the pronucleus stage (Figs. 4.11, 4.12, and 4.13). The acetylation of H3 at all of K9, K14, and K18 in somatic chromosomes followed the change in oocyte chromosomes. However, in 20% of somatic chromosomes did not show the reappearance of H3 acetylation although they showed A-T-like morphology or pronucleus-like structure (Fig. 4.14).

After electro-activation, the methylation of H3-K9 was maintained in oocyte chromosomes and somatic chromosomes until pronucleus stage (Fig. 4.15). However, in some oocytes, the intensity of Me-H3-K9 was lower in somatic chromosomes than that in oocytes.

4.4. DISCUSSION

Arrest at MII of pig oocytes was maintained for examined 5 h after nuclear transfer of somatic cells. During the time nuclear remodeling of pig granulosa cells took place in the oocytes. A series of phenomena were observed during the first 2 h, such as nuclear membrane disassembly, chromosome condensation to form metaphase-like configuration, decrease in histone H3 acetylation levels and increase in histone H3 phosphorylation levels. These results showed that the nuclear stage and modifications of histone H3 in injected somatic nuclei were controlled by MII cytoplasm.

In 10-15% of oocytes, somatic nuclei formed clumps of condensed chromosomes like as diakinesis stages of oocyte during maturation. The morphology was maintained after subsequent electro-activation. This result corresponded with the result of the integrity of nuclear membrane

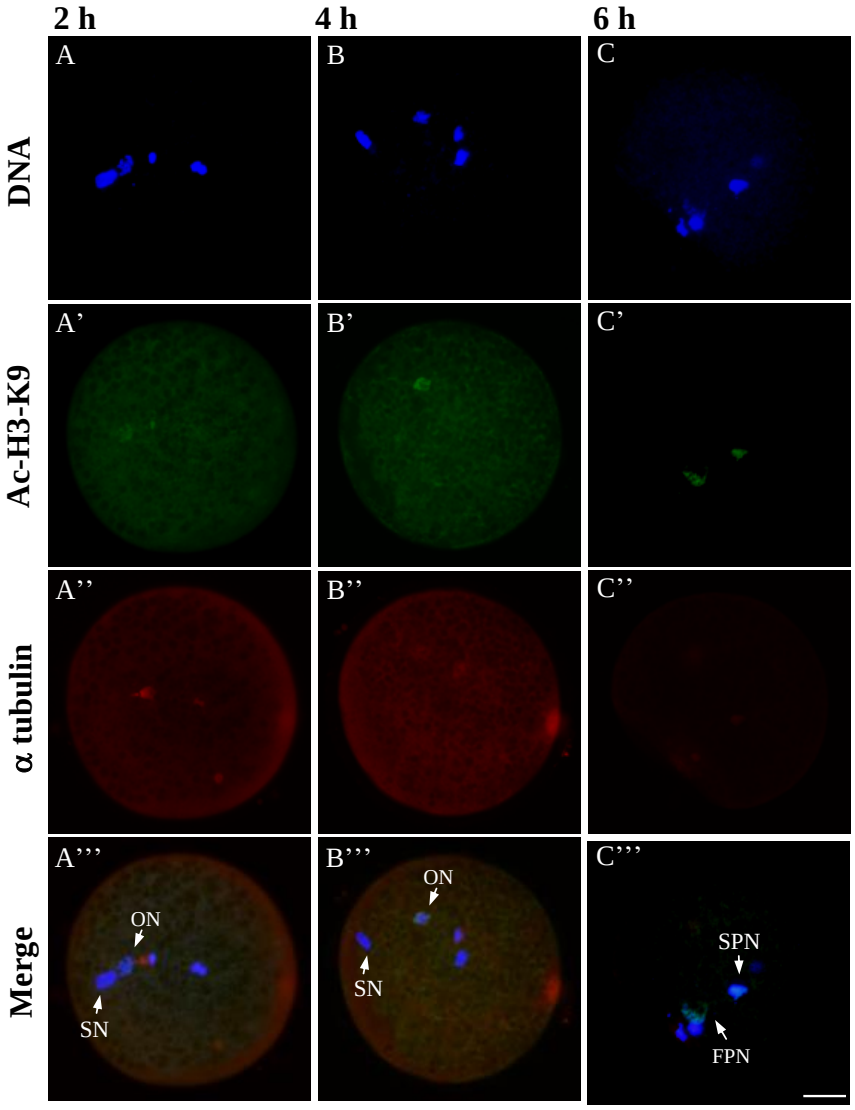

Fig. 4.11. Change in the acetylation levels of histone H3-K9 (Ac-H3-K9) of somatic cell nuclei injected into pig MII-oocytes followed by electro-activation. DAPI stained the chromosome (blue), anti-acetyl-H3-K9 and Alexa 488-labeled antibodies stained the acetylated H3-K9 (green), and anti-α tubulin and Alexa 568-labeled antibodies stained the microtubule (red). The oocytes were examined 0, 2, 4, and 6 h after electro-activation. ON: Oocyte nucleus, SN: Somatic nucleus, FPN: Female pronucleus, SPN: Somatic pronucleus. Scale bar = 30 μm.

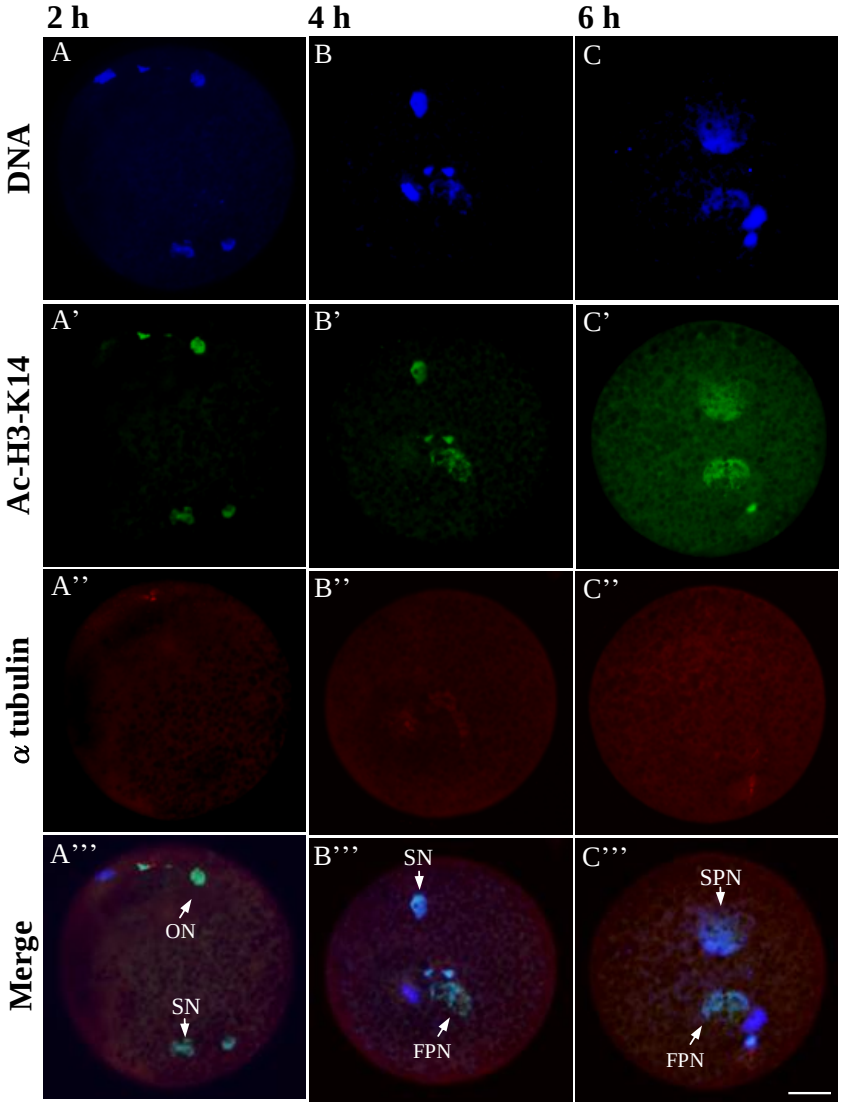

Fig. 4.12. Change in the acetylation levels of histone H3-K14 (Ac-H3-K14) of somatic cell nuclei injected into pig MII-oocytes followed by electro-activation. DAPI stained the chromosome (blue), anti-acetyl-H3-K14 and Alexa 488-labeled antibodies stained the acetylated H3-K14 (green), and anti-αtubulin and Alexa 568-labeled antibodies stained the microtubule (red). The oocytes were examined 0, 2, 4, and 6 h after electro-activation. ON: Oocyte nucleus, SN: Somatic nucleus, FPN: Female pronucleus, SPN: Somatic pronucleus. Scale bar = 30 μm.

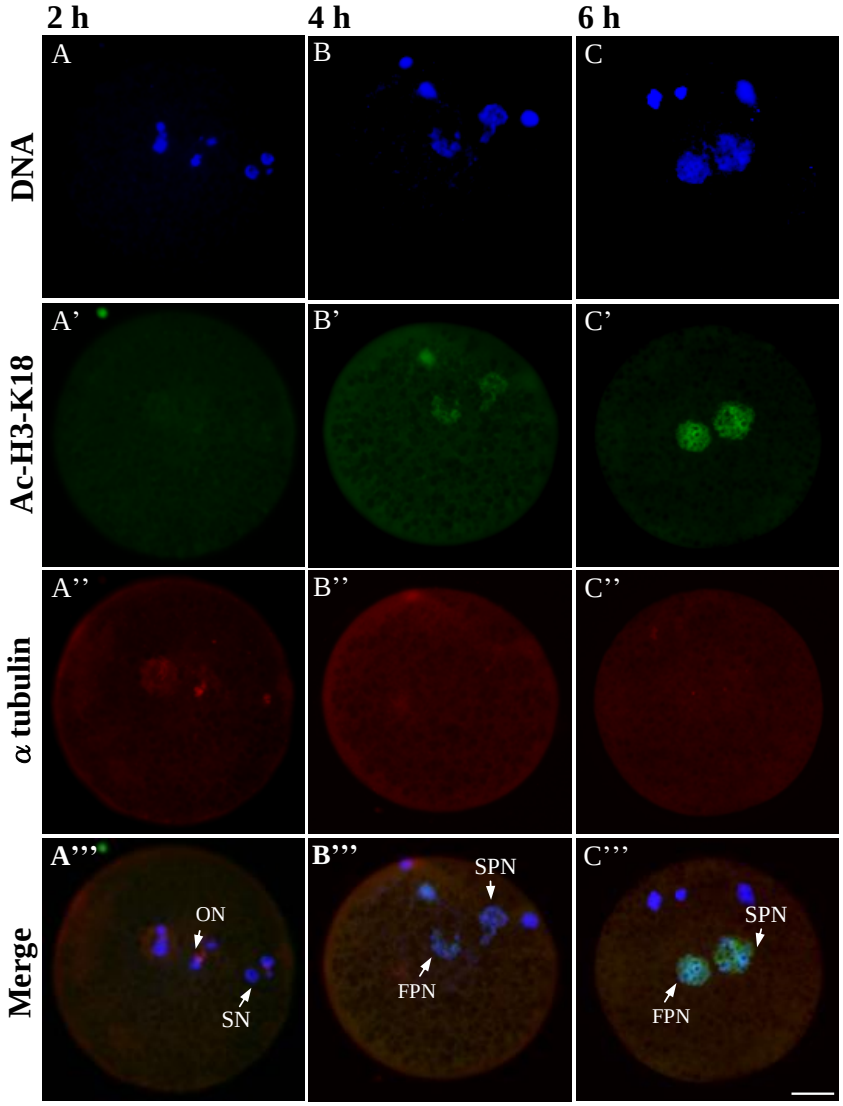

Fig. 4.13. Change in the acetylation levels of histone H3-K18 (Ac-H3-K18) of somatic cell nuclei injected into pig MII-oocytes followed by electro-activation. DAPI stained the chromosome (blue), anti-acetyl-histone H3-K18 and Alexa 488-labeled antibodies stained the acetylated H3-K18 (green), and anti-αtubulin and Alexa 568-labeled antibodies stained the microtubule (red). The oocytes were examined 0, 2, 4, and 6 h after electro-activation. ON: Oocyte nucleus, SN: Somatic nucleus, FPN: Female pronucleus, SPN: Somatic pronucleus. Scale bar = 30 μm.

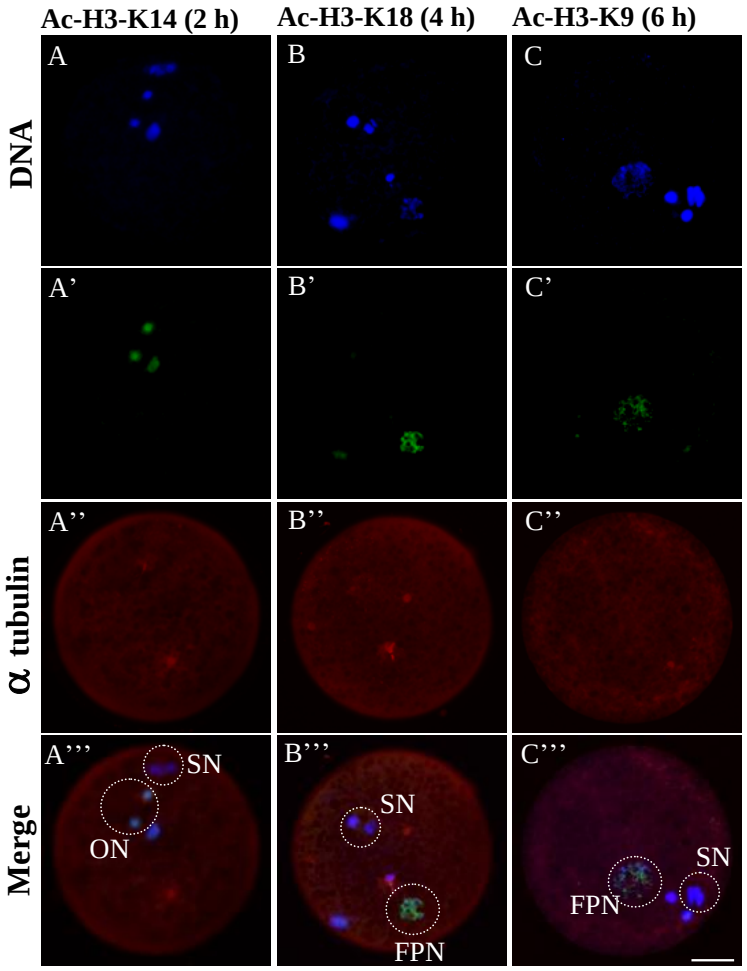

Fig. 4.14. Abnormal acetylation of histone H3-K14 (A'), H3-K18 (B'), and H3-K9 (C') of somatic nuclei injected into pig MII-oocytes followed by electro-activation. DAPI stained the chromosomes (blue), anti-acetyl-histone H3-K14, H3-K18, or H3-K9, and Alexa 488-labeled antibodies stained the Ac-H3-K14, Ac-H3-K18, or Ac-H3-K9 (green), and a anti-αtubulin and Alexa 568-labeled antibodies stained the microtubule (red). The oocytes were examined 0, 2, 4, and 6 h after electro-activation. ON: Oocyte nucleus, SN: Somatic nucleus, FPN: Female pronucleus, Scale bar = 30 μm.

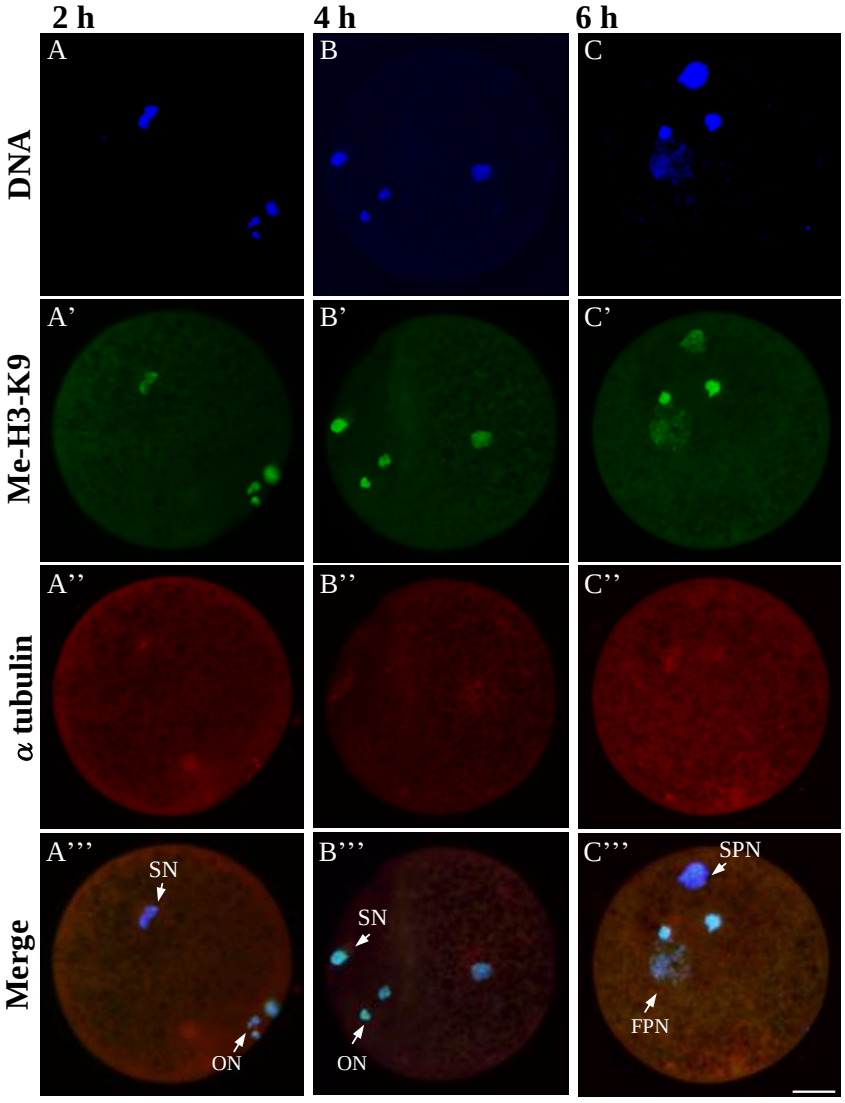

Fig. 4.15. Methylation levels of histone H3-K9 (Me-H3-K9) of somatic nuclei injected into pig MII-oocytes followed by electro-activation. DAPI stained the chromosome (blue), anti-methyl-H3-K9 and Alexa 488-labeled antibodies stained the methylated H3-K9 (green), and anti-α tubulin and Alexa 568-labeled antibodies stained the microtubule (red). The oocytes were examined 0, 2, 4, and 6 h after electro-activation. ON: Oocyte nucleus, SN: Somatic nucleus, FPN: Female pronucleus, SPN: Somatic pronucleus. Scale bar = 30 μm.

of the injected somatic cells by immunostaining with the anti-lamin A/C antibody. In the 10-15% of oocytes, the nuclear membrane of somatic cells did not breakdown completely even 2 h after nuclear transfer. Because the membranes still remained in the oocytes, the chromosomes of somatic cells could not be exposed to the oocyte cytoplasm directly. Therefore, the chromosomes counld not form highly condensed state as metaphase-like structure. As shown in Chapter 3, both Cdc2 kinase and histone H3 kinase activities are high in MII oocytes. However, it migh be happen in some MII-arrested oocytes, the Cdc2 kinase activity decreased and the activity was not enough for somatic nuclei to induce the membrane breakdown completely. Alternatively, the remaining nuclear membranes of the somatic cells might disturbed the recruitment of oocyte microtubules which were required for the spindle formation by the somatic nucleus. The clumps of condensed chromosomes were maintained even after electro-activation. The result suggests that nuclear membrane breakdown of somatic cell nuclei are important for the morphological change of the chromosomes, and the defect possibly concerns the abnormal chromosome segregation at the first mitosis of embryos (Nguyen et al., 2004). In addition, there were 20% of oocytes in which condensed somatic chromosomes were dispersed in ooplasm, out of the spindle. This abnormality would result in some oocytes that had more than 2 pronulei, for example 1 large and 2 small somatic pronuclei after electro-activation. It is suggested that most of nuclear transferred oocytes form abnormal spindles (Nguyen et al., 2004). Therefore, the abnormality resulted in the chaotically dispersed chromosomes and multiple formation of somatic pronuclei.

Although the chromosome morphology of somatic nuclei was different from oocyte nuclei to some extent, somatic cell chromosomes showed similar stage to those of oocytes after electro-activation. They showed metaphase- and anaphase-telophase-like stages and formed pronucleus-like structures. Especially, the phosphorylation and dephosphorylation of histone H3-S10 and H3-S28 of the somatic chromosomes changed in a similar manner to oocyte chromosomes. Histone H3-S10 and H3-S28 became phosphorylated after injection into mature oocytes, and dephosphorylated in the pronucleus-like structure after electro-activation. These results suggest that phosphorylation and dephosphorylation of histone H3 at S10 and S28 in injected somatic nuclei were controlled by oocyte cytoplasm.

Most genes in differentiated cells are regulated through epigenetic modifications that change in the chromosome and do not alter the DNA sequences (Kikyo and Wolffe, 2000). During

differentiation, somatic nuclei acquire highly specialized DNA and chromatin modifications which are thought to result in cellular memory of the differentiated state (Bird, 2002). Studies involving the modifications such as histone acetylation and methylation are thought to provide insights into the molecular mechanisms of redifferentiation in oocyte cytoplasm. It has been thought that the cytoplasm of the MII oocytes is able to reprogram the gene expression pattern of transferred somatic nuclei (Wilmut et al., 1997). In addition, it is suggested that acetylated histone molecules in chromatin are associated with increased gene expression (Tse et al., 1998). Therefore, histone H3 of transferred somatic nuclei should be deacetylated in the oocyes. In the present experiments, all of histone H3 acetylation levels of somatic cell nuclei were detected immediately after nuclear transfer. However, the acetylation levels decreased and completely disappeared 2 h after nuclear transfer. Thus, the cytoplasm of the MII oocytes could remove the acetyl groups from H3-K9, H3-K14, and H3-K18 in the transferred somatic nuclei. It suggests that histone deacetylase in oocyte cytoplasm deacetylates the somatic chromosomes.

Transcription is initiated in the one-cell stage embryos (Aoki et al., 1997). After activation, acetylation of H3-K14 and H3-K9 of oocyte chromosomes reappeared at AII-TII, perhaps preparing for the transcription at the one-cell stage. Reappearance of histone H3 acetylation in somatic chromosomes occurred in a similar time course to the oocyte chromosomes. These results suggest that acetylation of histone H3 at K9, K14, and K18 in injected somatic nuclei were controlled by oocyte cytoplasm.

However, there were 30% of oocytes in which somatic chromosomes showed low or no histone H3 acetylation although the morphological change of the chromosomes followed the change in oocyte chromosomes. Since acetylation in oocyte chromosomes reappeared after electro-activation, the result suggests that the preparation for the transcription was not sufficient in the somatic nuclei. This provides a clue for understading the cause of some results showing that epigenetic reprogramming was severely deficient in cloned embryos where aberrant patterns of gene expression occurred (Inoue et al., 2002; Niemann et al., 2002).

In normal fertilization, oocyte cytoplasm regulates and enhances the epigenetic asymmetry between parental genomes, and consequently, functional differences are observed between them during development in mammals. The epigenetic differences are enhanced in the zygote by means of DNA demethylation of the paternal genome shortly after fertilization, while the

maternal genome displays *de novo* methylation (Mayer et al., 2000). Santos et al. (2003) found that H3-K9 methylation was reprogrammed in parallel with DNA methylation in normal embryos. In the present experiment, the methylation of H3-K9 was observed in the somatic cell nuclei immediately after nuclear transfer and the methylation was maintained after 2 h, before electro-activation. During the time it could happen that the somatic nuclei were further methylated by the influence of oocyte cytoplasm. Arney et al. (2002) have reported that mouse zygotes after fertilization show a high level of histone H3-K9 methylation in the maternal genome. In contrast, the paternal genome has no methylation of histone H3-K9 at the early stages of development. The present results showed that after oocytes activation, the methylation of H3-K9 in somatic nuclei was still maintained in oocytes until pronucleus stage. Liu et al. (2004) suggested that in normal fertilization, the methylation of H3-K9 was absent in the male pronucleus in the mouse, because histone H3 was methylated in the oocyte chromatin, but undermethylated in the oocyte cytoplasmic pool. Moreover, after fertilization, the sperm chromatin exchanges their protamines for histones. Thus, the paternal chromatin perhaps incorporates hypomethylated histone H3. The results in the present experiment indicate that the methylation of histone H3-K9 in the transferred somatic nuclei were different from that of spermatozoa. The methylation of H3-K9 in somatic nuclei persists after oocyte activation.

In this study, the methylation level of H3-K9 of somatic chromosomes was lower than that of oocyte chromosomes in same MII oocytes and also after electro-activation. It is unknown whether erasure of the epigenetic mark of somatic nuclei can occur through active demethylation or histone exchange in the oocytes. Some possibilities might be thought about histone demethylation in the somatic nuclei. First, if demethylases exist, and they may erase the epigenetic mark of histone methylation of the somatic nuclei. Second, early reports demonstrated that *Xenopus* or human somatic nuclei injected into *Xenopus* oocytes lost 80-90% of the preradiolabelled nuclear proteins accompanied with significant incorporation of oocyte proteins (Gurdon et al., 1979). Because of the extreme difference of differentiation status between oocytes and somatic cells, these protein exchange events rise the possibility that methylated histones of somatic nuclei might be exchanged by the oocyte cytoplasmic histones.

However, under the experimental conditions in the present study, histone H3-K9 methylation in somatic nuclei was not diminished after oocyte activation. This persistence indicates that the

histone methylation probably retains the previous memory of cell differentiation. This incomplete erasure of preexisting methylation in the somatic nuclei will be one important reason why mammalian cloning often fails. This corresponds well with some reports that revealed the inefficient demethylation and inappropriate reestablishment of DNA methylation in transferred somatic nuclei (Bourc'his et al., 2001; Kang et al., 2002).

The results in this study showing the difference of histone acetylation and methylation between the oocyte nucleus and the transferred somatic nucleus would explain the different cloning efficacy using different donor cells with different epigenetic modifications, such as low levels of methylation and/or high levels of acetylation of histone H3. In summary, histone phosphorylation and acetylation, but not methylation of the transferred somatic nucleus is controled by oocyte cytoplasm. These results reinforce the fact that one of the key features of somatic nuclear transfer will be the establishment of the conditions that allow for erasure of heritable memory of differentiated cell types (Wade and Kikyo, 2002).

Chapter 5. Effects of Inhibition of Histone Deacetylase, Protein Synthesis and Tyrosine Phosphatase on the Chromosome Morphology and Histone H3 Modifications in Pig Oocytes

5.1. INTRODUCTION

It was suggested in Chapter 3 that the modulation of chromatin configurations from decondensed to peri-nucleolar heterochromatin sheath in GV involved decreased acetylation levels of histone H3 at K9, K14, and K18, and that these lysines were deacetylated during oocyte maturation. However, the regulation of this meiosis- or oocyte-specific deacetylation has not been elucidated. The acetylation and deacetylation of histones is thought to play important roles in various cellular functions. The basic mechanisms studied in other cell types indicate that the acetylation of core histones is essential in chromatin remodeling and transcription (Peterson and Workman, 2000; Agalioti et al., 2002). The discovery of transcription factors, co-activators and co-repressors having histone acetyltransferase (HAT) or histone deacetylase (HDAC) activity, revealed the role of histone acetylation in regulating gene expression (Strahl and Allis, 2000). Histones associated with active genes exhibit high levels of acetylation, while histones associated with repressed heterochromatin are hypoacetylated (Braunstein et al., 1993). Consistent with this paradigm, in general, HAT activates and HDAC represses transcription. Trichostatin A, a specific inhibitor of HDAC, induces cell-cycle arrest (Yamashita et al., 2003). In mammalian cells, pericentric heterochromatin is especially responsive to prolonged treatment with trichostatin A, which results in the defined regions to relocate at the periphery and lose the properties of retaining heterochromatin protein 1 (HP1) (Taddei et al., 2001). It is also suggested that HDAC is able to deacetylate histones during meiosis but not mitosis (Kim et al., 2003).

It is well documented that protein synthesis is required for the successful completion of meiotic maturation of oocytes from a variety of species including mammals (Schultz and Wassarman, 1977). Although protein synthesis is prominently decreased during mitosis, protein synthesis is active during oocyte maturation, and the newly synthesized proteins have vital roles

in the progress of meiosis (Schultz et al., 1979; Van Blerkom, 1981). If protein synthesis is inhibited during maturation, the activation of Cdc2 kinase and MAP kinase are inhibited, and meiosis stops in the mid-course (Hashimoto and Kishimoto, 1988; Sobajima et al., 1993). Cycloheximide, a protein synthesis inhibitor, is examined in some species such as mice (Schultz and Wassarman, 1977), rats (Ekholm and Magnusson, 1979) and pigs (Fulka et al., 1986). Although there are differences among mammalian species in the sensitivity of GVBD to cycloheximide, this inhibitor induces arrest of meiosis. In the pig, although the oocytes require the newly synthesized proteins for GVBD, premature condensation of chromosomes is induced in the GV without protein synthesis (Fulka et al., 1986; Kubelka et al., 1988). It has not been elucidated whether the protein synthesis is necessary for the histone modifications with the change in chromosome morphology in pig oocytes.

Protein phosphorylation occurs on specific serine, threonine, and tyrosine residues in specific proteins. Although the phosphorylation of protein-tyrosine residues seems to represent only a small fraction of the overall modification of cellular proteins by phosphorylation, this reversible alteration has been demonstrated to be involved in many critical aspects of cellular physiology (Hunter, 1989; Fischer et al., 1991). Reversible tyrosine phosphorylation mediates regulation of cell growth, cell division, and differentiation. In the nucleus of somatic cells, functionally, tyrosine phosphorylation is linked to the regulation of the transcription factor activity. Tyrosine phosphorylation and dephosphorylation appear to be key events at several distinct steps during the maturational process of oocytes. It is suggested that many nucleolar proteins are tyrosine phosphorylated in bovine oocytes during growth phase, and they are dispersed into the oocyte cytoplasm at GVBD (Fair et al., 2001). Sodium orthovanadate is a powerful inhibitor of many protein tyrosine phosphatases (PTPase) in mitosis and meiosis. Vanadate has been used to study the role of PTPase *in vitro* (Gordon, 1991). In mouse and rat oocytes, vanadate inhibits GVBD by inhibiting tyrosine dephosphorylation of Cdc2 kinase (Choi et al., 1992; Goren and Dekel, 1994). In pig oocytes, it inhibits GVBD almost completely at concentration of 250 μM and 500 μM (Aquino et al., 1995). Gowdy et al. (1998) have shown that vanadate causes chromosome decondensation in mitotic cells, with masses of condensed chromatin interspersed with interphase-like chromatin in a well defined round nucleus.

This chapter has the objective to examine whether meiosis-specific deacetylation and

phosphorylation of histone H3 are affected by the three different chemical inhibitors that have been known to regulate meiotic maturation of oocytes. The inhibitors were a HDAC inhibitor trichostatin A, a protein synthesis inhibitor cycloheximide, and a tyrosine phosphatase inhibitor vanadate. The results of Chapter 3 suggested that histone H3-K14 was highly acetylated in growing pig oocytes, and deacetylated during oocyte maturation. Therefore, the changes in acetylation of H3-K14 as well as phosphorylation of H3-S10 and H3-S28 were investigated in the oocytes treated by the inhibitors.

5.2. MATERIALS AND METHODS

5.2.1. Collection and Maturation Culture of Oocytes

OCGCs from follicles 4-6 mm in diameter were collected from pig ovaries and cultured in the same manner described in Section 2.2.1. OCGCs were cultured in the maturation medium with one of the inhibitors, trichostatin A (Sigma, Chemical Co.), cycloheximide (Wako Pure Chemical Industries Ltd., Osaka, Japan) and sodium orthovanadate (Nacalai Tesque Inc., Kyoto, Japan). After culture, oocytes were denuded of cumulus cells completely by hyaluronidase and gentle pipetting, then used for immunostaining, Western blot analysis, and kinase activity assay.

5.2.2. Experimental Designs

Experiment 1: Effect of trichostatin A (TSA) on the chromosome morphology and histone modifications

OCGCs were cultured in 0.5 ml of the maturation medium supplemented with or without 100 nM TSA for 42 h. Then oocytes were used for immunostaining experiment.

Experiment 2: Effect of cycloheximide (CHX) on the chromosome morphology and histone modifications

To examine the effect of CHX on the chromosome morphology and histone modifications, OCGCs were cultured in 0.5 ml of the maturation medium supplemented with or without 35 μM CHX for 42 h. Then oocytes were used for immunostaining experiment. To examine the effect of CHX on the activities of oocyte Cdc2 kinase, MAP kinase, and histone H3 kinase, OCGCs were

cultured for various time, 0, 3, 6, 9, 12, 15, 18, 21, 24, 27, and 42 h. Then the oocytes were used for kinase activity assay.

Experiment 3: Effect of vanadate (Va) on the chromosome morphology and histone modifications

To examine the effect of Va on the chromosome morphology and histone modifications, OCGCs were cultured in 0.5 ml of the maturation medium supplemented with or without 1 mM sodium orthovanadate for 42 h. Then the oocytes were used for immunostaining and Western blot analysis.

5.2.3. Immunofluorescent Microscopy

The method is described in Sections 2.2.3 and 3.2.4. The first antibodies used here were rabbit polyclonal anti-phospho-histone H3 at serine 10 (Cell Signaling Technology Inc.), rabbit polyclonal anti-phospho-histone H3 at serine 28 (Upstate, Cell Signaling Solutions), and rabbit polyclonal anti-acetyl-histone H3 at lysine 14 (Upstate, Cell Signaling Solutions) antibodies. To determine the integrity of the nuclear membrane, mouse monoclonal anti-lamin A/C antibody (Santa Cruz Biotechnology Inc.) was used. The conjugated second antibodies used here were Alexa Fluor 488-labeled goat anti-rabbit IgG (Molecular Probes Inc.) and Alexa Fluor 568-labeled goat anti-mouse IgG (Molecular Probes Inc.). The chromosomes were stained with 4, 6-diamidino-2-phenylindole (DAPI) (2 μg/ml; Molecular Probes Inc.). In the negative control, the oocytes were reacted with nonimmune rabbit serum instead of rabbit polyclonal first antibody.

5.2.4. Kinase Assay

The changes in the activities of Cdc2 kinase, MAP kinase, and histone H3 kinase in the oocytes were measured using the method described in Section 2.2.4.

5.2.5. Electrophoresis and Western Blotting

After culture, denuded oocytes were washed twice in PBS-PVA. Each group of 50 denuded oocytes was transferred into an Eppendorf tube with 15 μl of SDS sample buffer (Laemmli, 1970), boiled for 5 min, and stored at -20 ^{o}C before electrophoresis. After thawing, samples were run in 13% SDS-polyacrylamide gels, and proteins were transferred to hydrophobic

polyvinylidene difluoride membranes (Immobilin, Millipore Corporation, Bedford, MA) in a Trans-Blot SD semi-dry transfer cell (Bio-Rad Laboratories, Hurcules, CA) for 1.5 h at 2 mA/cm^2 in transfer buffer. The membrane were blocked with 10% fetal calf serum in PBS containing 0.1% Tween20 (PBS-Tween) for 2 h, then incubated with mouse monoclonal anti-phosphotyrosine antibody PY99 (1:500; Santa Cruz Biotechnology, Inc., CA) for 4 h at room temperature. After three washes in PBS-Tween, the membranes were treated with horseradish peroxidase-labeled anti-mouse Ig (1:1000, Dako Japan, Tokyo, Japan) in the blocking buffer for 1 h at room temperature. After three washes of 10 min each with PBS-Tween, peroxidase activity was visualized with ECL Western blotting detection system (Amersham Life Science, UK).

5.2.6. Statistical Analysis

At least 40 immunostained oocytes were examined by the immunofluorescent microscopy in each group. The values were analysed using the chi-square test. P values less than 0.05 were considered statistically significant.

5.3. RESULTS

5.3.1. Histone Deacetylase (HDAC) Inhibition Induces Maturation Arrest

Trichostatin A maintained H3-K14 acetylation. No oocytes underwent GVBD by trichostatin A treatment, while control oocytes had reached MII with deacetylation of H3-K14 after 42 h (Figs. 5.1B, 1D, and 5.2A). In addition, in the treated oocytes, chromosomes started to condense, and nuclei showed GVII-IV-like stage (Fig. 5.1B) and SC-GVI-like stage (Fig. 5.3B). However, no histone H3 phosphorylation at both S10 and S28 were observed in these chromosomes (Figs. 5.3B and 5.4B). This was different from that in oocytes during normal maturation where oocytes at GVII-IV stage had phosphorylated H3-S28 after 9-15 h of culture (in Chapter 3).

5.3.2. Protein Synthesis Inhibition Maintains Histone H3 Acetylation

Oocytes were incubated for 42 h with cycloheximide. The fluorescent signal of Ac-H3-K14 did not disappear and no oocyte underwent GVBD (Figs. 5.1C and 5.2B). On the other hand,

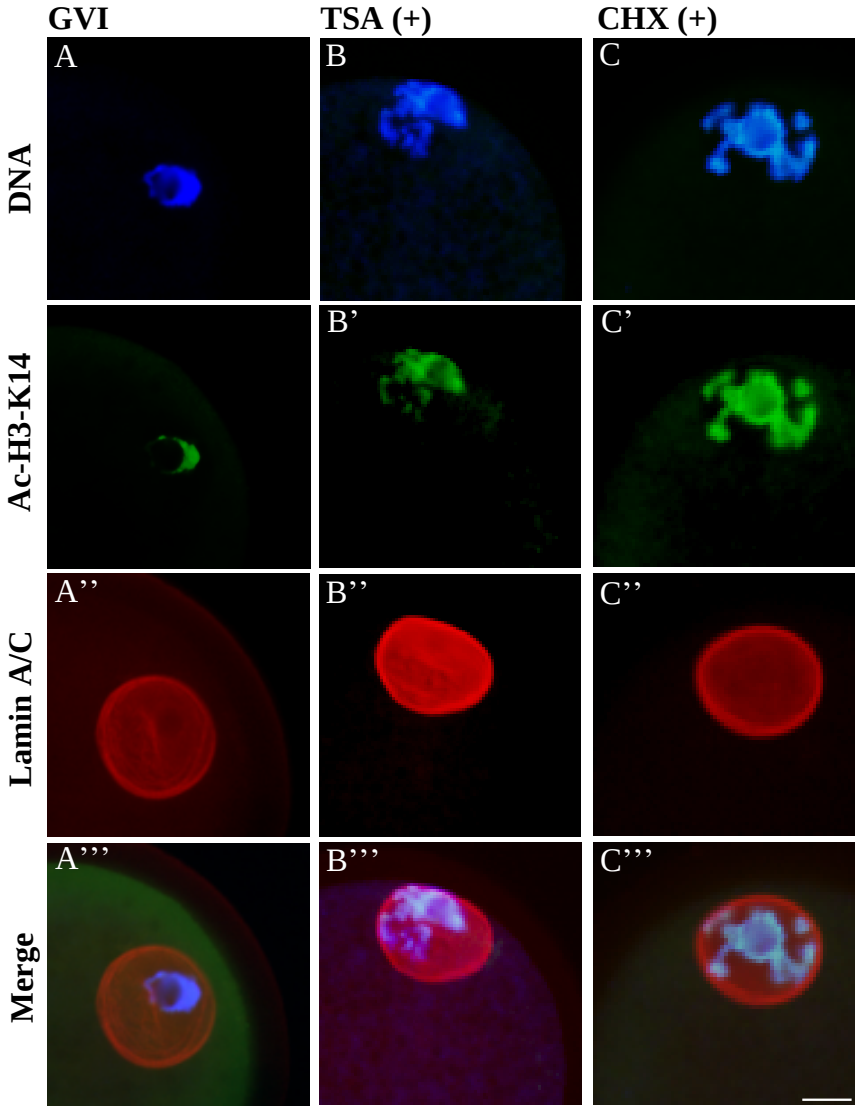

Fig. 5.1. Effects of trichostatin A (TSA) and cycloheximide (CHX) on the chromatin configuration, histone H3-K14 acetylation (Ac-H3-K14), and nuclear membrane of pig oocytes. Oocytes were cultured with or without TSA or CHX for 42 h, and then stained with DAPI for the chromatin (blue), anti-acetyl- histone H3-K14 and Alexa 488-labeled antibodies for the Ac-H3-K14 (green), and anti-lamin A/C and Alexa 568-labeled antibodies for the nuclear membrane (red). MI: Metaphase I. Scale bar = 20 μm.

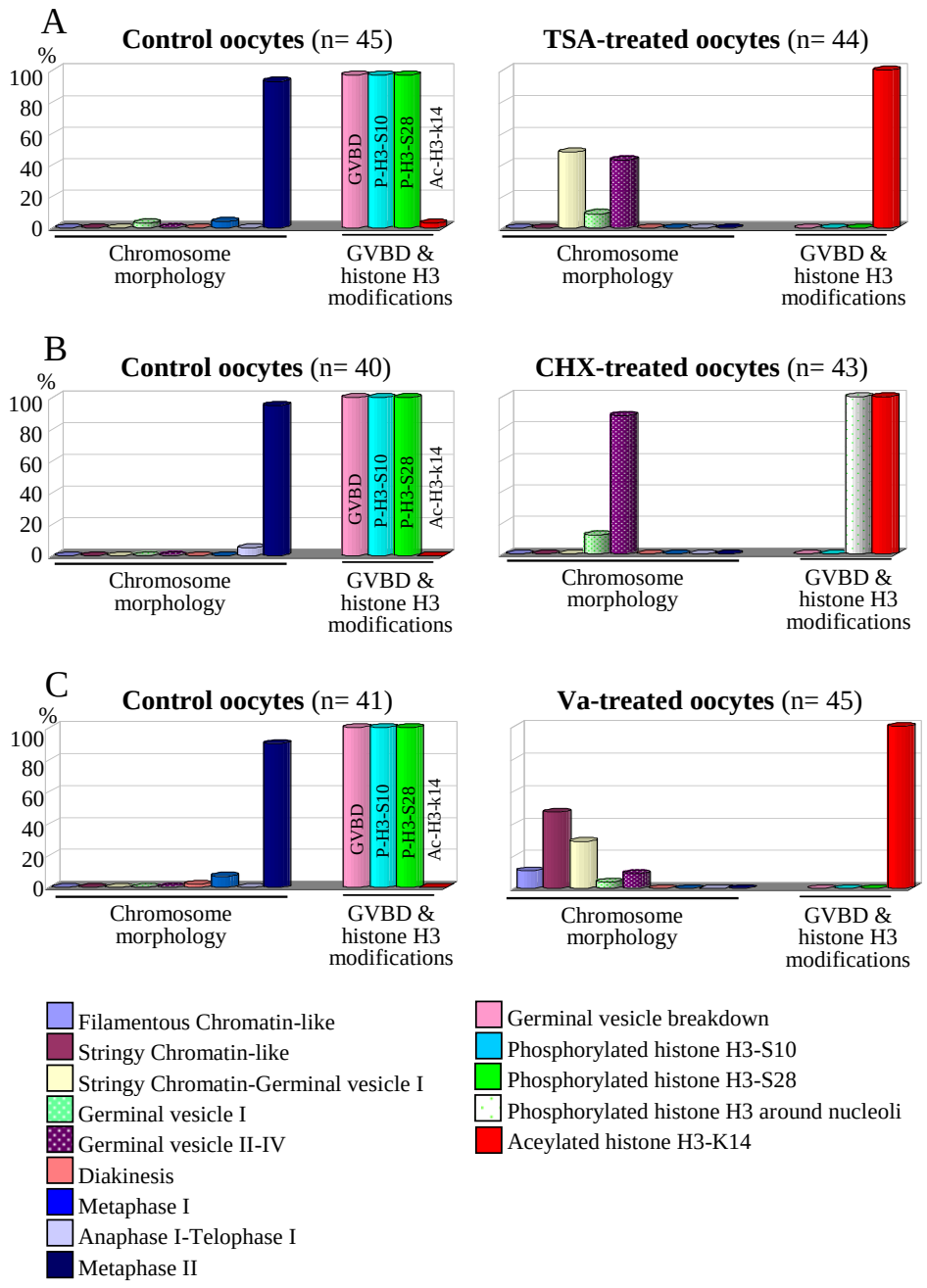

Fig. 5.2. Chromatin morphology, phosphorylation of histone H3-S10 and H3-S28, and acetylation of H3-K14 in the oocytes treated with A) Trichostatin A (TSA), B) Cycloheximide (CHX), or C) Vanadate (Va) for 42 h. This experiment was repeated 3 times.

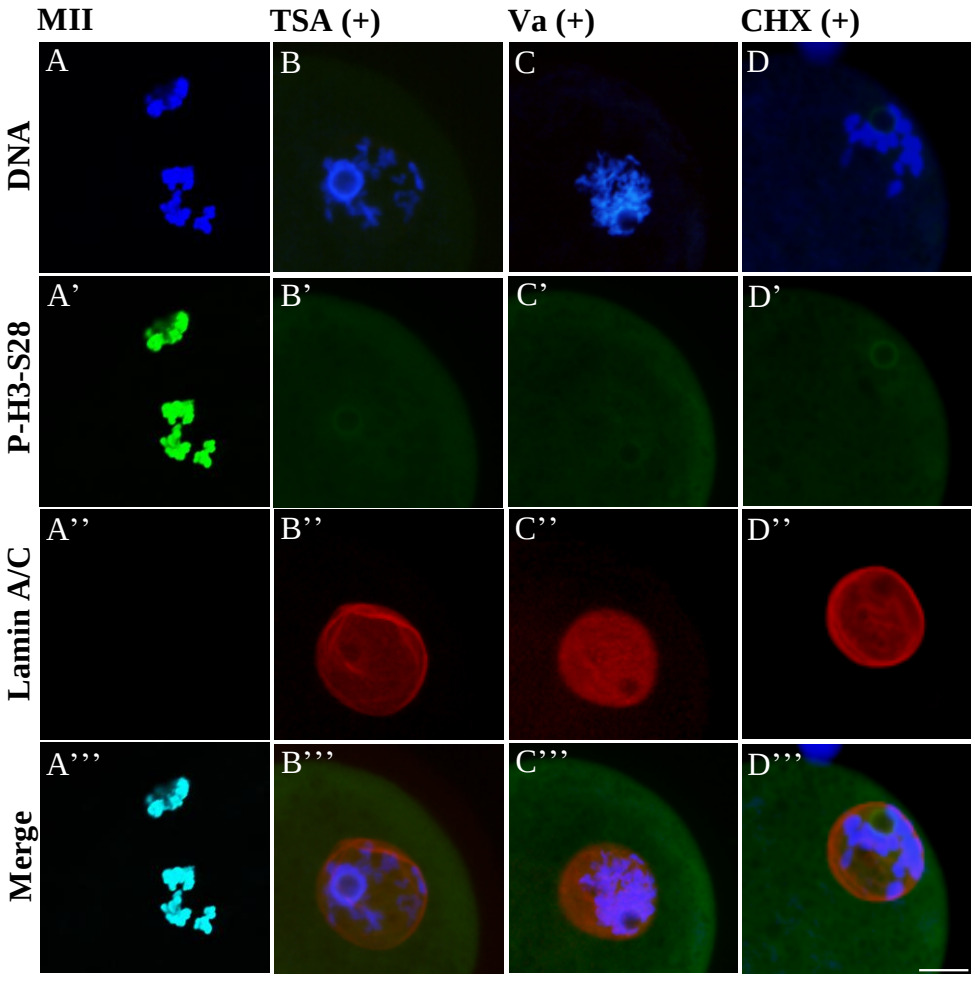

Fig. 5.3. Effects of trichostatin A (TSA), vanadate (Va) and cycloheximide (CHX), on the chromatin configuration, histone H3-S28 phosphorylation (P-H3-S28), and nuclear membrane of pig oocytes. Oocytes were cultured with or without TSA, Va, or CHX for 42 h, and then stained with DAPI for the chromatin (blue), anti-phospho-histone H3-S28 and Alexa 488-labeled antibodies for the P-H3-S28 (green), and anti-lamin A/C and Alexa 568-labeled antibodies for the nuclear membrane (red). MII: Metaphase II. Scale bar = 20 μm.

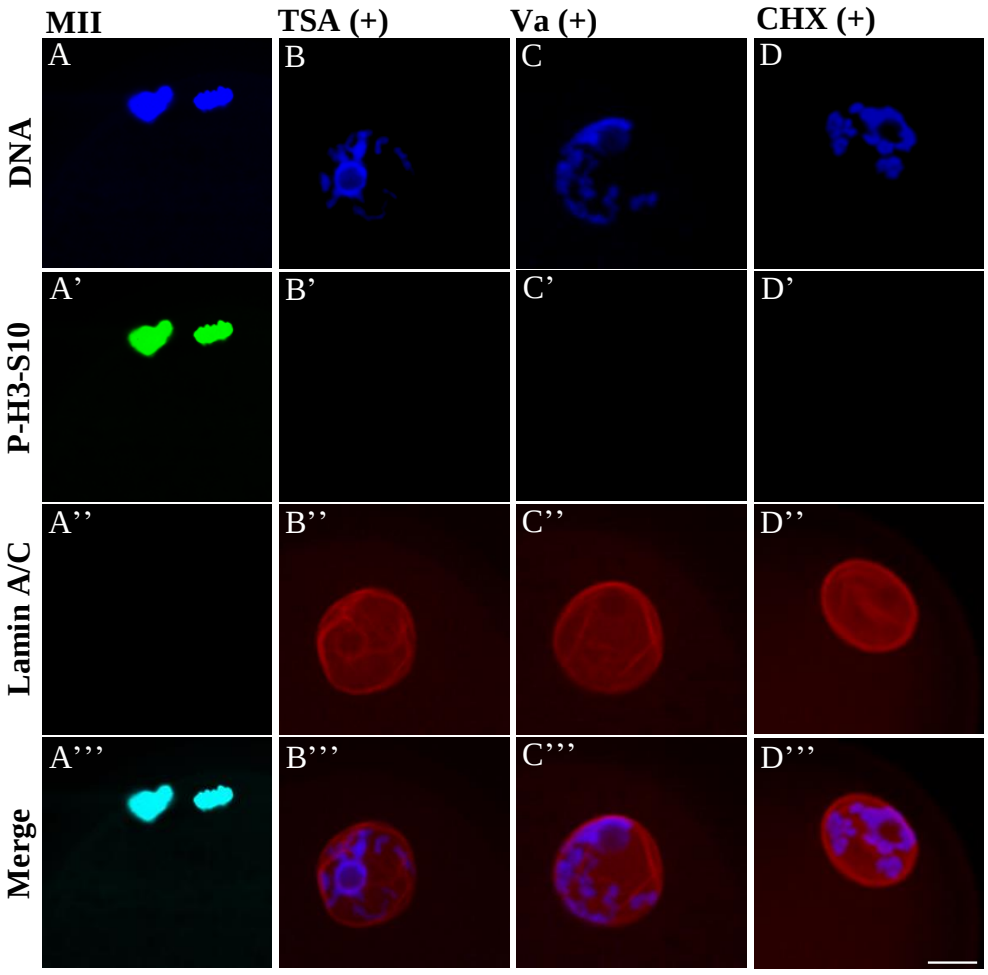

Fig. 5.4. Effects of trichostatin A (TSA), vanadate (Va) and cycloheximide (CHX), on the chromatin configuration, histone H3-S10 phosphorylation (P-H3-S10), and nuclear membrane of pig oocytes. Oocytes were cultured with or without TSA, Va, or CHX for 42 h, and then stained with DAPI for the chromatin (blue), anti-phospho-histone H3-S10 and Alexa 488-labeled antibodies for the P-H3-S10 (green), and anti-lamin A/C and Alexa 568-labeled antibodies for the nuclear membrane (red). MII: Metaphase II. Scale bar = 20 μm.

control oocytes reached MII and histone H3-K14 was deacetylated after 42 h (Figs. 5.1A and 5.2B).

The activities of Cdc2 kinase and MAP kinase were measured in cycloheximide-treated oocytes. Both of them were inactive during the treatment (Fig. 5.5). On the other hand, in control oocytes, Cdc2 kinase became active after 24 h of culture, then MAP kinase became active in MI oocytes after 27 h (Fig. 5.5). In cycloheximide-treated oocytes, histone H3 kinase was also inactive during the treatment, while it was high in control oocytes at MI and MII (Fig. 5.6).

In cycloheximide-treated oocytes, chromosomes condensed in the GV (Figs. 5.1, 5.3 and 5.4). The condensed chromosomes had no histone phosphorylation at S10 (Fig. 5.4D), while histone H3-S28 was phosphorylated at a low level around the nucleolus after 42 h (Figs. 5.2B and 5.3D).

5.3.3. Tyrosine Phosphatase Inhibition Causes Chromatin Decondensation and Maintenance of Histone H3 Acetylation

In vanadate-treated oocytes, the chromatin configuration changed from condensed heterochromatin ring around the nucleolus to decondensed morphology like filamentous stage or sringy stage in growing oocytes. No oocytes underwent GVBD by the treatment after 42 h of culture (Figs. 5.2C, 5.7B, and 5.7C). In the oocytes, there were intense fluorescente signals of acetylation of H3-K14 even after 42 h of treatment (Figs. 5.2C, 5.7B', and 5.7C'), while control oocytes reached MII with deacetylation of H3-K14 (Figs. 5.7D and D'). In addition, vanadate-treated oocytes had no histone H3 phosphorylation at both S10 and S28 (Figs. 5.2C, 5.3C' and 5.4C').

Immunoblot analyses using anti-phosphotyrosine antibodies confirmed the effect of vanadate on tyrosine phosphorylation of oocyte proteins. Vanadate caused a massive accumulation of various tyrosine phosphorylated proteins with different molecular weights (Fig. 5.8).

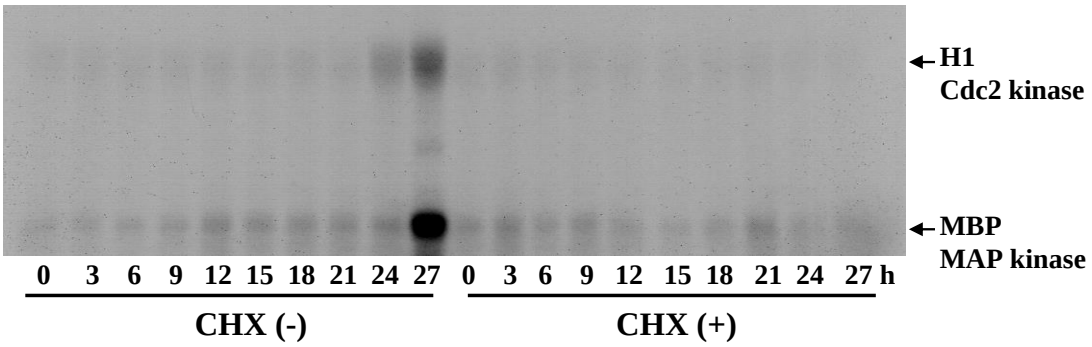

Fig. 5.5. The autoradiograph showing the changes in Cdc2 kinase and MAP kinase activities during meiotic resumption of pig oocytes. Pig oocytes were cultured in the medium with (+) or without (-) cycloheximide (CHX). Histone H1 (H1) and myelin basic protein (MBP) were used for the substrates of Cdc2 kinase and MAP kinase, respectively. The lower figures present the hours of maturation culture.

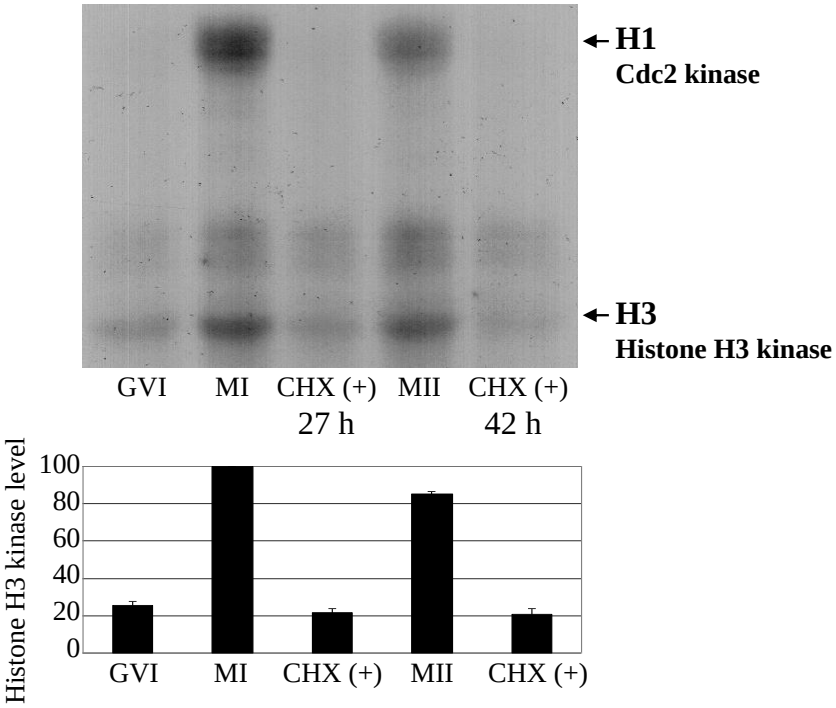

Fig. 5.6. The autoradiograph showing the changes in Cdc2 kinase and histone H3 kinase activities during maturation of pig oocytes. Pig oocytes were cultured in the medium with (+) or without (-) cycloheximide (CHX). Histone H1 (H1) and histone H3 (H3) were used for the substrates of Cdc2 kinase and histone H3 kinase, respectively. The lower figures present the meiotic stages are Germinal vesicle stage I (GVI), Metaphase I (MI), Metaphase II (MII) and the time of CHX treatment (CHX(+) 27 h and CHX(+) 42 h).

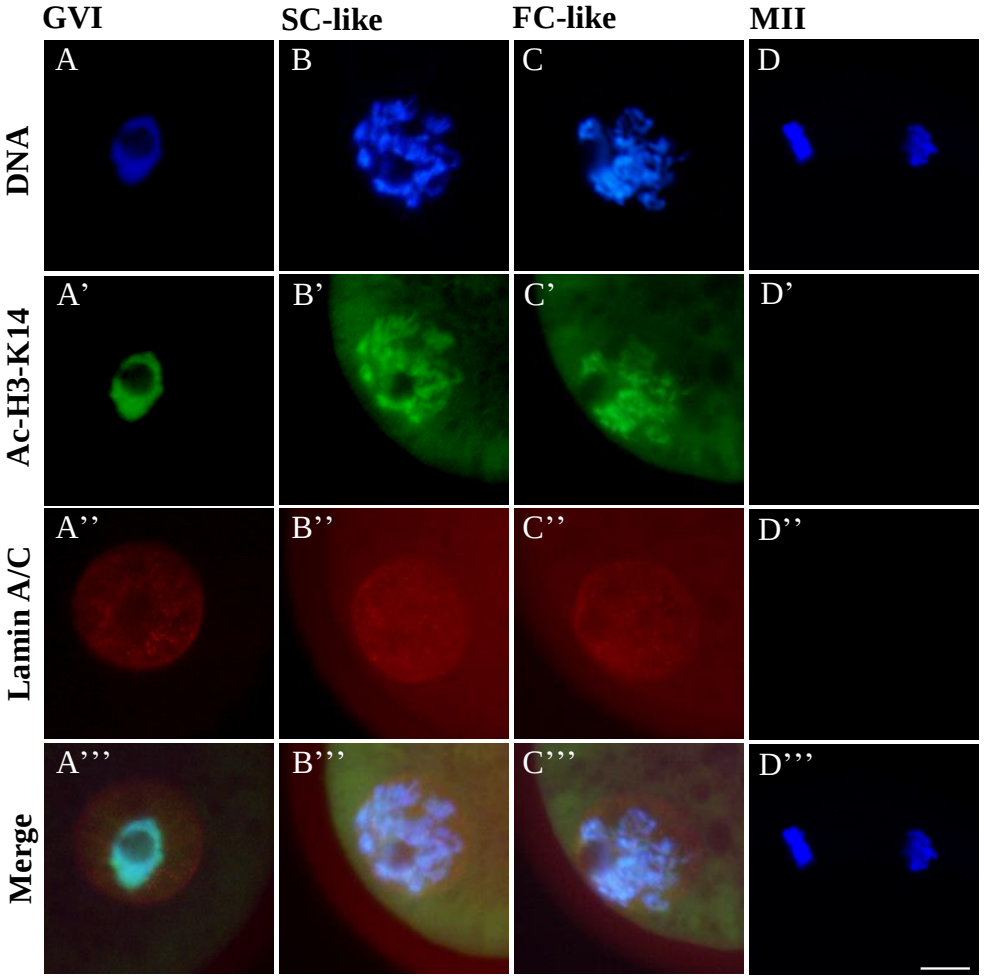

Fig. 5.7. Effects of vanadate (Va) on the chromatin configuration, histone H3-K14 acetylation (Ac-H3-K14), and nuclear membrane of pig oocytes. Oocytes were cultured with or without Va for 42 h, and then stained with DAPI for the chromatin (blue), anti-acetyl histone H3-K14 and Alexa 488-labeled antibodies for the Ac-H3-K14 (green), and anti-lamin A/C and Alexa 568-labeled antibodies for the nuclear membrane (red). GVI: Germinal vesicle stage I, SC-like Stringy chromatin stage by the vanadate treatment. FC-like: filamentous chromatin stage by the vanadate treatment. Scale bar = 20 μm.

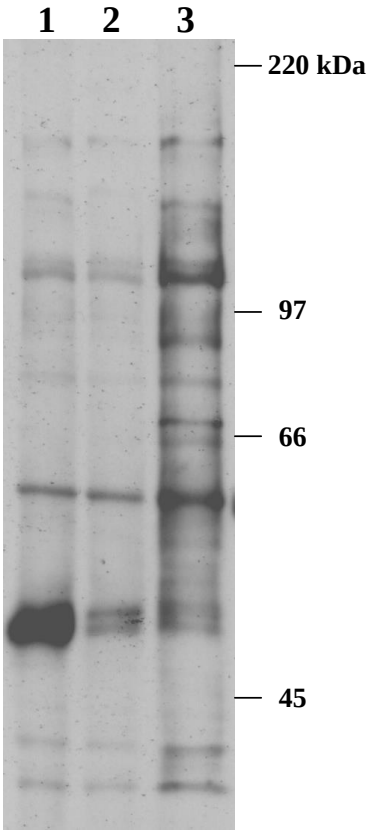

Fig. 5.8. Tyrosine-phophorylated proteins in pig oocytes treated with vanadate. **1**: immature oocytes collected from 4-6 mm follicles. **2**: oocytes cultured for 42 h for maturation. **3**: oocytes treated with vanadate for 42 h. Mouse monoclonal anti-phosphotyrosine antibody PY99 was used.

5.4. DISCUSSION

The results presented here showed that inhibition of HDAC by trichostatin A induced oocyte arrest at the GV stage. In addition, both of cycloheximide and vanadate induced oocyte arrest. In all of the arrested oocytes, acetylation of histone H3-K14 was maintained. The results also suggest that tyrosine phosphatase(s) and newly synthesized proteins are required for deacetylation of histone H3-K14 as well as GVBD.

Trichostatin A maintains the H3-K14 acetylation, although the chromosome morphology changed to GVII-IV-like stage in treated oocytes. It was shown in Chapter 3 that histone H3-S28 is phosphorylated in chromosomes of GVII-IV stages during normal oocyte maturation. The chromosomes in trichostatin-A treated oocytes condensed in a different manner from the oocytes in normal maturation.

Since many kinds of proteins are known to be synthesized specifically during maturation, and they are required for the successful completion of meiotic maturation of oocytes, the association between protein synthesis and H3-K14 deacetylation was examined in pig oocytes. The result showed that the cycloheximide induced arrest of oocytes with inactivity of both Cdc2 kinase and MAP kinase. It maintained the acetylation of H3-K14 although chromosomes started to condense. The configuration of chromosomes looked similar to that in trichostatin A-treated oocytes, and dephosphorylation of H3-S10 and acetylation of H3-K14 were maintained, although the phosphorylation of H3-S28 appeared at the periphery of the nucleolus in cycloheximide-treated oocytes. It was indicated in Chapter 3 that phosphorylation of H3-S28 might be one of the key events initiating meiotic chromosome condensation, therefore, it might affect the beginning of chromosome condensation in the treated oocytes. However, the histone H3 kinase activity did not increase during the treatment. The phosphorylation of H3-S28 was possibly induced through the decreased activity of H3-S28 phosphatase induced by cycloheximide. A burst of phosphorylation of H3-S10 and H3-S28 could not be induced because of the low activities of histone H3 kinase and Cdc2 kinase. Nevertheless, these results demonstrate that the newly synthesized proteins are essential for the histone H3 phosphorylation and deacetylation during meiotic resumption of pig oocytes.

Chromatin configuration of vanadate-treated oocytes was different from trichostatin A- or

cycloheximide-treated oocytes. It has been suggested that sodium orthovanadate causes mitotic cells to revert to an interphase-like state (Anderson et al., 1998). Gowdy et al. (1998) suggested that tyrosine phosphatase inhibitors caused chromosome decondensation and nuclear envelope reformation in mitotic cells. The present experiments showed that in the vanadate-treated pig oocytes, condensed heterochromatin decondensed to filamentous or sringy configuration. In the oocytes, histone H3 was not phosphorylated at both S10 and S28. These results suggest that the inhibitor of tyrosine phosphatases inhibits the condensation of chromosomes and induces the decondensation of heterochromatin. In vanadate-treated oocytes, intense fluorescent signal of Ac-H3-K14 was detected even after 42 h. This indicates that the tyrosine phosphatase inhibitor maintained the acetylation of H3-K14 during the treatment. The result of immunoblot analyses using anti-phosphotyrosine antibodies confirmed the effect of vanadate on tyrosine phosphorylation of oocyte proteins. Vanadate caused a massive accumulation of tyrosin phosphorylated proteins with different molecular weights. This indicates that the tyrosine phosphatase inhibitor induces tyrosine phosphorylation of some proteins which in turn inhibit HDAC or promote HAT activity to maintain the acetylation of histone H3 in the oocytes, because it has been shown that the balance between the activities of HAT and HDAC determines the acetylation status of histones (Yamagoe et al., 2003).

In summary, the three different inhibitors used in the experiments prevented the meiotic resumption of pig oocytes. Although the chromatin configurations were different among treatments, acetylation of histone H3-K14 and dephosphorylation of H3-S10 were maintained. Based on the results in Chapter 3 and here, it is possible that deacetylation of histone H3-K14 is a prerequisite to the phosphorylation of H3-S10.

Chapter 6. General Summary

In mammalian fetal ovaries, oogonia enter the meiotic cell cycle to become primary oocytes, and then they are arrested at the diplotene stage of the first meiotic prophase. During this arrest, some of the oocytes start to grow. They increase in volume with the change in chromatin morphology. Fully-grown oocytes resume meiosis under the stimulation of gonadotropic hormones, and mature to metaphase II. During this oocyte maturation, chromosomes start to condense, and Cdc2 kinase and MAP kinase become active. The chromosome condensation is the first step of the oocyte maturation and has been thought to be induced by Cdc2 kinase. However, the mechanism of the chromosome condensation has not been understood completely. Morphological change in chromosomes in somatic cells has been implicated by histone modifications. Histone N-terminal tails provide sites for a variety of post-translational modifications including acetylation, phosphorylation, and methylation. The sites for the modifications are clustered within the first 30 amino acids of core histones, and the juxtaposition of the modification sites provides potential cross-regulation of different modificational events.

The main objective of this research was to investigate the regulation of chromosome morphology by histone modification in pig oocytes during the growth, maturation, and activation. In addition, the study was carried out to determine the involvement of histone H3 modifications in the change in chromosome morphology of the somatic nuclei transferred into *in vitro*-matured pig oocytes. Finally, the possible involvement of histone modifications induced by some inhibitors that had been shown to affect on chromosome morphology in pig oocytes was investigated.

In Chapter 2, the correlation between chromosome condensation and histone H3 phosphorylation at serine 10 (H3-S10) during maturation of pig oocytes was examined. The phosphorylation of histone H3-S10 was first detected in the clump of condensed chromosomes at the diakinesis stage after 18 h of culture, and thereafter it was maintained until metaphase II. The kinase assay showed that histone H3 kinase activity was low in the oocytes at the germinal vesicle stage and increased markedly at the diakinesis stage, and that the high activity was maintained until metaphase II. To elucidate the involvement of Cdc2 kinase, MAP kinase, and histone H3 kinase on the chromosome condensation and histone H3 phosphorylation, the effects

of protein phosphatase 1/2A (PP1/PP2A) inhibitors on the chromosome condensation, phosphorylation of histone H3-S10, and activities of histone H3, Cdc2, and MAP kinases were investigated. The results showed that inhibitors of PP1/PP2A induced rapid chromosome condensation associated with histone H3-S10 phosphorylation after 2 h of treatment (Fig. 6.1). Both histone H3 kinase and MAP kinase were activated in the treated oocytes, although Cdc2 kinase was not activated. In oocytes treated with a PP1/PP2A inhibitor (calyculin A) and a MEK inhibitor (U0126), neither Cdc2 kinase nor MAP kinase was activated, although histone H3 kinase was still activated and the chromosomes condensed with histone H3-S10 phosphorylation. The inhibitor experiments made clear that the chromosome condensation correlated with histone H3 kinase activity, but not with Cdc2 kinase and MAP kinase activities. These results demonstrate the phosphorylation of histone H3-S10 occurs in condensed chromosomes during maturation of pig oocytes.

In Chapter 3, correlation between the morphological change of chromatin/chromosome and histone H3 phosphorylation, acetylation, and methylation was investigated throughout oocyte growth, maturation, and activation. The results indicated that the modulation of chromatin configurations from decondensed state to peri-nucleolar heterochromatin sheath during oocyte growth involved the change in the levels of histone H3 acetylation at lysine 9 (H3-K9), H3-K14, and H3-K18. The phosphorylation of histone H3-S10 and H3-S28 was not involved in the change in the chromatin morphology in growing oocytes. The data also showed that the complete acquisition of histone H3 methylation corresponded to the formation of heterochromatin in fully-grown oocytes. Early in oocyte maturation, phosphorylation of H3-S28 was detected in condensing chromosomes in the oocytes at GVII-IV stage after 9 h of maturation culture, and then histone H3-S10 was phosphorylated. During the maturation, the histone H3 acetylation levels decreased dramatically, however, methylation of histone H3-K9 was maintained. After electro-activation of matured oocytes, acetylation of H3-K14, H3-K9, and H3-K18 reappeared at anaphase II, telophase II, and the pronucleus stage, respectively. The reappearance of acetylated H3-K9 was concomitant with the drop of phosphorylation levels of H3-S10 and H3-S28 at this stage. Chromosomes were completely decondensed and H3-S10 was completely dephosphorylated at the time of pronucleus formation, while fluorescent signal of acetylated H3-K9 increased. The methylation of H3-K9 was maintained during maturation and after

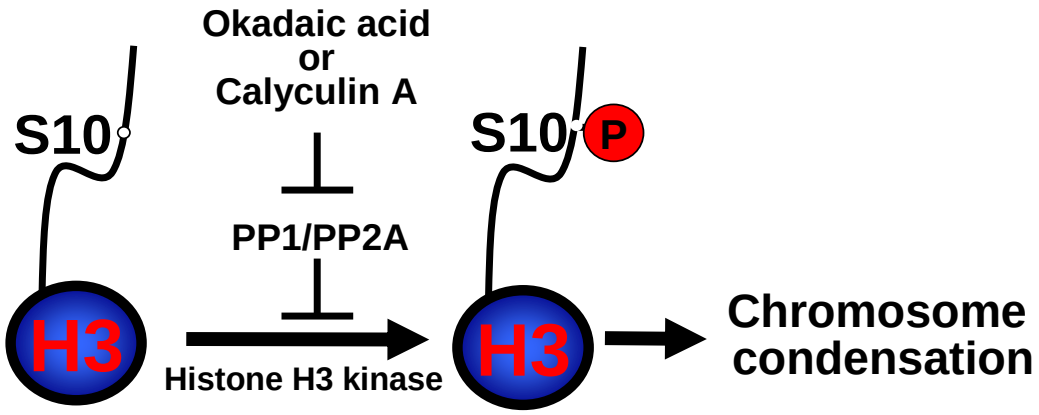

Fig. 6.1. A hypothetical model showing how PP1/PP2A inhibition induces histone H3 phosphorylation leading to chromosome condensation in pig oocytes.

activation until pronucleus stage in the oocytes. These findings suggest that chromatin morphology and chromosome condensation/decondensation of pig oocytes are regulated by acetylation/deacetylation and phosphorylation/dephosphorylation of histone H3. It was also shown that the oocytes in secondary follicles lacked histone H3-K9 methylation and the methylation was established correlative with oocyte growth. Although histone acetylation and phosphorylation were reversible, the stable methylation of H3-K9 was maintained throughout the oocyte maturation and activation. Furthermore, it is suggested that the ordered phosphorylation of histone H3 at S10 and S28 is thought to be influenced by other modifications, acetylation of neighboring lysines in the histone H3 molecule.

In Chapter 4, nuclei of somatic cells were transferred into *in vitro*-matured pig oocytes, and their histone H3 phosphorylation, acetylation, and methylation were investigated in relation to the change in the chromosome morphology. A series of phenomena were observed in the somatic nuclei during the first 2 h after nuclear transfer; chromosome condensation to form metaphase-like configuration, nuclear membrane disassembly, decrease in histone H3 acetylation levels, and increase in histone H3 phosphorylation levels. These results showed that nuclear remodeling including histone H3 modifications of injected somatic nuclei took place in the oocytes under the regulation of oocyte cell cycle. In the next experiment, pig oocytes injected with nuclei of somatic cells were electro-activated, and the chromosome morphology of oocytes and somatic cell nuclei was examined in correlation with their histone modifications in the same ooplasm. In most of the case, somatic chromosomes showed similar morphological change to those of oocytes, they progressed to anaphase II-telophase II-like stage, and then formed pronucleus-like structures. They also showed similar change in histone H3 phosphorylation and acetylation as oocytes. These results suggest that histone H3 phosphorylation and acetylation, but not methylation, of transferred somatic nuclei are controlled by oocyte cytoplasm.

In Chapter 5, it was examined whether meiosis-specific deacetylation and phosphorylation of histone H3 were affected by three different chemical inhibitors that had known to regulate meiotic maturation of oocytes. The inhibitors were a histone deacetylase (HDAC) inhibitor trichostatin A, a protein synthesis inhibitor cycloheximide, and a tyrosine phosphatase inhibitor vanadate. The results showed that HDAC inhibition induced maturation arrest, protein synthesis inhibition maintained histone H3 acetylation, and tyrosine phosphatase inhibition caused

heterochromatin decondensation and maintenance of histone H3 acetylation. The data indicated that all the three different inhibitors prevented the meiotic resumption of pig oocytes. Although induced chromatin configurations were different among treatments, acetylation of histone H3-K14 and dephosphorylation of H3-S10 were maintained.

The correlation of juxapositional histone H3 modifications during the growth, maturation and activation of pig oocytes can be summarized in a model as follows (Fig. 6.2). During their growth phase, histone H3-K9 becomes methylated for establishment of the maternal gene imprinting and histone H3-K9, H3-K14, and H3-K18 are acetylated for their transcriptional activity. When the fully-grown oocytes are stimulated by gonadotropins and start their maturation, histone H3-S28 and then H3-S10 become phosphorylated for the meiotic chromosome condensation. The phosphorylation of H3-S10 is accompanied by the deacetylation of H3-K9, H3-K14, and H3-K18. In oocytes at metaphase I and II, histone H3 at S10 and S28 are phosphorylated and K9, K14, and K18 are deacetylated completely. After activation of mature oocytes, H3-S10 and then H3-S28 become dephosphorylated for decondensation of chromosomes and H3-K9, H3-K14, and H3-K18 are reacetylated for preparing the zygotic transcription. Although histone acetylation and phosphorylation are reversible, the stable methylation of H3-K9 is maintained throughout the oocyte maturation and activation.

The oocyte growth, maturation, and activation are complex processes, which include transcription, meiotic arrest with condensed heterochromatin, chromosome condensation and decondensation, two consecutive meiotic divisions, and genomic imprinting, for producing the female gamete, egg. The work described in this dissertation suggests that oocytes have unique ability to manage these complex processes through the histone, at least core histone H3 modifications in chromatin. The phosphorylation of histone H3 is the first sign of oocyte maturation, and the balance of histone H3 kinase and PP1/PP2A activities regulates the phosphorylation leading to the chromosome condensation. The acetylation of histone H3 during oocyte growth and reacetylation after oocyte activation perhaps concern the transcriptional activities. The deacetylation during oocyte maturation and after somatic nuclear transfer may concern in erasing some memories in oocyte growth and differentiated state, respectively, to create the undifferentiated or totipotent embryos. Since the sites for the modifications are within the short histone tail, the juxtaposition of the modification sites is thought to provide

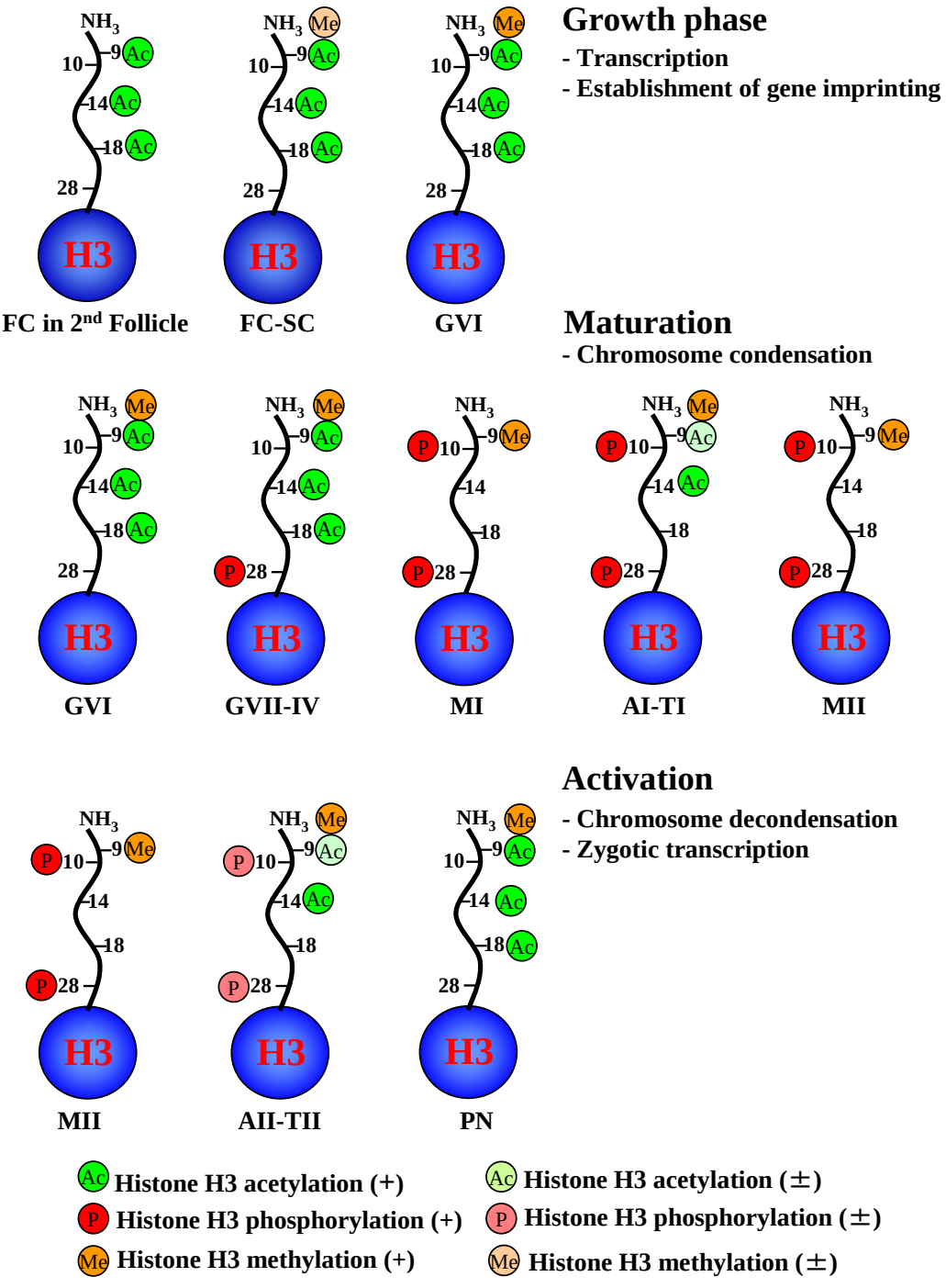

Fig. 6.2. A model of the histone H3 modifications during the growth, maturation, and activation in pig oocytes.

cross-regulations of different modifications. Deacetylation of histone H3-K14 is a prerequisite to the phosphorylation of histone H3-S10. When histone deacetylases are inhibited, histone H3 is not phosphorylated and the meiotic resumption is arrested. In contrast to the phosphorylation and acetylation, the energetic stability of histone H3 methylation through the maturation and activation perhaps contributes to the oocyte maternal epigenetic memory.

REFERENCES

Agalioti T, Chen G, Thanos D. Deciphering the transcriptional histone acetylation code for a human gene. *Cell*. 2002; 111(3):381-392.

Allfrey VG, Faulkner R, Mirsky AE. Acetylation and methylation of histones and their possible role in the regulation of RNA synthesis. *Proc Natl Acad Sci U S A.* 1964; 51:786-794.

Anderson HJ, de Jong G, Vincent I, Roberge M. Flow cytometry of mitotic cells. *Exp Cell Res.* 1998; 238(2):498-502.

Aoki F, Schultz RM. DNA replication in the 1-cell mouse embryo: stimulatory effect of histone acetylation. *Zygote*. 1999; 7(2):165-172.

Aoki F, Worrad DM, Schultz RM. Regulation of transcriptional activity during the first and second cell cycles in the preimplantation mouse embryo. *Dev Biol.* 1997; 181(2):296-307.

Aquino FP, Naito K, Cruz LC, Sato E, Toyoda Y. Effects of vanadate on meiotic maturation of porcine oocytes in vitro. *J Reprod Dev* 1995; 41:271-276.

Arents G, Burlingame RW, Wang BC, Love WE, Moudrianakis EN. The nucleosomal core histone octamer at 3.1 A resolution: a tripartite protein assembly and a left-handed superhelix. *Proc Natl Acad Sci U S A.* 1991; 88(22):10148-10152.

Arney KL, Bao S, Bannister AJ, Kouzarides T, Surani MA. Histone methylation defines epigenetic asymmetry in the mouse zygote. *Int J Dev Biol.* 2002; 46(3):317-320.

Bachman KE, Rountree MR, Baylin SB. Dnmt3a and Dnmt3b are transcriptional repressors that exhibit unique localization properties to heterochromatin. *J Biol Chem.* 2001; 276(34):32282-32287.

Bachvarova R. Gene expression during oogenesis and oocyte development in mammals. *Dev Biol (N Y 1985)*. 1985; 1:453-524.

Bannister AJ, Zegerman P, Partridge JF, Miska EA, Thomas JO, Allshire RC, Kouzarides T. Selective recognition of methylated lysine 9 on histone H3 by the HP1 chromo domain. *Nature*. 2001; 410(6824):120-124.

Bird A. DNA methylation patterns and epigenetic memory. *Genes Dev*. 2002; 16(1):6-21.

Bourc'his D, Le Bourhis D, Patin D, Niveleau A, Comizzoli P, Renard JP, Viegas-Pequignot

E. Delayed and incomplete reprogramming of chromosome methylation patterns in bovine cloned embryos. *Curr Biol*. 2001; 11(19):1542-1546.

Braunstein M, Rose AB, Holmes SG, Allis CD, Broach JR. Transcriptional silencing in yeast is associated with reduced nucleosome acetylation. *Genes Dev.* 1993, 7(4):592-604.

Campbell KH, Loi P, Otaegui PJ, Wilmut I. Cell cycle co-ordination in embryo cloning by nuclear transfer. *Rev Reprod.* 1996; 1(1):40-46.

Chadee DN, Hendzel MJ, Tylipski CP, Allis CD, Bazett-Jones DP, Wright JA, Davie JR. Increased Ser-10 phosphorylation of histone H3 in mitogen-stimulated and oncogene-transformed mouse fibroblasts. *J Biol Chem.* 1999; 274:24914-24920.

Chatot CL. Ziomek CA. Bavister BD. Lewis JL. Torres I. An improved culture medium supports development of random-bred 1-cell mouse embryos in vitro. *J Reprod Fertil.* 1989; 86:679-688.

Cheung P, Allis CD, Sassone-Corsi P. Signaling to chromatin through histone modifications. *Cell.* 2000a; 103(2):263-271.

Cheung P, Tanner KG, Cheung WL, Sassone-Corsi P, Denu JM, Allis CD. Synergistic coupling of histone H3 phosphorylation and acetylation in response to epidermal growth factor stimulation. *Mol Cell*. 2000b; 5(6):905-915.

Choi T, Aoki F, Yamashita M, Nakahama Y, and Kohmoto K. Direct activation of $p34^{cdc2}$ protein kinase without preceding phosphorylation during meiotic cell cycle in mouse oocytes. *Biomed Res.* 1992; 13:423-427.

Christians E, Boiani M, Garagna S, Dessy C, Redi CA, Renard JP, Zuccotti M. Gene expression and chromatin organization during mouse oocyte growth. *Dev Biol*. 1999; 207(1):76-85.

Crosio C, Fimia GM, Loury R, Kimura M, Okano Y, Zhou H, Sen S, Allis CD, Sassone-Corsi P. Mitotic phosphorylation of histone H3: spatio-temporal regulation by mammalian Aurora kinases. *Mol Cell Biol.* 2002; 22:874-885.

De La Fuente R, Eppig JJ. Transcriptional activity of the mouse oocyte genome: companion granulosa cells modulate transcription and chromatin remodeling. *Dev Biol.* 2001; 229:224-236.

de Smedt V, Crozet N, Gall L. Morphological and functional changes accompanying the

acquisition of competence in ovarian goat oocyte. *J Exp Zool. 1994*; 269:128-139.

De Sousa PA, Dobrinsky JR, Zhu J, Archibald AL, Ainslie A, Bosma W, Bowering J, Bracken J, Ferrier PM, Fletcher J, Gasparrini B, Harkness L, Johnston P, Ritchie M, Ritchie WA, Travers A, Albertini D, Dinnyes A, King TJ, Wilmut I. Somatic cell nuclear transfer in the pig: control of pronuclear formation and integration with improved methods for activation and maintenance of pregnancy. *Biol Reprod*. 2002; 66(3):642-650.

Dedieu T, Gall L, Crozet N, Sevellec C, Ruffini S. Mitogen-activated protein kinase activity during goat oocyte maturation and the acquisition of meiotic competence. *Mol Reprod Dev.* 1996; 45:351-358.

Di Agostino S, Rossi P, Geremia R, Sette C. The MAPK pathway triggers activation of Nek2 during chromosome condensation in mouse spermatocytes. *Development* 2002; 129:1715-1727.

Edmondson DG, Davie JK, Zhou J, Mirnikjoo B, Tatchell K, Dent SY. Site-specific loss of acetylation upon phosphorylation of histone H3. *J Biol Chem.* 2002; 277(33):29496-29502.

Ekholm C, Magnusson C. Rat oocyte maturation: effects of protein synthesis inhibitors. *Biol Reprod*. 1979; 21(5):1287-1293.

Fair T, Hulshof SCJ, Hyttel P, Greve T, and Boland M. Nucleus ultrastructure and transcriptional activity of bovine oocytes in preantral and early antral follicles. *Mol Reprod Dev.* 1997; 46:208-215.

Fair T, Hyttel P, Greve T, and Boland M. Nucleus structure and transcriptional activity in relation to oocytes diameter in cattle. *Mol Reprod Dev.* 1996; 43:503-512.

Fair T, Hyttel P, Lonergan P, Boland MP. Immunolocalization of nucleolar proteins during bovine oocyte growth, meiotic maturation, and fertilization. *Biol Reprod*. 2001; 64(5):1516-1525.

Fiil A. Oogenesis in the malaria Mosquito Anopheles gambiae. Cell Tissue Res. 1976; 167(1):23-35.

Fischer EH, Charbonneau H, Tonks NK. Protein tyrosine phosphatases – a diverse family of intracellular and transmembrane enzymes. *Science.* 1991; 253: 401-406.

Fissore RA, He CL, Vande Woude GF. Potential role of mitogen-activated protein kinase during meiosic resumption in bovine oocytes. *Biol Reprod*. 1996; 55:1261-1270.

Fulka J Jr, Loi P, Ledda S, Moor RM, Fulka J. Nucleus transfer in mammals: how the oocyte cytoplasm modifies the transferred nucleus. *Theriogenology.* 2001; 55(6):1373-1380.

Fulka J Jr, Motlik J, Fulka J, Jilek F. Effect of cycloheximide on nuclear maturation of pig and mouse oocytes. *J Reprod Fertil*. 1986; 77(1):281-285.

Gavin AC, Tsukitani Y, Schorderet-Slatkine S. Induction of M-phase entry of prophase-blocked mouse oocytes through microinjection of okadaic acid, a specific phosphatase inhibitor. *Exp Cell Res* 1991; 192:75-81.

Gerace L, Burke B. Functional organization of the nuclear envelope. *Annu Rev Cell Biol*. 1988; 4:335-374.

Giet R, Glover DM. Drosophila aurora B kinase is required for histone H3 phosphorylation and condensin recruitment during chromosome condensation and to organize the central spindle during cytokinesis. *J Cell Biol.* 2001; 152:669-682.

Gordon JA. Use of vanadate as protein-phosphotyrosine phosphatase inhibitor. *Methods Enzymol*. 1991; 201:477-482.

Goren S, Dekel N. Maintenance of meiotic arrest by a phosphorylated p34cdc2 is independent of cyclic adenosine 3',5'-monophosphate. *Biol Reprod*. 1994; 51(5):956-962.

Goto H, Yasui Y, Nigg EA, Inagaki M. Aurora-B phosphorylates Histone H3 at serine28 with regard to the mitotic chromosome condensation. *Genes Cells.* 2002; 7:11-17.

Gowdy PM, Anderson HJ, Roberge M. Entry into mitosis without Cdc2 kinase activation. *J Cell Sci*. 1998; 111 (Pt 22):3401-3410.

Guo XW, Th'ng JPH, Swank RA, Anderson HJ, Tudan C, Bradbury EM, Roberge M. Chromosome condensation induced by fostriecin does not require $p34^{cdc2}$ kinase activity and histone H1 hyperphosphorylation, but is associated with enhanced histone H2A and H3 phosphorylation. *EMBO J.* 1995; 14:976-985.

Gurdon JB, Laskey RA, De Robertis EM, Partington GA. Reprogramming of transplanted nuclei in amphibia. I*nt Rev Cytol Suppl*. 1979; (9):161-178.

Haccard O, Jessus C, Cayla X, Goris J, Merlevede W, Ozon R. In vivo activation of a microtubule-associated protein kinase during meiotic maturation of the Xenopus oocyte. *Eur J Biochem.* 1990; 192:633-642.

Hans F, Dimitrov S. Histone H3 phosphorylation and cell division. *Oncogene.* 2001;

20:3021-3027.

Hashimoto N, Kishimoto T. Regulation of meiotic metaphase by a cytoplasmic maturation-promoting factor during mouse oocyte maturation. *Dev Biol.* 1988; 126(2):242-252.

Hendzel MJ, Wei Y, Mancini MA, Van Hooser A, Ranalli T, Brinkley BR, Bazett-Jones DP, Allis CD. Mitosis-specific phosphorylation of histone H3 initiates primarily within pericentromeric heterochromatin during G2 and spreads in an ordered fashion coincident with mitotic chromosome condensation. *Chromosoma.* 1997; 106:348-360.

Hirao Y, Tsuji Y, Miyano T, Okano A, Miyake M, Kato S, Moor RM. Association between $p34^{cdc2}$ levels and meiotic arrest in pig oocytes during early growth. *Zygote.* 1995; 3:325-332.

Hsu JY, Sun ZW, Li X, Reuben M, Tatchell K, Bishop DK, Grushcow JM, Brame CJ, Caldwell JA, Hunt DF, Lin R, Smith MM, Allis CD. Mitotic phosphorylation of histone H3 is governed by Ipl1/aurora kinase and Glc7/PP1 phosphatase in budding yeast and nematodes. *Cell.* 2000; 102:279-291.

Hunter T. Protein-tyrosine phosphatases: the other side of the coin. *Cell* 1989; 58:1013-1016.

Inoue K, Kohda T, Lee J, Ogonuki N, Mochida K, Noguchi Y, Tanemura K, Kaneko-Ishino T, Ishino F, Ogura A. Faithful expression of imprinted genes in cloned mice. *Science.* 2002; 295(5553):297.

Inoue M, Naito K, Aoki F, Toyoda Y, Sato E. Activation of mitogen-activated protein kinase during meiotic maturation in porcine oocytes. *Zygote.* 1995; 3:265-271.

Inoue M, Naito K, Nakayama T, Sato E. Mitogen-activated protein kinase translocates into the germinal vesicle and induces germinal vesicle breakdown in porcine oocytes. *Biol Reprod.* 1998; 58:130-136.

Jaskelioff M, Peterson CL. Chromatin and transcription: histones continue to make their marks. *Nat Cell Biol.* 2003; 5(5):395-399.

Jenuwein T, Allis CD. Translating the histone code. *Science*. 2001; 293(5532):1074-1080.

Jeppesen P, Turner BM. The inactive X chromosome in female mammals is distinguished by a lack of histone H4 acetylation, a cytogenetic marker for gene expression. *Cell.* 1993; 74(2):281-289.

Kanayama N, Miyano T, Lee J. Acquisition of meiotic competence in growing pig oocytes correlates with their ability to activate Cdc2 kinase and MAP kinase. *Zygote.* 2002; 10:261-270.

Kang YK, Park JS, Koo DB, Choi YH, Kim SU, Lee KK, Han YM. Limited demethylation leaves mosaic-type methylation states in cloned bovine pre-implantation embryos. *EMBO J.* 2002; 21(5):1092-1100.

Kasinathan P, Knott JG, Moreira PN, Burnside AS, Jerry DJ, Robl JM. Effect of fibroblast donor cell age and cell cycle on development of bovine nuclear transfer embryos in vitro. *Biol Reprod*. 2001; 64(5):1487-1493

Kaszas E, Cande WZ. Phosphorylation of histone H3 is correlated with changes in the maintenance of sister chromatid cohesion during meiosis in maize, rather than the condensation of the chromatin. *J Cell Sci.* 2000; 113:3217-3226.

Kato Y, Tani T, Tsunoda Y. Cloning of calves from various somatic cell types of male and female adult, newborn and fetal cows. *J Reprod Fertil*. 2000; 120(2):231-237.

Kikyo N, Wolffe AP. Reprogramming nuclei: insights from cloning, nuclear transfer and heterokaryons. *J Cell Sci.* 2000; 113 (Pt 1):11-20.

Kim JM, Liu H, Tazaki M, Nagata M, Aoki F. Changes in histone acetylation during mouse oocyte meiosis. *J Cell Biol.* 2003; 162(1):37-46.

Kopecny V, Landa V, Malatesta M, Martin TE, Fakan S. Immunoelectron microscope analyses of rat germinal vesicle-stage oocyte nucleolus-like bodies. *Reprod Nutr Dev.* 1996; 6:667-679.

Kruhlak MJ, Hendzel MJ, Fischle W, Bertos NR, Hameed S, Yang XJ, Verdin E, Bazett-Jones DP. Regulation of global acetylation in mitosis through loss of histone acetyltransferases and deacetylases from chromatin. *J Biol Chem.* 2001; 276(41):38307-38319.

Kubelka M, Anger M, Kalous J, Schultz RM, Motlik J. Chromosome condensation in pig oocytes: lack of a requirement for either cdc2 kinase or MAP kinase activity. *Mol Reprod Dev.* 2002; 63:110-118.

Kubelka M, Motik J, Fulka J Jr, Prochazka R, Rimkevicova Z, Fulka J. Time sequence of germinal vesicle breakdown in pig oocytes after cycloheximide and P-aminobenzamidine

block. *Gamete Res.* 1988; 19(4):423-431.

Kwon YG, Lee SY, Choi Y, Greengard P, Nairn AC. Cell cycle-dependent phosphorylation of mammalian protein phosphatase 1 by cdc2 kinase. *Proc Natl Acad Sci U S A.* 1997; 94:2168-2173.

Lachner M, O'Carroll D, Rea S, Mechtler K, Jenuwein T. Methylation of histone H3 lysine 9 creates a binding site for HP1 proteins. *Nature*. 2001; 410(6824):116-120.

Laemmli UK. Cleavage of structural proteins during the assembly of the head of bacteriophage T4. *Nature.* 1970; 227:680-685.

Lee J, Miyano T, Moor RM. Localisation of phosphorylated MAP kinase during the transition from meiosis I to meiosis II in pig oocytes. *Zygote.* 2000; 8:119-125.

Liu H, Kim JM, Aoki F. Regulation of histone H3 lysine 9 methylation in oocytes and early pre-implantation embryos. *Development.* 2004; 131(10):2269-2280.

Lu Q, Dunn RL, Angeles R, Smith GD. Regulation of spindle formation by active mitogen-activated protein kinase and protein phosphatase 2A during mouse oocyte meiosis. *Biol Reprod.* 2002; 66:29-37.

Lucifero D, Mann MR, Bartolomei MS, Trasler JM. Gene-specific timing and epigenetic memory in oocyte imprinting. *Hum Mol Genet.* 2004; 13(8):839-849.

Luger K, Mader AW, Richmond RK, Sargent DF, Richmond TJ. Crystal structure of the nucleosome core particle at 2.8 A resolution. *Nature.* 1997; 389(6648):251-260.

Masui Y, Markert CL. Cytoplasmic control of nuclear behavior during meiotic maturation of frog oocytes. *J Exp Zool*. 1971; 177(2):129-145.

Mateescu B, England P, Halgand F, Yaniv M, Muchardt C. Tethering of HP1 proteins to chromatin is relieved by phosphoacetylation of histone H3. *EMBO Rep*. 2004; 5(5):490-496.

Mayer W, Niveleau A, Walter J, Fundele R, Haaf T. Demethylation of the zygotic paternal genome. *Nature*. 2000; 403(6769):501-502.

Millward TA, Zolnierowicz S, Hemmings BA. Regulation of protein kinase cascades by protein phosphatase 2A. *Trends Biochem Sci.* 1999; 24:186-191.

Miyano T, Lee J, Fulka J. Jr. G2/M transiton of pig oocytes: How do oocytes initiate maturation? *Reprod Med Biol.* 2003; 2:91-99.

Miyano T, Lee J. Change in cyclin B1 and MAP kinase molecules during maturation and fertilization of pig oocytes. In: Miyamoto H, Manabe N (eds.), *Reproductive Biotechnology. Kyoto: Hokuto Shobo;* 2001:9-19.

Moor RM, Trounson AO. Hormonal and follicular factors affecting maturation of sheep oocytes in vitro and their subsequent developmental capacity. *J Reprod Fertil.* 1977; 49:101-109.

Motlik J, Crozet N, Fulka J. Meiotic competence in vitro of pig oocytes isolated from early antral follicles. *J Reprod Fertil.* 1984; 72:323-328.

Motlik J, Fulka J. Breakdown of the germinal vesicle in pig oocytes in vivo and in vitro. *J Exp Zool.* 1976; 198:155-162.

Murnion ME, Adams RR, Callister DM, Allis CD, Earnshaw WC, Swedlow JR. Chromatin-associated protein phosphatase 1 regulates aurora-B and histone H3 phosphorylation. *J Biol Chem.* 2001; 276:26656-26665.

Murray AW. Creative blocks: cell cycle checkpoints and feed back controls. *Nature* 1992; 359:599-604.

Nebreda AR, Gannon JV, Hunt T. Newly synthesized protein(s) must associate with p34cdc2 to activate MAP kinase and MPF during progesterone-induced maturation of Xenopus oocytes. *EMBO J.* 1995; 14(22):5597-5607.

Nguyen VT, Kure-bayashi S, Harayama H, Nagai T, Miyake M. Stage-specific effects of the osmolarity of a culture medium on the development of parthenogenetic diploids in the pig. *Theriogenology.* 2003; 59(3-4):719-734.

Nguyen VT, Wakayama S, Kishigami S, Wakayama T. Spindle morphogenesis and the morphology of chromosome in mouse nuclear transfer: an abnormal stage in cloning of mice. *Reprod Fertil Dev.* 2004; 16 (1,2):153.

Niemann H, Wrenzycki C, Lucas-Hahn A, Brambrink T, Kues WA, Carnwath JW. Gene expression patterns in bovine in vitro-produced and nuclear transfer-derived embryos and their implications for early development. *Cloning Stem Cells*. 2002; 4(1):29-38.

Nigg EA. Cellular substrates of $p34^{cdc2}$ and its companion cyclin-dependent kinases. *Trends Cell Biol.* 1993; 3:296-301.

Nurse P. Universal control mechanism regulating onset of M phase. *Nature* 1990; 344:503-508.

Obata Y, Kaneko-Ishino T, Koide T, Takai Y, Ueda T, Domeki I, Shiroishi T, Ishino F, Kono

T. Disruption of primary imprinting during oocyte growth leads to the modified expression of imprinted genes during embryogenesis. *Development*. 1998; 125(8):1553-1560.

Obata Y, Kono T. Maternal primary imprinting is established at a specific time for each gene throughout oocyte growth. *J Biol Chem.* 2002; 277(7):5285-5289.

Onishi A, Iwamoto M, Akita T, Mikawa S, Takeda K, Awata T, Hanada H, Perry AC. Pig cloning by microinjection of fetal fibroblast nuclei. *Science*. 2000; 289(5482):1188-1190.

Peter M, Nakagawa J, Doree M, Labbe JC, Nigg EA. In vitro disassembly of the nuclear lamina and M phase-specific phosphorylation of lamins by cdc2 kinase. *Cell.* 1990; 61:591-602.

Peter M, Sanghera JS, Pelech SL, Nigg EA. Mitogen-activated protein kinases phosphorylate nuclear lamins and display sequence specificity overlapping that of mitotic protein kinase $p34^{cdc2}$. *Eur J Biochem.* 1992; 205:287-294.

Peterson CL, Workman JL. Promoter targeting and chromatin remodeling by the SWI/SNF complex. *Curr Opin Genet Dev.* 2000; 10(2):187-192.

Picard A, Capony JP, Brautigan DL, Doree M. Involvement of protein phosphatases 1 and 2A in the control of M phase-promoting factor activity in starfish. J *Cell Biol*. 1989; 109: 3347-3354.

Polejaeva IA, Chen SH, Vaught TD, Page RL, Mullins J, Ball S, Dai Y, Boone J, Walker S, Ayares DL, Colman A, Campbell KH. Cloned pigs produced by nuclear transfer from adult somatic cells. *Nature.* 2000; 407(6800):86-90.

Rea S, Eisenhaber F, O'Carroll D, Strahl BD, Sun ZW, Schmid M, Opravil S, Mechtler K, Ponting CP, Allis CD, Jenuwein T. Regulation of chromatin structure by site-specific histone H3 methyltransferases. *Nature*. 2000; 406(6796):593-599.

Rime H, Huchon D, Jessus C, Goris J, Merlevede W, Ozon R. Characterization of MPF activation by okadaic acid in Xenopus oocyte. *Cell Differ Dev.* 1990; 29:47-58.

Santos F, Zakhartchenko V, Stojkovic M, Peters A, Jenuwein T, Wolf E, Reik W, Dean W. Epigenetic marking correlates with developmental potential in cloned bovine preimplantation embryos. *Curr Biol*. 2003; 13(13):1116-1121.

Sassone-Corsi P, Mizzen CA, Cheung P, Crosio C, Monaco L, Jacquot S, Hanauer A, Allis CD. Requirement of Rsk-2 for epidermal growth factor-activated phosphorylation of

histone H3. *Science.* 1999; 285:886-891.

Schmitt A, Gutierrez GJ, Lénárt P, Ellenberg J, Nebreda AR. Histone H3 phosphorylation during Xenopus oocyte maturation: regulation by the MAP kinase/p90Rsk pathway and uncoupling from DNA condensation. *FEBS Lett.* 2002; 518:23-28.

Schultz RM, Davis W Jr, Stein P, Svoboda P. Reprogramming of gene expression during preimplantation development. *Exp Zool.* 1999; 285(3):276-282.

Schultz RM, Letourneau GE, Wassarman PM. Program of early development in the mammal: changes in patterns and absolute rates of tubulin and total protein synthesis during oogenesis and early embryogenesis in the mouse. *Dev Biol.* 1979; 68(2):341-359.

Schultz RM, Wassarman PM. Biochemical studies of mammalian oogenesis: Protein synthesis during oocyte growth and meiotic maturation in the mouse. *J Cell Sci.* 1977; 24:167-194.

Sette C, Barchi M, Bianchini A, Conti M, Rossi P, Geremia R. Activation of the mitogen-activated protein kinase ERK1 during meiotic progression of mouse pachytene spermatocytes. *J Biol Chem.* 1999; 274:33571-33579.

Shibuya EK, Boulton TG, Cobb MH, Ruderman JV. Activation of p42 MAP kinase and the release of oocytes from cell cycle arrest. *EMBO J.* 1992; 11:3963-3975.

Smith GD, Sadhu A, Mathies S, Wolf DP. Characterization of protein phosphatases in mouse oocytes. *Dev Biol.* 1998; 204:537-549.

Sobajima T, Aoki F, Kohmoto K. Activation of mitogen-activated protein kinase during meiotic maturation in mouse oocytes. *J Reprod Fertil.* 1993; 97:389-394.

Sontag E, Fedorov S, Kamibayashi C, Robbins D, Cobb M, Mumby M. The interaction of SV40 small tumor antigen with protein phosphatase 2A stimulates the map kinase pathway and induces cell proliferation. *Cell.* 1993; 75:887-897.

Strahl BD, Allis CD. The language of covalent histone modifications. *Nature.* 2000; 403(6765):41-45.

Struhl K. Histone acetylation and transcriptional regulatory mechanisms. *Genes Dev.* 1998; 12(5):599-606.

Sugiyama K, Sugiura K, Hara T, Sugimoto K, Shima H, Honda K, Furukawa K, Yamashita S, Urano T. Aurora-B associated protein phosphatases as negative regulators of kinase activation. *Oncogene.* 2002; 21:3103-3111.

Sun QY, Blumenfeld Z, Rubinstein S, Goldman S, Gonen Y, Breitbart H. Mitogen- activated protein kinase in human eggs. *Zygote.* 1999; 7:181-185.

Sun QY, Wu GM, Lai L, Bonk A, Cabot R, Park KW, Day BN, Prather RS, Schatten H. Regulation of mitogen-activated protein kinase phosphorylation, microtubule organization, chromatin behavior, and cell cycle progression by protein phosphatases during pig oocyte maturation and fertilization in vitro. *Biol Reprod.* 2002; 66:580-588.

Szöllösi D. Oocyte maturation. In "*Reproduction in Mammals and Man*." (eds. Thibault C, Levasseur MC, Hunter RHF) Paris: Ellipses, 1993; 307-325.

Taddei A, Maison C, Roche D, Almouzni G. Reversible disruption of pericentric heterochromatin and centromere function by inhibiting deacetylases. *Nat Cell Biol*. 2001; 3(2):114-120.

Tamaru H, Selker EU. A histone H3 methyltransferase controls DNA methylation in Neurospora crassa. *Nature.* 2001; 414(6861):277-283.

Tani T, Kato Y, Tsunoda Y. Direct exposure of chromosomes to nonactivated ovum cytoplasm is effective for bovine somatic cell nucleus reprogramming. *Biol Reprod*. 2001; 64(1):324-330.

Tse C, Hansen JC. Hybrid trypsinized nucleosomal arrays: identification of multiple functional roles of the H2A/H2B and H3/H4 N-termini in chromatin fiber compaction. *Biochemistry.* 1997; 36:11381-11388.

Tse C, Sera T, Wolffe AP, Hansen JC. Disruption of higher-order folding by core histone acetylation dramatically enhances transcription of nucleosomal arrays by RNA polymerase III. *Mol Cell Biol*. 1998; 18(8):4629-4638.

Turner BM. Histone acetylation as an epigenetic determinant of long-term transcriptional competence. *Cell Mol Life Sci*. 1998; 54(1):21-31.

Van Blerkom J. Structural relationship and posttranslational modification of stage-specific proteins synthesized during early preimplantation development in the mouse. *Proc Natl Acad Sci U S A.* 1981; 78(12):7629-7633.

Van Hooser A, Goodrich DW, Allis CD, Brinkley BR, Mancini MA. Histone H3 phosphorylation is required for the initiation, but not maintenance, of mammalian chromosome condensation. *J Cell Sci.* 1998; 111:3497-3506.

Wade PA, Kikyo N. Chromatin remodeling in nuclear cloning. *Eur J Biochem*. 2002; 269(9):2284-2287.

Wakayama T, Perry AC, Zuccotti M, Johnson KR, Yanagimachi R. Full-term development of mice from enucleated oocytes injected with cumulus cell nuclei. *Nature.* 1998; 394(6691):369-374.

Wakayama T, Yanagimachi R. Effect of cytokinesis inhibitors, DMSO and the timing of oocyte activation on mouse cloning using cumulus cell nuclei. *Reproduction.* 2001; 122(1):49-60.

Walker SC, Shin T, Zaunbrecher GM, Romano JE, Johnson GA, Bazer FW, Piedrahita JA. A highly efficient method for porcine cloning by nuclear transfer using in vitro-matured oocytes. *Cloning Stem Cells.* 2002;4(2):105-112

Wei Y, Mizzen CA, Cook RG, Gorovsky MA, Allis CD. Phosphorylation of histone H3 at serine 10 is correlated with chromosome condensation during mitosis and meiosis in Tetrahymena. *Proc Natl Acad Sci U S A.* 1998; 95:7480-7484.

Wei Y, Yu L, Bowen J, Gorovsky MA, Allis CD. Phosphorylation of histone H3 is required for proper chromosome condensation and segregation. *Cell.* 1999; 97:99-109.

Wells DN, Misica PM, Tervit HR. Production of cloned calves following nuclear transfer with cultured adult mural granulosa cells. *Biol Reprod*. 1999; 60(4):996-1005.

Wilmut I, Schnieke AE, McWhir J, Kind AJ, Campbell KH. Viable offspring derived from fetal and adult mammalian cells. *Nature.* 1997; 385(6619):810-813.

Wu J, Grunstein M. 25 years after the nucleosome model: chromatin modifications. *Trends Biochem Sci*. 2000, 5(12):619-623.

Wutz A, Smrzka OW, Schweifer N, Schellander K, Wagner EF, Barlow DP. Imprinted expression of the Igf2r gene depends on an intronic CpG island. *Nature*. 1997; 389(6652):745-749.

Yamagoe S, Kanno T, Kanno Y, Sasaki S, Siegel RM, Lenardo MJ, Humphrey G, Wang Y, Nakatani Y, Howard BH, Ozato K. Interaction of histone acetylases and deacetylases in vivo. *Mol Cell Biol*. 2003; 23(3):1025-1033.

Yamashita Y, Shimada M, Harimoto N, Rikimaru T, Shirabe K, Tanaka S, Sugimachi K. Histone deacetylase inhibitor trichostatin A induces cell-cycle arrest/apoptosis and hepatocyte differentiation in human hepatoma cells. *Int J Cancer.* 2003; 103(5):572-576.

Zhang J, Xu F, Hashimshony T, Keshet I, Cedar H. Establishment of transcriptional competence in early and late S phase. *Nature.* 2002; 420(6912):198-202.

ACKNOWLEDGMENTS

I am especially grateful to Professor Takashi Miyano for his supervision during 5 years of my study at Laboratory of Reproductive Biology and Biotechnology in Kobe University, and for his kind help in supporting my study in Japan by his valuable suggestions and discussions. I am very grateful to Professor Seishiro Kato and Professor Masashi Miyake for their encouragement and valuable suggestions on my study. I would like to express my thanks to Associate Professor Hiroshi Harayama for his valuable suggestions on analysis of the data. I also thank Professor Usio Kikkawa and Professor Yasuo Fukami for the critical reading of my dissertation and suggestions. I thank Miss Emi Yamaoka who has contributed to my experiments. I would like to express my thanks to all of my Japanese friends in my laboratory for their valuable suggestions and technical advices on my experiments and their encouragement, especially for their helps in improving of my Japanese.

I am very grateful to Dr. Teruhiko Wakayama for providing me with the opportunity to do some experiments in his lab, Laboratory for Genomic Reprogramming, CDB, RIKEN-Kobe, and for his technical support and supervising my study during the time doing experiments in his lab. And I also would like to thank to all of researchers and staffs of his lab.

I would like to express my thanks to Kobe University, the 21st Century COE program for supporting my study and my reports in the conferences in Japan also in abroad. I am grateful to Kinoshita Foundation whose scholarship supported me during the time that I study in Kobe University. I would like to thank the staff of the Meat Inspection Office of Kobe City for supplying pig ovaries.

Finally, I would like to express my indebtedness to my parents, my husband, my daughter and son, for the patience and tolerance that they have shown me during the study of my doctoral dissertation.